August 2001 ECN-C–01-032

PEMSWECS

Performance Evaluation Methods for Autonomous, Applications Orientated Wind Turbine Systems:

Systems with batteries

J.T.G. Pierik

Distribution

NEL:
R. Dunlop 1 – 5
W.K. Lee 6

DEWI:
J. Gabriel 7

Fortis:
J. Kuikman 8

IT Power:
Francis Crick 9

Ciemat:
L.M. Arribas 10
I. Cruz 11

Cermak Peterka Petersen:
B.C. Cochran 12

RES:
R. Hunter 13

NREL:
H. Link 14
T. Forsyth 15
J. van Dam 16

Philips:
A. de Bijl 17

Novem:
J. ’t Hooft 18

ECN:
F.W. Saris 19
W. Schatborn 20
H.J.M. Beurskens 21
L.G.J. Jansen 22
L. Rademakers 23
A. Curvers 24
E. Werkhoven 25
A. van der Werff 26
H. Snel 27
J.A. Eikelboom 28
E. Wiggelinkhuizen 29
M. van Leeuwen 30
F. van Hulle 31
P. Schaak 32
T. G. van Engelen 33
E. van der Hooft 34
J.T.G. Pierik 35
ECN Wind Energy Archive 36 – 49
ECN Central Archive 50

Abstract

This report describes measurements and simulations to determine a method for the power performance evaluation of autonomous wind turbine systems. The method applies to small systems, equipped with a permanent magnet generator in the turbine, a diode rectifier and batteries. The analysis concentrates on the effect of the load on the power-wind speed curve of the turbine. It is shown that, although the effect of the load on the DC voltage is substantial, a 30% variation is not unusual, the effect on the power curve is relatively small. The effect on the annual averaged energy production, although dependent on the wind regime, is also expected to be small: in the range of 5%. This justifies a simple method for the measurement of the power curve.

Acknowledgement

This work has been executed in the JOULE III programme on Renewable Energy, on a partial grant of the European Commission and the ECN Generic R&D programme financed by the Ministry of Economic Affairs of the Netherlands.

Project	:	Power Performance Evaluation Methods for Autonomous,
	:	Applications Oriented Wind Turbine Systems
EC Project nr	:	JOR3-CT98-0262
ECN Project nr	:	7.4063

The author likes to thank Erwin Werkhoven, Arno van der Werff and Peter Vink for their efforts to make the measurement system work and Tim van Engelen for his help with the estimation of tranferfunctions.

Keywords

power performance, stand-alone wind turbines, wind energy, electric power, electrical models

CONTENTS

List of symbols

δ	load angle	^{o}
ϕ	angle between current and voltage phasor (phase angle)	^{o}
ω	electrical angular frequency	rad/s
f	electrical frequency	Hz
P	power	kW
Q	reactive power	kVA
S	apparent power	kVA
u, U	AC voltage	V
E	electro motive force (EMF)	V
i, I	current	A
$\hat{}$	amplitude of a sinusoidal quantity	-
$\vec{}$	phasor	-
l, L	inductance	H
l_{afd}	mutual inductance stator-field	H
r, R	resistance	Ω
X	reactance	Ω
subscript $_d$	d-as	-
subscript $_q$	q-as	-
subscript $_f$	field	-
subscript $_{s,\,a}$	stator	-
subscript $_g$	generator	-
subscript $_r$	rotor	-
subscript $_{eq}$	equivalent	-
subscript $_{dc}$	direct current	-
subscript $_i$	internal	-
subscript $_p$	polarisation	-
superscript ^{e}	EMF reference frame	-
superscript ^{u}	stator voltage reference frame	-
superscript ^{o}	open circuit	-
n, N	rotational speed	rpm
σ	standard deviation	-
nr	number of samples in bin	-
s_{Pi}	cat. A uncertainty, deduced from measurements, in power	kW
u_{Pi}	cat. B uncertainty, related to instruments and data acquisition, in power	kW
Ψ	magnetic flux	Vs
AH	amp hours	Ah
T	temperature	C
SOC	state of charge	%
C_p	power coefficient	-
V_w	wind speed	m/s
T_{av}	pre-averageing time	s
H	probability distribution	-
h	probability density	-
E_{annual}	annual average energy production	J/y
A_r	rotor area	m^2
A	Weibull scale factor	-
k	Weibull shape factor	-
Γ	Gamma function	-
EF	E_{tur}/E_{aero}	-
CF	capacity factor	-
C_{bat}	battery capacity	Ah

1. INTRODUCTION

The PEMSWECS project "Power Performance Evaluation Methods for Autonomous, Applications Oriented Wind Turbine Systems" is a joint project of National Engineering Laboratory NEL (UK), Deutches Windenergie-Institute DEWI (Germany) and ECN, executed within the framework of the Joule III programme. This report gives the results of the ECN contribution to the project.

The general goal of PEMSWECS is to:
- understand real load behaviour of stand alone systems;
- predict real load performance;
- perform measurements to verify the prediction;
- recommend a method for the performance evaluation of stand alone wind turbine systems.

The ECN contribution concentrates on systems with permanent magnet generator, diode rectifier and batteries. This type of autonomous system is very common for autonomous applications in the range of a few hundred watts to several kilowatts.

Contrary to medium and large size turbines, most small turbines operate "stand-alone", i.e. not grid connected. Grid connected performance evaluation methods may not be suitable for these systems for a number of reasons [7]:
- the effect of turbulence and turbine dynamics on power performance can be significant;
- the turbine performance will depend on type and the variation of the electrical load;
- mechanical and electrical efficiencies can be low.

Especially the effect of the load on the system behavior will make stand alone systems more difficult to evaluate. The IEC standard 61400-12 deals with power performance testing of grid connected wind turbines, and is a suitable starting point, but for the reasons mentioned, it does not cover the typical aspects of stand alone systems. To give an example: if the turbine is equipped with a permanent magnet generator and the load is a battery fed through a diode or thyristor rectifier, the battery voltage will fluctuate and influence the wind turbine power-speed curve and thus the power output at a given wind speed.

When quantifying stand-alone system behaviour, a good understanding of the interaction between turbine and load seems crucial for two reasons:
- to be able to choose realistic conditions for measurements;
- to translate measured behaviour to real load behaviour at an end user.

A method will be determined for realistic tests. The results of the Standardising Performance Claims project [4] will be the starting point. This project aimed at a test to quantify the behaviour of small wind turbines under "standard conditions", and concentrated on battery charging systems. The project recommended two measurements to characterize a system: one at 95% and one at 112% of the nominal battery voltage.

A second aspect to consider is the choice of the sampling rate and averaging period in the determination of a power curve. There are indications that the smaller the turbine, the shorter the averaging period that should be used [5]. Using a long averaging period will lead to loss of information and a longer measurement time.

Project approach

The tasks in the PEMSWECS project are:

- choice of 3 relevant system types, viz. systems with different loads, control and operation;
- evaluation of the system operation by:
  – modelling;
  – measurements;
- determination of the system characteristics:
  – which variables should be measured;
  – which variables determine the power curve;
  – how should the power curve be measured and evaluated;
- estimation of the power performance of the chosen systems;
- recommendation of measurement and evaluation method.

Contents of this report

Chapter 2 gives an overview of possible configurations of stand alone systems. The three system configurations investigated in this project are described. Each of the partners in the PEMSWECS project performed measurements on a different system. Chapter 3 describes the Fortis Montana wind turbine system used for measurements to develop a method at ECN. The measurement equipment is described in chapter 4. Chapter 5 deals with the test to define system characteristics. The effect of the averaging time on the measured power curve is analysed. To understand the differences in operation, system configurations are examined through model calculations in chapters 6. The parameters required in the models are determined from measurements. Chapter 7 discusses the effect of the parameter which is believed to have the largest effect on the power performance: the DC voltage. Chapter 8 translates observed changes in DC voltage and power curve to changes in annual energy production for a number of wind regimes. From these results, conclusions for a power performance evaluation method for autonomous wind turbine systems with batteries are drawn in chapter 9.

2. STAND ALONE SYSTEMS

2.1 Configurations

The stand alone systems examined in this project will serve as a source of electric power. There is a large market for mechanical wind pumps world wide, but these turbines differ considerably from what is generally known as battery chargers and these systems are excluded from this project. First, the differences in lay-out and operation of a number of configurations will be summarized. From these configurations, the systems to be tested in this project, have been chosen.

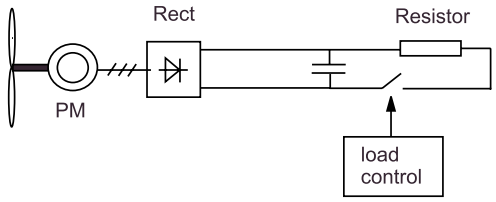

Figure 2.1 *Configuration 1: Permanent Magnet WT + Rectifier + DC load*

Configuration 1 is the most simple one. The turbine is equipped with a permanent magnet generator and is operated in variable speed mode. The DC load is a set of resistors which is directly connected to a diode bridge rectifier. The generator terminal AC voltage is of variable amplitude and frequency. The ratio between the AC and DC voltage of the rectifier is fixed. The current and the electric power delivered by the generator depend on the difference between the generator internal voltage, the EMF and the DC voltage. For a permanent magnet generator, the EMF only depends on the rotor speed.

To get a better match between the turbine and the load, a load controller is introduced. The controller closes a switch if the voltage reaches a given setpoint and opens the switch if the voltage falls below this value. A hysteresis band may be included. The load controller could be left out, but this dramatically reduces the energy capture at low wind speeds. This demonstrates that the operating point of the turbine is not only determined by the aerodynamic characteristics of the rotor, but also by the load and the DC voltage.

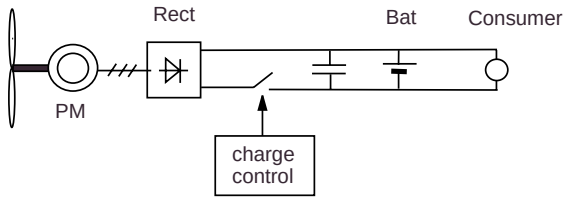

Figure 2.2 *Configuration 2a: Permanent Magnet WT + Rectifier + Batteries + DC load, open circuit control*

In many cases stand alone systems include batteries (figure 2.2). This is often the case if the end user requires electric power for different applications and desires partial independence of the wind resource. If the wind power exceeds the

consumer load, the surplus is stored in case the batteries are not fully charged. Again, the turbine operates at variable speed and produces power at variable voltage and frequency.

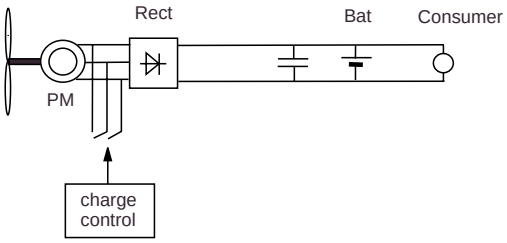

Figure 2.3 *Configuration 2b: Permanent Magnet WT + Rectifier + Batteries + DC load, short circuit control*

The batteries in configuration 2a are protected against high voltages and overcharging by a charge controller. In the example of figure 2.2 the wind turbine is simply disconnected from the batteries (open circuit option) but other options are also feasible:

- the wind turbine generator is short circuited (figure 2.3);
- a resistive load is switched on, either on the AC or the DC side of the rectifier (figure 2.4). Often a voltage controlled high frequency solid state switch is used.

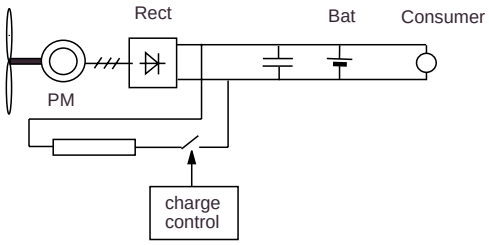

Figure 2.4 *Configuration 2c: Permanent Magnet WT + Rectifier + Batteries + DC load, dumpload control*

The open circuit option will require an aerodynamic or mechanical speed limitation, since the turbine will run unloaded. It may result in a high open circuit voltage and in noise. The short circuit option (figure 2.3) will require a generator able to withstand a prolonged short circuit and it may stop the turbine completely. Option 2c (figure 2.4) diverts the power to a different load and the turbine will remain near its current point of operation. It may also continue charging at a reduced level, depending on the implementation of the control.

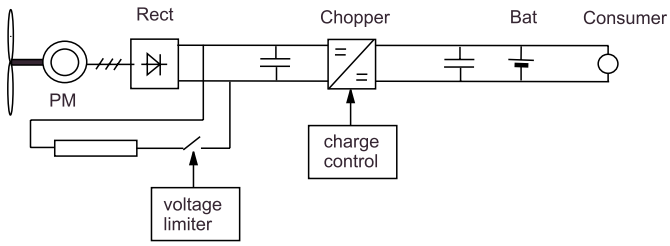

Figure 2.5 *Configuration 3: Permanent Magnet WT + Rectifier + Chopper + Batteries + DC load*

The battery current can also be controlled by means of a chopper (figure 2.5). The chopper acts as a DC transformer: it reduces the DC voltage (buck or downchopper) or increases it (boost or upchopper). By changing the duty cycle of the chopper, the ratio of the voltages on both sides is set, and a sophisticated charge control can be achieved. The wind turbine can be operated at a higher voltage and the voltage range may be wider.

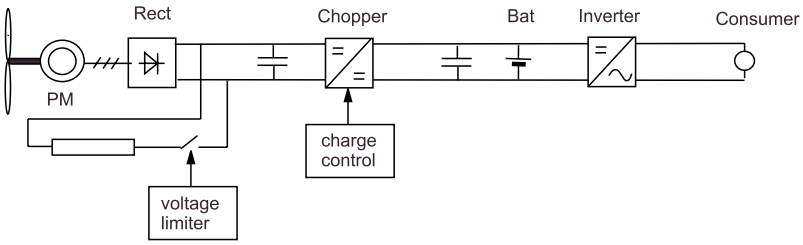

Figure 2.6 *Configuration 4: Permanent Magnet WT + Rectifier + Chopper + Batteries + Invertor + AC load*

In some systems an inverter is added to the system (figure 2.6) to produce a sinusoidal voltage and to be able to apply standard AC loads. In the past a thyristor controlled inverter was used in combination with filters and reactive power compensation [1]. With the advance of high frequency power electronic switches, like IGBTs, the filters can be small and no reactive power compensation is needed. This increases the feasibility of this option considerably. A voltage is produced with little distortion and the frequency and amplitude are controlled.

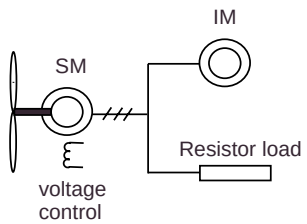

Figure 2.7 *Configuration 5: Synchronous Machine WT + Induction Machine + AC load*

In Configuration 5 the turbine and the load are coupled on an AC level. A synchronous generator is used in order to control the voltage. If the speed increases, the field is reduced. No storage is included, which means that the frequency

can only be controlled by adjusting the resistive load. Otherwise, the frequency changes freely with the wind speed. The system is relatively simple but the matching of the rotor and the load is critical since there is a strong electrical interaction between rotor and load.

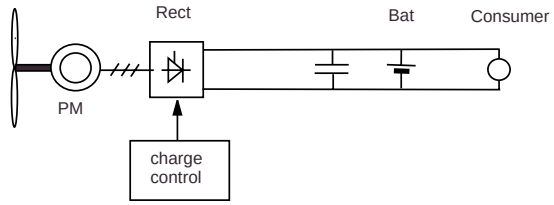

Figure 2.8 *Configuration 6: Permanent Magnet WT + Thyristor Rectifier + Batteries + DC load*

In systems with a controllable rectifier, figure 2.8, the angle between the AC voltage and AC current can be controlled to limit the active current and a solid state switch is not required. In the past, grid connected variable speed turbines have used this option, with a second thyristor bridge on the grid side of the DC link. Since not all aerodynamic power will be absorbed under all circumstances, this configuration requires speed limitation. This option can be used in stand alone systems but a thyristor controlled rectifier is not often found in small systems. The characteristics of a system with batteries are described in [13].

Table 2.1 *Examples of commercial and prototype systems*

	Manufacturer	Rated power
Config 1	Proven	6 kW
Config 2	Fortis	4 kW
	Whisper	0.9 kW
Config 3	Fortis	4 kW
Config 4	Fortis	4 kW
Config 5	Tocardo	4 kW

2.2 Test Systems

2.2.1 Test System 1: NEL

The first test system is a Configuration 1 system. Figure 2.9 gives the lay-out. This system is tested by NEL. The load is controlled by firing an IGBT, based on the value of the DC voltage. The voltage setpoint is constant.

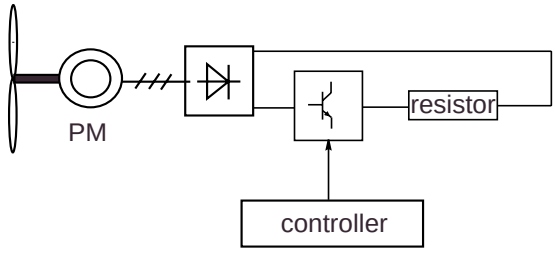

Figure 2.9 *System 1 (NEL): Permanent Magnet generator, rectifier and resistive load*

2.2.2 Test System 2: ECN

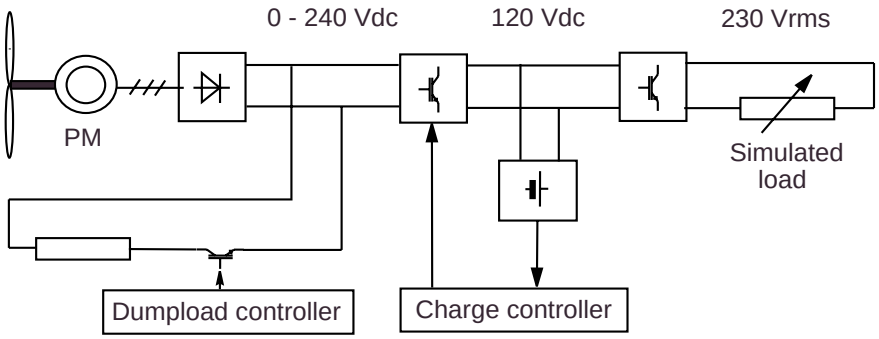

Figure 2.10 *System 2 (ECN initial setup): Batteries + inverter + AC load*

The second test system was originally a Configuration 4 system in figure 2.10, including an inverter for AC power. However, the operation of the dumpload controller in combination with the chopper turned out to be problematic. After a number of components were destroyed, the system was converted to a Configuration 2c type by bypassing the chopper and reducing the DC voltage level of the rectifier and dumpload. This proved to be successful. This configuration is shown in figure 2.11 and is described in more detail in chapter 3.

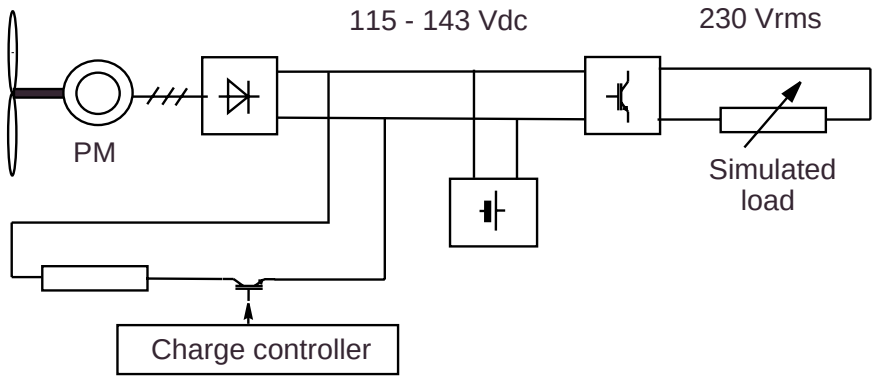

Figure 2.11 *System 2 (ECN final setup): Batteries + inverter + AC load*

2.2.3 Test System 3: DEWI

The third test system is a Configuration 5 system with a synchronous generator in the turbine and a resistive load. A controller switches load resistors, the speed of the turbine is constant. In this way, the turbine is operated similar to a grid connected constant speed turbine. This configuration is more relevant for stand alone systems which include a back-up generator set, mostly a diesel genset. The back-up genset will supply any power shortages. The grid frequency in a Wind-Diesel system is kept constant by either the diesel genset or a dumpload. The configuration without back-up genset is shown in figure 2.12 and is tested by DEWI.

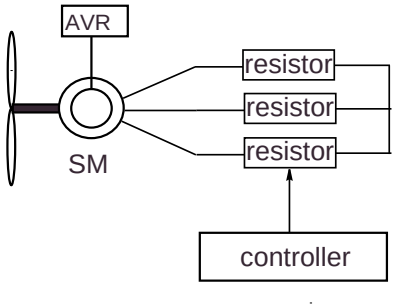

Figure 2.12 *System 3 (DEWI): Constant speed system*

Standard synchronous machines are equipped with AVRs: automatic voltage controllers, which keep the voltage constant if the speed does not deviate too much from the rated speed, i.e. the speed corresponding to 50 Hz. Measurements at DEWI have been taken at a number of different speeds and show that the voltage is proportional to the speed. The power-speed curve is strongly influenced by the chosen speed setpoint, as can be expected, but the $C_p(\lambda)$ curve is not. Operation is similar to the grid connected case.

3. DESCRIPTION OF ECN TEST SYSTEM

The system tested at the ECN test site is a Fortis Montana wind turbine with diode rectifier, controllable dumpload, batteries and a Sunpower PV UP 5000 converter. Table 3.1 lists the characteristic data of the Fortis Montana wind turbine [9].

Table 3.1 *Fortis Montana 4000 turbine data*

Rotor diameter	5 m
Number of blades	3
Blade type	NACA 4415
Material	glass fiber reinforced polyester
Optimal tip speed ratio	9
Cut in wind speed	3.5 m/s
Rated wind speed	12 m/s
Survival wind speed	60 m/s

Gear ratio	direct drive

Yaw system	inclined hinged tail vane
Power limitation	inclined hinged tail vane
Turbine brake	short circuit switch on generator

Generator	3 phase, permanent magnet
Rated power	4 kW
Nr of pole pairs	9
Rated speed	300 rpm
Max speed	420 rpm
Frequency	0-70 Hz
Load	diode rectifier
	switchable dumpload
	batteries at 120 Vdc
	single phase 230 Vrms converter

Tower	guyed steel tube, tiltable
Hub height	6, 12, 18 or 24 m

The operation of the yaw system and aerodynamic power limitation of the Fortis turbine indicated in figure 3.1. The rotor is eccentrically mounted. At an increase in wind speed, the yaw moment will increase, turning the nacelle anti-clockwise. This moment is counteracted by the vane, which is hinged and the hinge axis is tilted. The vane will be lifted by the yawing of the nacelle and this results in a clockwise moment around the yaw axis. The balance of the two moments determines the yaw angle at a given wind speed.

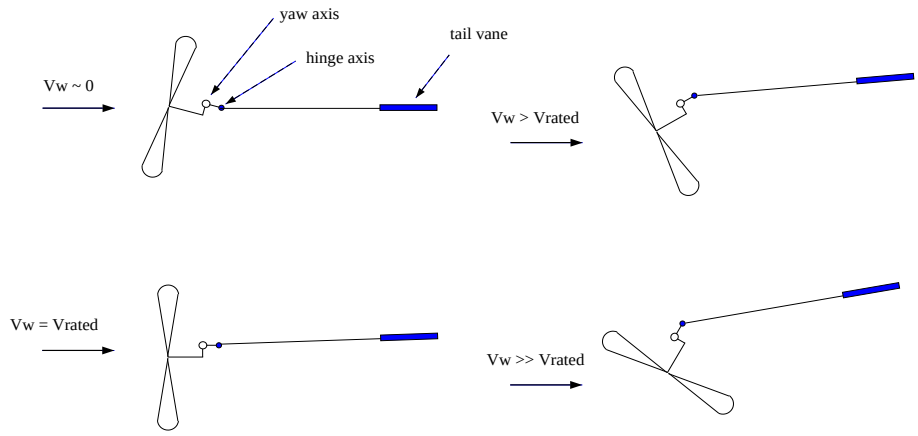

Figure 3.1 *Inclined hinge tail vane and eccentric nacelle mounting*

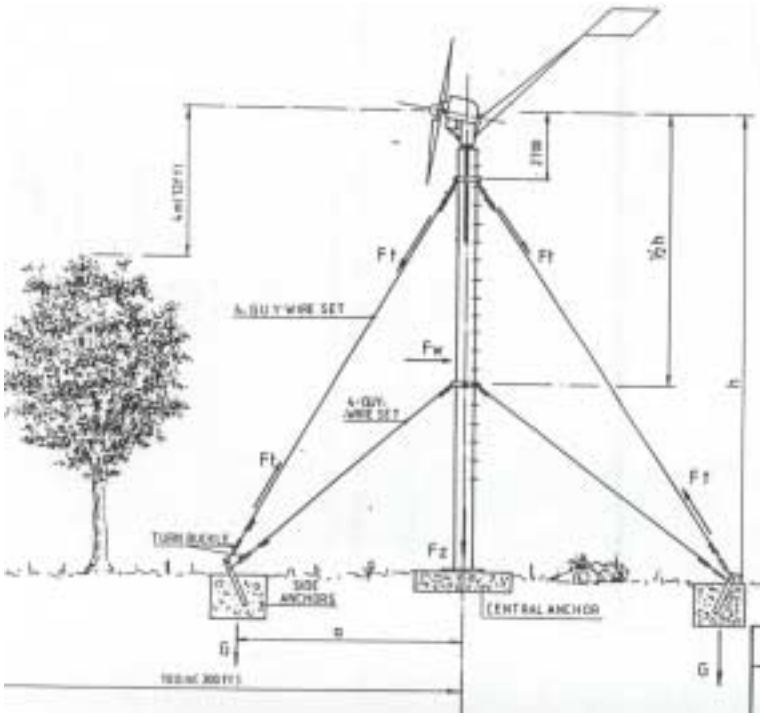

Figure 3.2 *Fortis turbine (from Instructions for assembly of Fortis Montana 4000 by J. Kuikman)*

The main electrical components (figures 3.3 and 3.4) are:

- a 3 phase permanent magnet generator with a full diode bridge rectifier;
- a dumpload controller consisting of a voltage controlled FET and a dumpload capable of dissipating 5 kW;
- a string of ten 12 V batteries;
- a capacitor between rectifier and batteries;
- a bi-directional single phase DC-AC converter operating between 120 Vdc and 230 Vac to create a single phase grid.

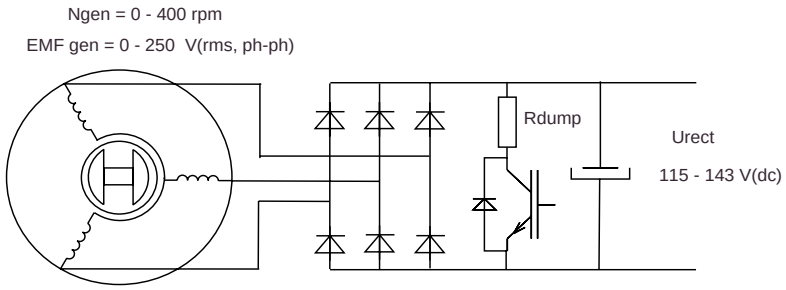

Figure 3.3 *Permanent magnet generator, diode rectifier and dumpload*

The bi-directional converter is part of a Sunpower PV UP 5000, of which the downchopper section is bypassed. In the Fortis system, the converter will only work in one direction, since no power source is connected to the AC side. The converter is designed to produce a sinusoidal output voltage of 230V and 50 Hz, suitable for all standard electrical appliances (see table 3.2).

The turbine will start to produce power when the phase to phase AC voltage exceeds the battery voltage, typically 120 V, since this is the minimum voltage required to open the diodes. Initially the current loading the input capacitor of the downchopper will flow discontinuously. The inductance in the circuit is relatively small, only due to the stator of the generator. When wind speed increases the turbine will increase in speed, the AC voltage will go up and the current will flow continuously. The capacitor will be loaded to a voltage above battery voltage and the batteries will be charged. The turbine speed is dictated by the wind speed and the capacitor voltage. If the batteries are charged the capacitor voltage will increase further. When a value of 143 V is reached, the dumpload is switched on bij the dumpload controller and all surplus power is fed to the dumpload.

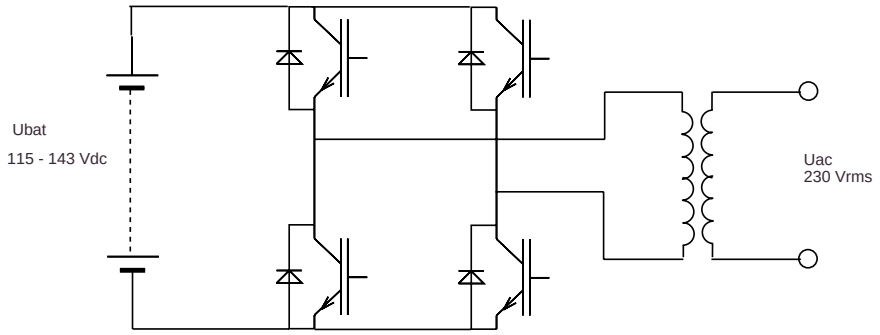

Figure 3.4 *Batteries and bi-directional converter*

Table 3.2 *Sunpower PV UP 5000 data*

Type	PV UP 5000
INPUT DC (Windturbine rectifier)	
Recommended generator power	5000 W
Operating mode	Input voltage control 166 V
Ground fault detection	yes
Protection against wrong polarity	yes
Overvoltage protection	varistors in conjunction with arc protection
INPUT AC (Grid / Diesel Generator)	
Grid input voltage	196 - 253 Vac
Input frequency range	48 - 52 Hz
BATTERY	
Number of cells in series	60
Nominal operating voltage	120 Vdc
Battery regulator & charging mode	step-down regulator
Battery temperature compensation	battery temperature measurement
Battery voltage indication	LED
OUTPUT DATA	
Output power	5000 VA
Output power derating between 45 - 65 ^{o}C	5 % per ^{o}C
Output voltage	230 V / 50 Hz
Inverter efficiency > 15 % output power	90 - 92 %
Output current shape	sinus
Harmonic distortion of output current	< 3 %
Power factor cos phi (charging state)	1
Isolation solargenerator-grid	transformer
Ambient temperature range	0...45 ^{o}C
Realtive humidity	95 % non condensing
GENERAL	
Status indications with LED	SG o.k., Grid Voltage o.k., Fault, Operation
Dimensions (Width x Height x Length) ca. cm	52 x 58 x 36
Weight (ca.)	60 kg
STANDARDS	
Protection class	1
EMV	EN 50081, Teil 1 / EN 50082, Teil 1
Compliance	CE 73 / 23 / EEC
Case Protection	indoor (opt. outdoor casing)

4. MEASUREMENT SYSTEM

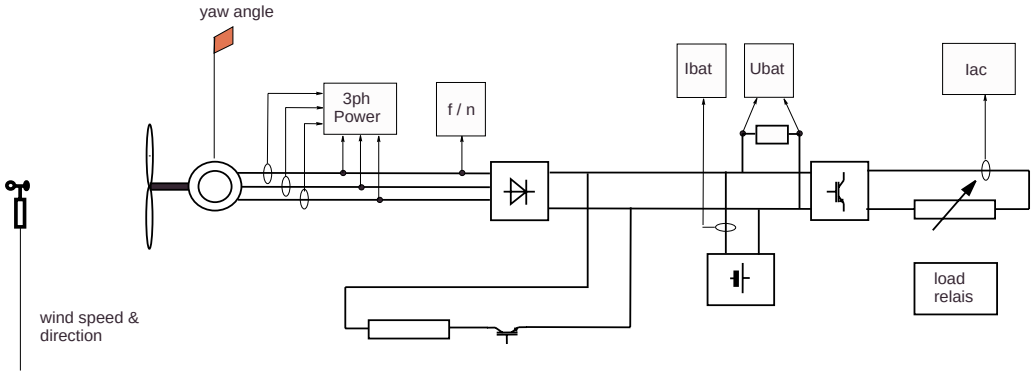

Figure 4.1 *Measurement equipment installed in Fortis Montana system*

The Fortis Montana system was set up at position B of the ECN test site. The meteo mast was located at about 15 m from the turbine at a position of 26 degrees clockwise looking from the meteo mast to the turbine (North is 0 degrees). This meant that measurement data in a sector between 355 and 55 degrees was rejected. A second sector between 130 and 170 degrees was rejected due to the position of the anemometer. The temperature measurement turned out to be defect and the temperature reading was replaced by values measured at a nearby mast. During the second half of the measurement period the clamp measuring the AC current started to produce wrong readings. All AC current clamp readings were rejected, which did not result in a problem because this measurement was a redundant: the same information was available from a recording of the load relay position. Table 4.1 lists the make and type of the measurement equipment used.

Table 4.1 *Measurement equipment, type and accuracy*

Device	Make	Type	Accuracy	Remarks
Wind speed meter	Mierij	018	1.5%	
Wind speed print	Mierij	050	n.a.	
Wind direction meter	Mierij	032	1.4 degree	
Air pressure sensor	Druck	PDCR 901	0.1%	
Air pressure print	Mierij	078	0.1%	
Precipitation detector	Mierij	085	–	
Air temperature meter	Mierij	070	2 degrees	
Electronic filters	Mierij	079		-3 dB at 20 Hz
AC current transformer	Hobut	25/5	3%	
Three phase power meter	BBC	GTU289	0.2%	45-50 Hz
Yaw angle meter	ECN	DEAL0539	0.1 degree	
Electronic filters	ECN	–		-3 dB at 20 Hz
Frequency-current converter	Jaquet	FWT1613AC230	0.2%	
DC current shunt	n.a.	n.a.	0.5%	
Isolated amplifier	Phoenix	2810913	0.1%	
Resistors	n.a.	n.a.	1%	
ADC card	NI	AT-MIO-64E-3	0.1%	
AC Current clamp	HEME	100	1 A	

5. TEST TO DEFINE SYSTEM CHARACTERISTICS

5.1 Power curve measurement

The IEC standard 61400-12 describes power performance testing of grid connected wind turbines and is a suitable starting point for the determination of a method for autonomous systems. Figure 5.1 gives a summary of the method in the IEC standard.

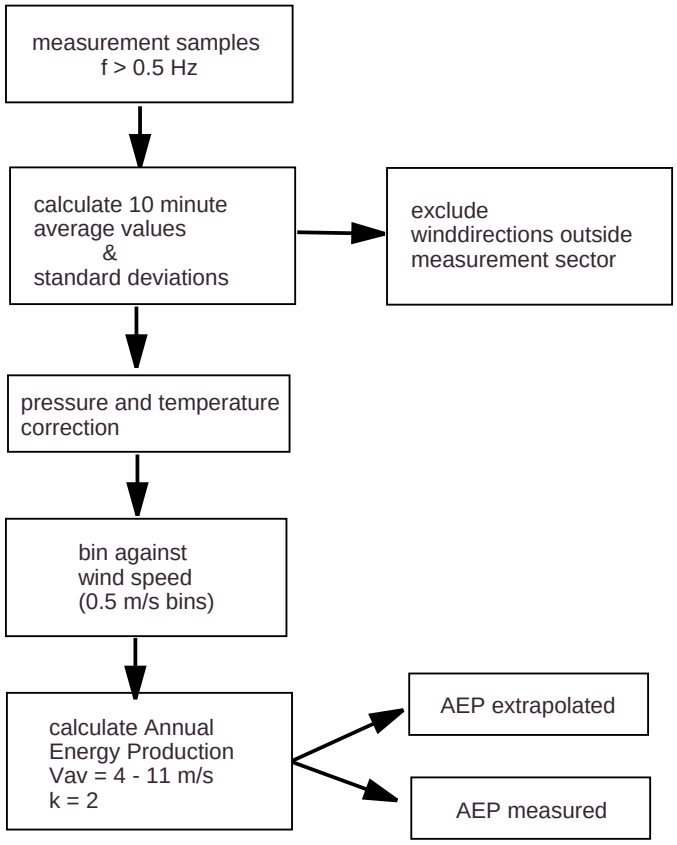

Figure 5.1 *Flow diagram of the power performance testing method in IEC 61400-12*

This project will concentrate on a power performance method for autonomous systems with batteries. First, the effect of the pre-averaging time is investigated. The 10 minutes suggested in the IEC standard 61400-12 is probably too long for the small scale systems found in autonomous applications.

5.2 Effect of the pre-averaging time

There are two basic mechanism causing an imperfect correlation between the measured wind speed and electric power [5]:

- poor correlation between the measured wind and the actual wind experienced by the entire rotor;
- poor correlation due to the inertial lag of the system responding to changes in the ambient wind speed.

Time averaging reduces the effects of poor point-to-point correlation and inertial lag: it works as a low pass filter. High frequency wind fluctuations are filtered out and the inertial lag is masked if the pre-averaging time exceeds the response time constant. The averaging time should be chosen in relation to the system's response time. If it is chosen too short, the amount of scatter will be increased, which may result in misinterpretation of the measurements. If it is taken too long, important information may be filtered out and measurement time is increased.

Hansen and Hausfeld [5] analyse this problem by deriving a the transfer function for an arbitrary turbine. This transfer function is a low pass filter as well. It is split up in its basic components, representing:

- the time needed to travel from anemometer to turbine rotor;
- the averaging effect of the rotor disc compared to a point measurement of the wind;
- the mechanical and electrical inertia of the system.

Since a wind turbine is a highly nonlinear system and the measurement conditions will vary, the overall time constant is expected to vary as well. The analysis shows a variation of a factor 2-4 in calculated overall time constant. Secondly the size of the turbine plays an important role. An increase in rotor diameter will shift the cutoff frequency of the low pass filter to a lower frequency.

Hansen and Hausfeld suggest to choose the averaging time of the measurements equal to the cutoff frequency of the turbine transfer function since this will guarantee the best information transfer in the measurements. This frequency is defined by a decrease of -3 dB (a factor 0.5) in the turbine response. This method will be adopted in the PEMSWECS study. For small stand alone systems this will result is a considerable reduction of the pre-averaging time compared to the IEC 61400-12 recommendation of 10 minutes mentioned in the previous section.

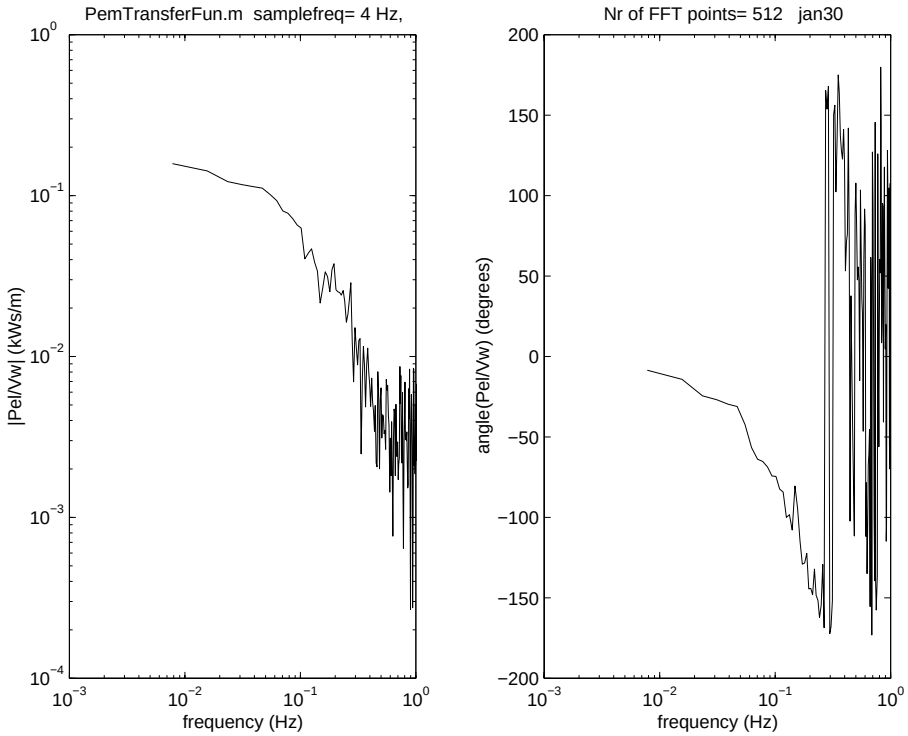

Figure 5.2 *Transfer function* $\mathrm{d}P_{el}/\mathrm{d}V_w$ *estimated from a 8 hour measurement*

Figure 5.2 gives the transfer function from wind speed to electric power for the Fortis Montana system, estimated from an 8 hour measurement with sample frequency of 4 Hz and a length of the measurement sample used in the FFT of 512 data points (128 s). The static gain value $\Delta P_{el}/\Delta V_w$ is about 0.2 kW/(m/s), which corresponds to the value estimated from the P(V) curve. A reduction by a factor 2 of this value is reached at a frequency of 0.05 Hz, suggesting an optimal averaging time of 20 s. Compared to the values found in [5], it corresponds to those given for small turbines and favourable measurement conditions. However, the estimate should be taken as an indication, since it will depend on the operating conditions. To check this result, the power curves of the Fortis turbine will be determined for a number of sampling frequency and the differences will be analysed. For comparison, the transfer function from rotor speed to power dP_{el}/dN is also determined (figure 5.3). In this case the time constant is 33 seconds at a different phase shift: in this case the phase shift is zero and independent of the frequency.

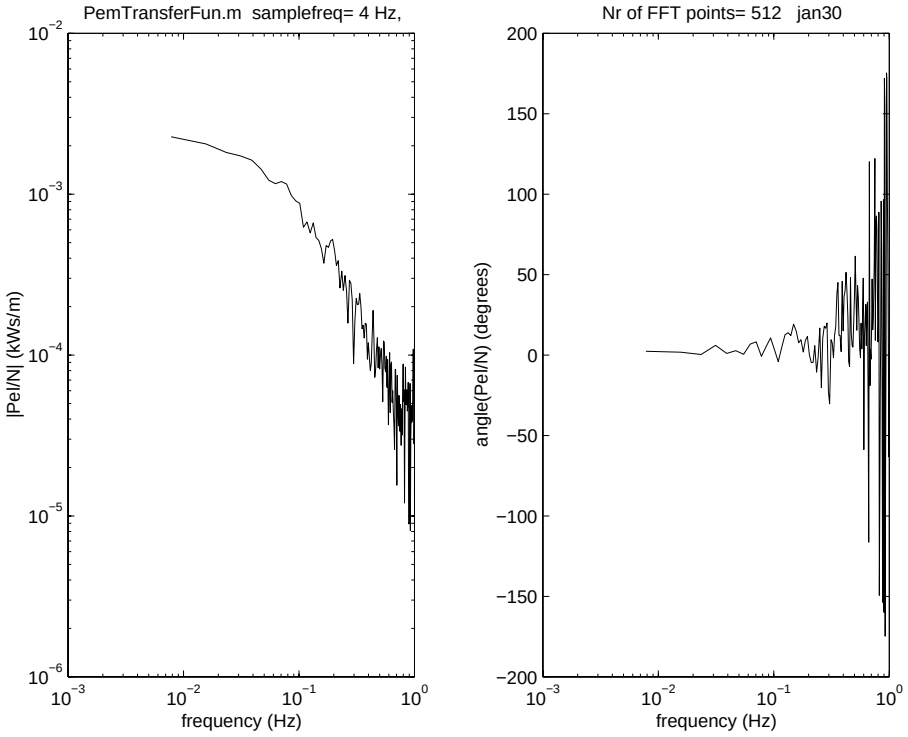

Figure 5.3 *Transfer function* $\mathrm{d}P_{el}/\mathrm{d}N$ *estimated from a 8 hour measurement*

5.3 Measured Fortis Montana Power Curves

To determine the power curves of the Fortis Montana turbine about 100 hours of measurement data were recorded at a sample frequency of 4 Hz. The measurement were taken under variable AC load, simulating real load conditions, and covering the full range of DC voltage: 115 to 143 V. The raw data was processed by means of a number of Matlab routines. First, the raw data was plotted to check for any inconsistencies or irregularities. Secondly, all data was corrected for temperature and pressure, followed by averaging over 10, 30, 60, 120, 300 and 600 seconds. The averaged data was subsequently binned against wind speed and rotor speed to investigate the effect of the averaging time.

Figure 5.4 shows the effect of the temperature and pressure correction. The maximum correction is about 5 %. Figure 5.5 gives the resulting Power-Rotor

speed curves for 10, 30, 60 and 600 seconds. In the low speed region the differences are very small. Speeds above 260 rpm show small deviation which may be caused by the small number of data in the 600 seconds bins or insufficient filtering for the 10 seconds bins. The 30 and 60 seconds results are practically the same over the full range of operation. This is in agreement with the results in the previous section. Figure 5.6 shows the Power - Wind speed curves for 10, 30, 60 and 600 seconds averaging time. Again, the differences are small for all bins below 10 m/s, where all bins have enough data (see table 5.1). This justifies the choice of a pre-averaging time of 30 s.

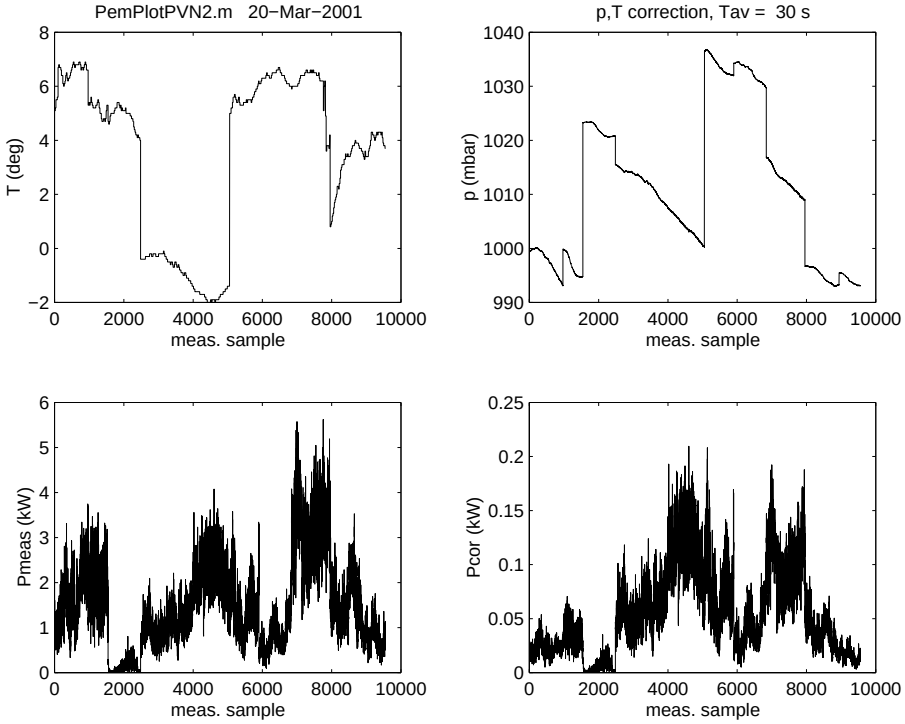

Figure 5.4 *Temperature and pressure correction of measured power*

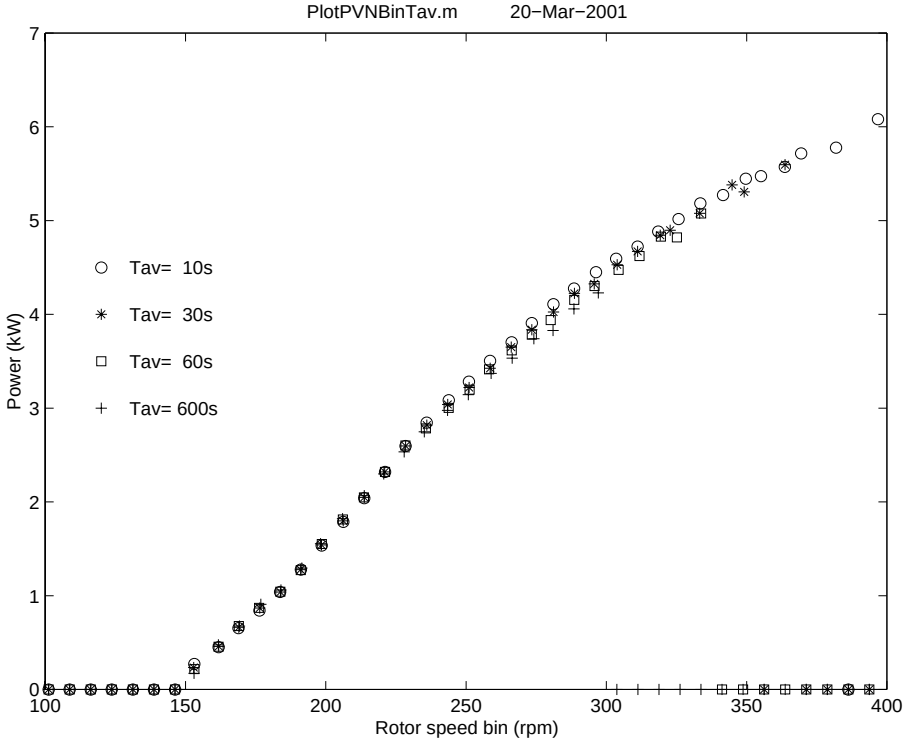

Figure 5.5 *Power-Rotor speed curves for 4 averaging times*

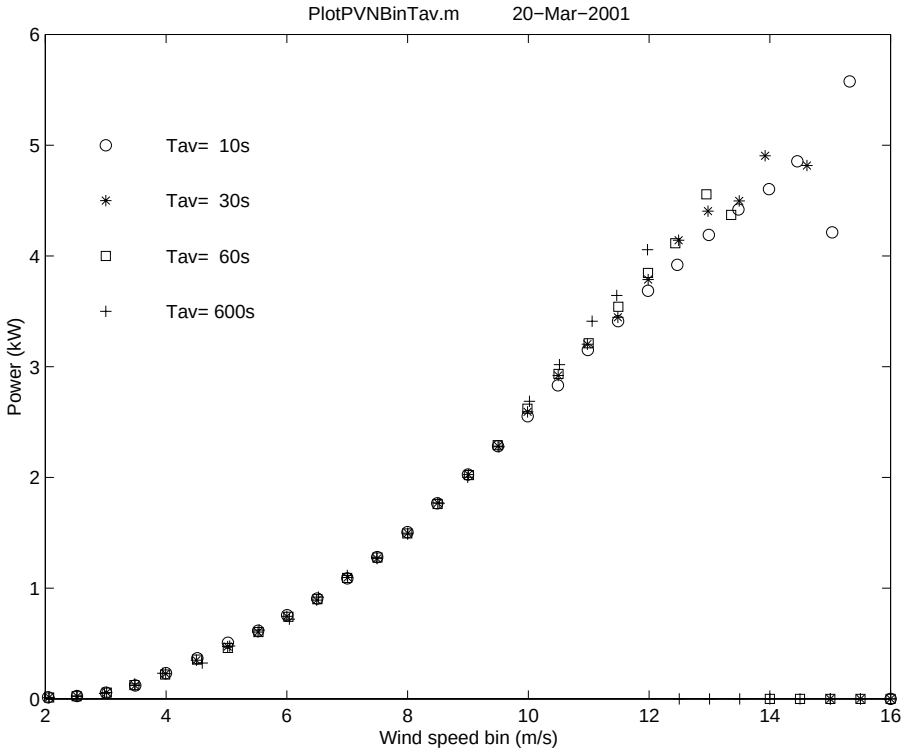

Figure 5.6 *Power-Wind speed curves for 4 averaging times*

Table 5.1 *Measured P(N) and P(V) values for averaging period of 30 s*

N_i (rpm)	P_i (kW)	$\sigma(P_i)$ (kW)	nr_i (-)		V_i (m/s)	P_i (kW)	$\sigma(P_i)$ (kW)	nr_i (-)	s_{Pi} (kW)	u_{Pi} (kW)
146.2	0.0000	0.0000	0		2.063	0.0145	0.0124	62	0.0015	0.0300
152.9	0.2333	0.0985	422		2.527	0.0234	0.0166	170	0.0012	0.0300
161.8	0.4589	0.1399	432		3.014	0.0579	0.0330	230	0.0021	0.0300
168.9	0.6630	0.1428	776		3.485	0.1208	0.0490	196	0.0035	0.0301
176.4	0.8680	0.1800	990		3.992	0.2268	0.0609	191	0.0044	0.0302
183.8	1.0391	0.1901	1071		4.503	0.3494	0.1043	154	0.0084	0.0306
191.0	1.2777	0.1693	1064		5.019	0.4733	0.1253	276	0.0075	0.0311
198.4	1.5408	0.1574	831		5.523	0.6039	0.1526	453	0.0071	0.0317
206.2	1.7983	0.1469	657		6.001	0.7453	0.1763	719	0.0065	0.0326
213.7	2.0486	0.1234	634		6.494	0.8917	0.1845	868	0.0062	0.0337
221.0	2.3194	0.1392	596		7.007	1.0962	0.2008	914	0.0066	0.0354
228.4	2.5960	0.1471	391		7.494	1.2671	0.2115	854	0.0072	0.0371
236.0	2.8191	0.1767	279		8.003	1.4978	0.2379	819	0.0083	0.0396
243.4	3.0390	0.1793	203		8.498	1.7701	0.3019	696	0.0114	0.0428
251.1	3.2205	0.1647	171		9.005	2.0262	0.3393	673	0.0130	0.0460
258.6	3.4260	0.1267	137		9.498	2.2830	0.3599	629	0.0143	0.0495
266.1	3.6506	0.1399	109		9.987	2.5916	0.3998	556	0.0169	0.0538
273.4	3.8359	0.1274	60		10.494	2.9199	0.4563	408	0.0225	0.0586
281.1	4.0256	0.1285	53		10.977	3.2026	0.4673	244	0.0299	0.0629
288.6	4.2238	0.1167	47		11.483	3.4467	0.5037	223	0.0337	0.0666
295.6	4.3256	0.1103	32		11.983	3.7871	0.4877	99	0.0490	0.0719
303.8	4.5284	0.1013	14		12.488	4.1422	0.5299	66	0.0652	0.0775
311.1	4.6708	0.1032	18		12.974	4.4048	0.5707	22	0.1216	0.0817
319.2	4.8440	0.1236	12		13.492	4.4978	0.6053	6	0.2470	0.0832
322.7	4.8965	0.1229	2		13.923	4.9050	0.5945	7	0.2247	0.0898
333.2	5.0778	0.0848	4		14.615	4.8161	0.0000	1	0.0000	0.0883
344.8	5.3814	0.0000	1		15.000	0.0000	0.0000	0	-	0.0300
349.1	5.3056	0.0427	2							
356.2	0.0000	0.0000	0							

The Fortis turbine is equipped with a passive yaw system to maximize the power at low wind by aligning the turbine to the wind direction (yaw angle zero) and to limit the power at high wind by increasing the yaw angle. Figure 5.7 shows that the turbine starts operation with a yaw angle of 30 degrees and that the angle slightly increases for an increase in wind speed. This increase is too small to explain the observed decrease in power coefficient (figure 5.8), which is mainly caused by stalling of part of the rotor.

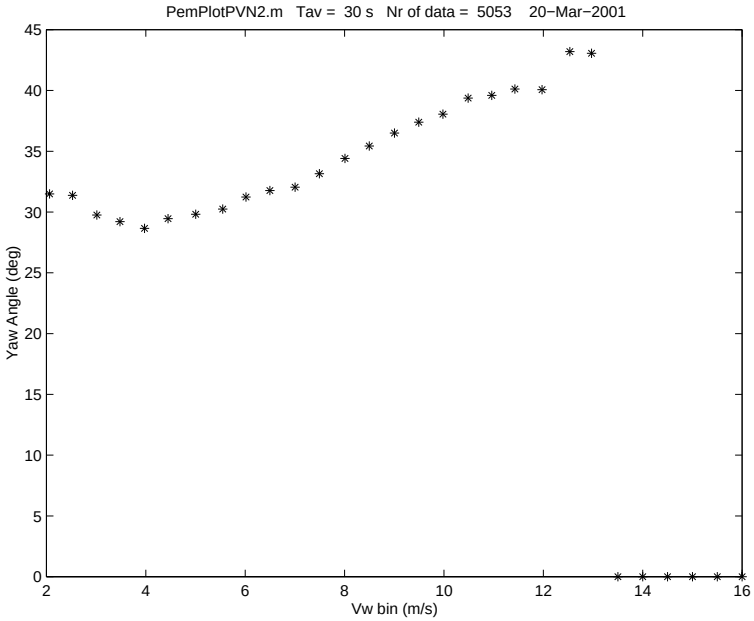

Figure 5.7 *Yaw angle binned against wind speed for 30 seconds averaging time*

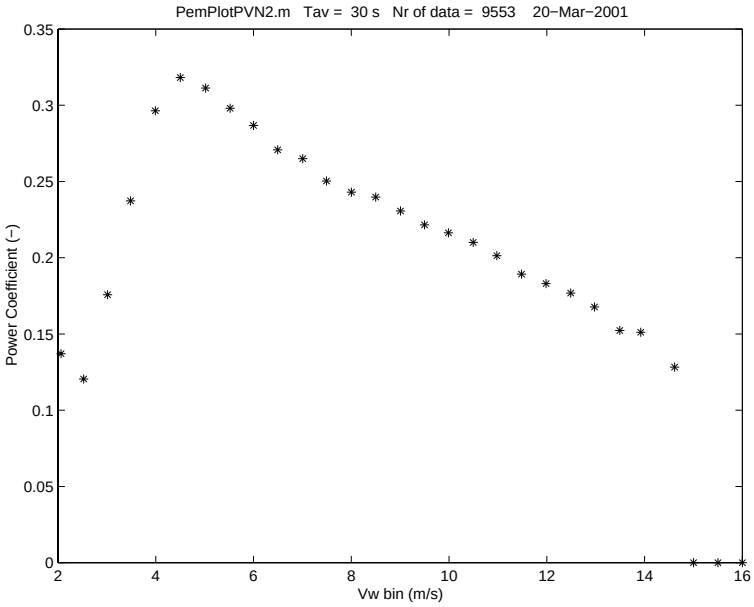

Figure 5.8 *Power coefficient binned against wind speed for 30 seconds averaging time*

Figure 5.9 gives an impression of the area of operation of the DC voltage and the rotor speed. The upper limit of 143 V is caused by the dumpload controller. On average, the voltage follows a path which increases with the rotor speed. At a speed above 250 rpm, the voltage is practically always at its maximum value.

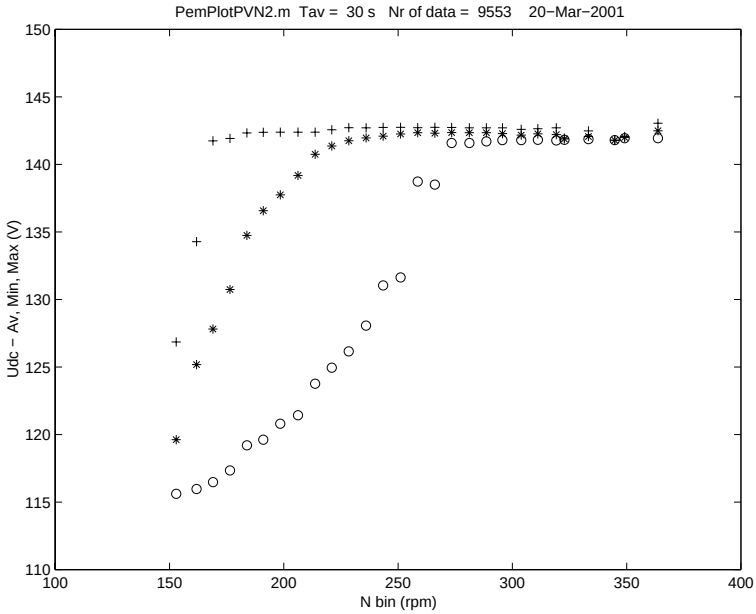

Figure 5.9 *Voltage-rotor speed curve for 30 seconds averaging time: average, minimum and maximum values*

When the DC voltage is binned against the DC current, another interesting aspect of systems with batteries is demonstrated (see figure 5.10). It shows that the DC voltage strongly depends on the DC current. This is caused by the internal resistance of the batteries, as described in more detail in chapter 6. Discharge causes a voltage decrease, while the relation between a charge current and the voltage appears to be less clear. This is caused by the irregular operation of the dumpload controller, which is obscured by the binning of the data.

In figure 5.11 the voltage is plotted against the discharge current to determine the internal resistance of the batteries. Only the inverter is in operation during this measurement, the turbine was stopped. A value $R_{bat} = 0.18\Omega$ is found. Not all samples are on a straight line due to the dynamic behaviour of batteries. After a change in current it takes some time to reach a new steady state. These dynamic effects are not expected to be very relevant for the power performance of the system and are neglected.

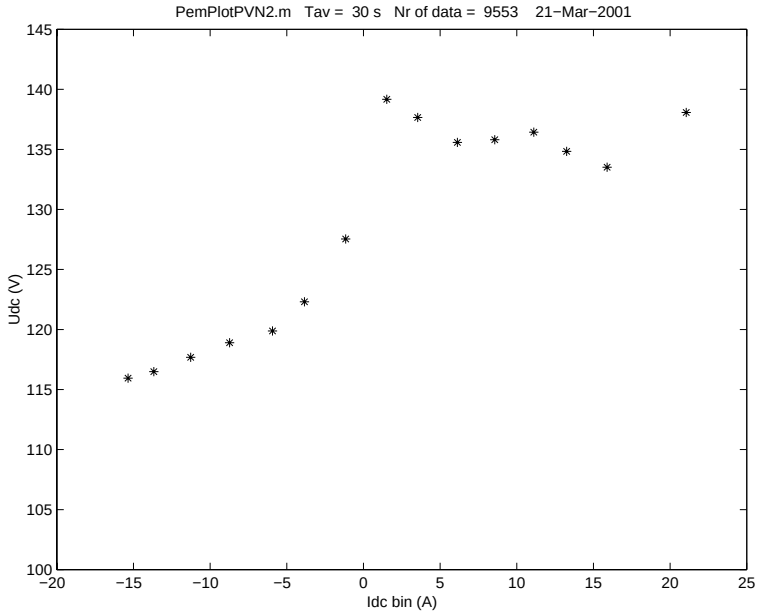

Figure 5.10 *DC voltage binned against DC current*

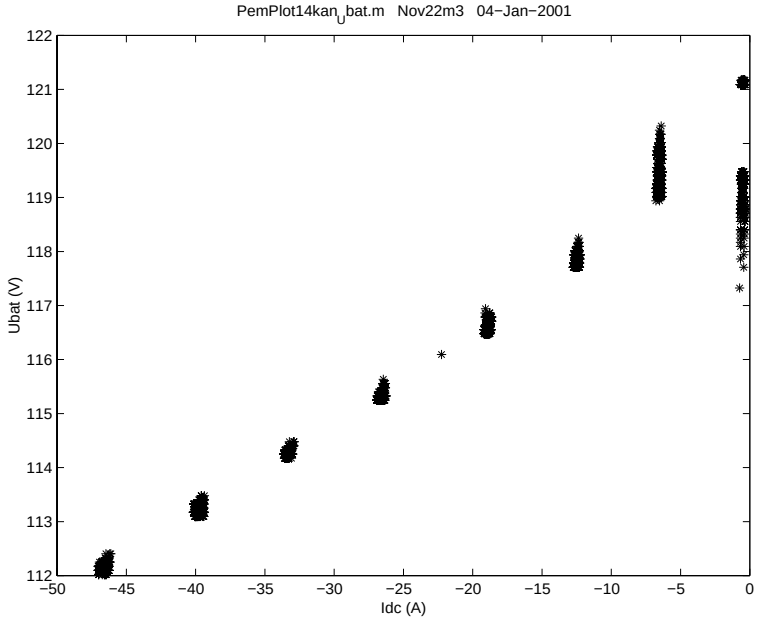

Figure 5.11 *Battery voltage for a fixed number of discharge currents*

6. UNDERSTANDING REAL LOAD BEHAVIOUR: MODELLING

Estimation of the power performance of a stand-alone system requires insight into the operation of the system. To understand the characteristics of the systems tested in PEMSWECS project, component models are useful. The emphasis in these models will be on power performance, i.e. the minute to minute behaviour of the system. Dynamic phenomena with time constants less than 30 seconds are less relevant for the power performance. This was already demonstrated in the development of design tools for wind-diesel systems [15, 3].

The following component models are required:
- turbine rotor;
- permanent magnet generator;
- diode bridge rectifier;
- batteries;
- inverter and AC load;
- dumpload and load controller;

All component models will be quasi-steady state with one exception: the battery model includes the state of charge (SOC) of the batteries. In the electrical models accurate voltage and current phase relations are desired without making the models too complicated.

Outcome of the system model are the steady-state characteristics of the system, viz. the power-rotor speed and power-wind speed curves, for various system conditions. This information is used for a better understanding of the parameters that influence the power performance of the system and it is the input for step 2 of the investigation: modelling of the power performance. Matlab was chosen as programming language, since some of the models already existed in Matlab. The next sections give a description of the component models. This is followed by a number of calculation examples. The power performance model is described in chapter 8.

6.1 Component Models

6.1.1 Rotor

The rotor model has to give the aerodynamic power as a function of wind speed and rotor speed with reasonable accuracy. For the purpose of power performance evaluation the rotor model can be simple: for a pitch or yaw angle controlled turbine $C_p(\lambda, \theta)$ curves, with θ the pitch or yaw angle, are sufficient. If the turbine is stall controlled, a single $C_p(\lambda)$ curve is sufficient.

However, small turbines sometimes have complicated power limitation devices when compared to the previous options. The devices are often passive and depend in some cases on a complicated equilibrium between aerodynamic forces on the rotor and a tail vane or on centrifugal forces. The turbines included in this project limit aerodynamic power by:
- tail vane and eccentric nacelle mounting (ECN system, see figure 3.1);
- flexible connection of blades to hub (a combination of pitching and coning: NEL system);
- stall plus coning/pitching (DEWI system).

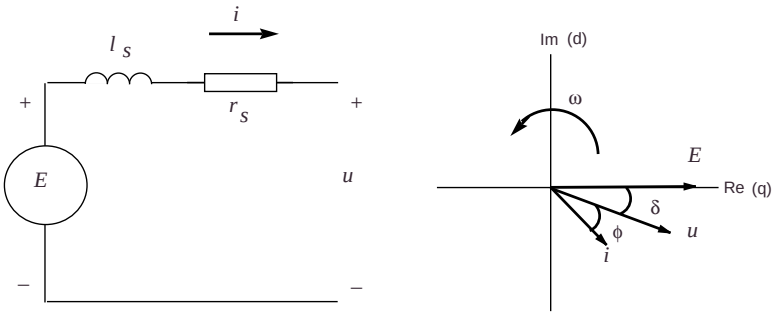

Figure 6.1 *Equivalent circuit of a synchronous or Permanent Magnet generator (EMF is reference)*

Modelling these effects is complicated [14] and is beyond the scope of the project. For the ECN test system, measurements show that the yaw angle does not play an important role, and therefore the model can be simple: a single $C_p(\lambda)$ curve is sufficient.

6.1.2 Permanent Magnet generator with diode bridge

Figure 6.1 shows the equivalent circuit and phasor diagram of a synchronous generator in a reference frame fixed to the EMF E i.e. the rotor field of the machine. Subscripts are used to indicate the components direction (d for direct and q for quadrature axis):

Time variant:			Time invariant:		
$\vec{E}(t)$	=	$\vec{E}\,\mathrm{e}^{j\omega t}$	$\vec{E}$	=	$\hat{E}$
$\vec{u}(t)$	=	$\vec{u}\,\mathrm{e}^{j\omega t}$	$\vec{u}$	=	$\hat{u}\,\mathrm{e}^{-j\delta}$
				=	$u_q + ju_d$
			u_d	=	$-\hat{u}\sin\delta$
			u_q	=	$\hat{u}\cos\delta$
$\vec{i}(t)$	=	$\vec{i}\,\mathrm{e}^{j\omega t}$	$\vec{i}$	=	$\hat{i}\,\mathrm{e}^{-j(\delta+\phi)}$
				=	$i_q + ji_d$
			i_d	=	$-\hat{i}\sin(\delta+\phi)$
			i_q	=	$\hat{i}\cos(\delta+\phi)$

The load angle δ is defined from $\vec{u}$ to $\vec{E}$ and is positive if $\vec{E}$ precedes $\vec{u}$ with respect to the direction of rotation ω. The phase angle ϕ is defined from $\vec{i}$ to $\vec{u}$ and is positive if $\vec{u}$ proceeds $\vec{i}$. The steady state equations for the a synchronous machine, assuming generator convention, are [2]:

$$u_d = -r_s i_d - \omega l_s i_q \tag{6.1}$$

$$u_q = -r_s i_q + \omega l_s i_d + \hat{E} \tag{6.2}$$

$$\hat{E} = \omega l_{afd} I_f \tag{6.3}$$

$$P = \frac{3}{2}(u_d i_d + u_q i_q) \tag{6.4}$$

Equation 6.4 assumes the amplitude invariant parameter set in the Park transformation.

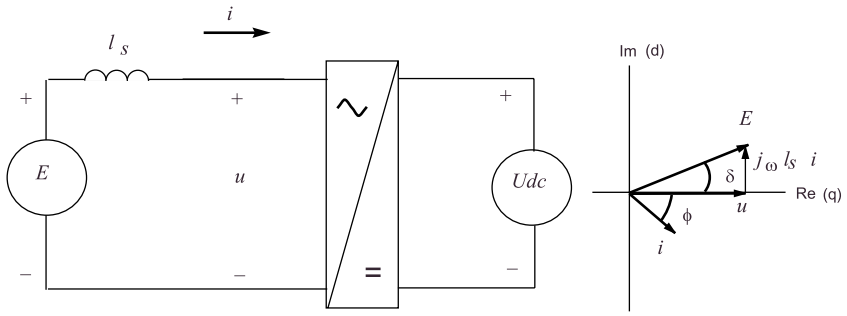

Figure 6.2 *Equivalent circuit of a Permanent Magnet generator with rectifier (stator voltage is reference)*

To simplify the calculation, the stator resistance r_s is neglected. A change of reference frame will result in a set of equations which can be solved without iteration: rotation over load angle δ will make the stator voltage phasor the reference direction. Figure 6.2 shows the new coordinate system. The following table compares the time-invariant parts both sets of equations. A superscript is used to indicate the reference system (e for EMF reference frame and u for stator voltage reference frame):

EMF phasor ref. frame (fig 6.1):

$$
\begin{aligned}
\vec{E^e} &= \hat{E} \\
&= E_q^e \\
E_d^e &= 0 \\
\vec{u^e} &= \hat{u}\, \mathrm{e}^{-j\delta} \\
&= u_q^e + j u_d^e \\
&= \hat{u}(\cos\delta - j\sin\delta) \\
\vec{i^e} &= \hat{i}\, \mathrm{e}^{-j(\delta+\phi)} \\
&= i_q^e + j i_d^e \\
&= \hat{i}(\cos(\delta+\phi) - j\sin(\delta+\phi)) \\
\vec{u^e} &= -j\omega l_s \vec{i^e} + \vec{E^e} \\
u_q^e + j u_d^e &= -j\omega l_s (i_q^e + j i_d^e) + \hat{E} \\
u_d^e &= -\omega l_s i_q^e \\
u_q^e &= \omega l_s i_d^e + \hat{E} \\
\hat{E} &= \omega l_{afd} I_f \\
P^e &= \tfrac{3}{2}(u_d^e i_d^e + u_q^e i_q^e)
\end{aligned}
$$

Stator voltage phasor ref. frame (fig 6.2):

$$
\begin{aligned}
\vec{E^u} &= \hat{E}\, \mathrm{e}^{j\delta} \\
&= E_q^u + j E_d^u \\
&= \hat{E}(\cos\delta + j\sin\delta) \\
\vec{u^u} &= \hat{u} \\
&= u_q^u \\
u_d^u &= 0 \\
\vec{i^u} &= \hat{i}\, \mathrm{e}^{-j\phi} \\
&= i_q^u + j i_d^u \\
&= \hat{i}(\cos\phi - j\sin\phi) \\
\vec{u^u} &= -j\omega l_s \vec{i^u} + \vec{E^u} \\
u_q^u &= -j\omega l_s (i_q^u + j i_d^u) + (E_q^u + j E_d^u) \\
0 &= -\omega l_s i_q^u + E_d^u \\
u_q^u &= \omega l_s i_d^u + E_q^u \\
\hat{E} &= \omega l_{afd} I_f \\
P^u &= \tfrac{3}{2}(u_d^u i_d^u + u_q^u i_q^u)
\end{aligned}
$$

Summarizing:

$$u_d^u = 0 \tag{6.5}$$

$$u_q^u = \hat{u} \tag{6.6}$$

$$0 = -\omega l_s \hat{i}\cos\phi + \hat{E}\sin\delta \tag{6.7}$$

$$\hat{u} = -\omega l_s \hat{i}\sin\phi + \hat{E}\cos\delta \tag{6.8}$$

In most stand-alone systems a permanent magnet generator is used. This implies that the rotor field is constant, so E is linear with the angular speed. In machines with salient poles, the stator inductance l_s will dependent on the direction, i.e. $l_d \neq l_q$. Since the rectifier is a diode bridge, the phase angle ϕ equals zero. This

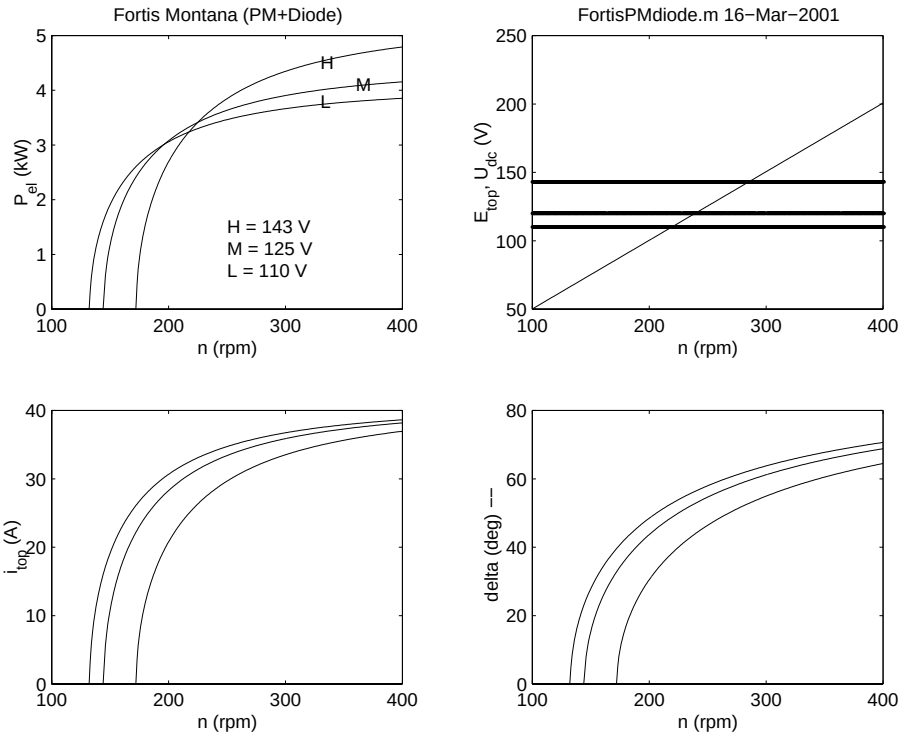

Figure 6.3 *Power-Speed curves of Fortis Montana for 3 DC voltages*

results in the following set of equations for the permanent magnet generator:

$$\hat{E} = \omega\Psi_{afd} \tag{6.9}$$
$$i_d^u = 0 \tag{6.10}$$
$$i_q^u = \hat{i} \tag{6.11}$$
$$0 = -\omega l_q \hat{i} + \hat{E}\sin\delta \tag{6.12}$$
$$\hat{u} = \hat{E}\cos\delta \tag{6.13}$$

This result is combined with the relation for the voltage on both sides of the diode bridge:

$$\hat{u} = \frac{\pi U_{dc}}{3\sqrt{3}} \tag{6.14}$$

Rewriting the equations in the sequence of evaluation:

$$\hat{E} = \omega\Psi_{afd} \tag{6.15}$$
$$\hat{u} = \frac{\pi U_{dc}}{3\sqrt{3}} \tag{6.16}$$
$$\cos\delta = \frac{\hat{u}}{\hat{E}} \tag{6.17}$$
$$\hat{i} = \frac{\hat{E}\sin\delta}{\omega l_q} \tag{6.18}$$
$$P = \frac{3}{2}\hat{u}\hat{i} \tag{6.19}$$

Figure 6.3 shows the results for the Fortis Montana turbine for three values of the DC voltage: 110, 125 and 143 V. The value of 110 V is the lower limit

of the battery voltage at maximum discharge current. When the batteries are full, the dumpload controller keeps the DC voltage at 143 V. The current of the generator is limited by the voltage drop across the stator inductance and depends on the DC voltage. The figure shows that the maximum AC current is about 40 A. At 140 DC this limits the power to about 5 kW. Whether this power will actually be produced, depends on the aerodynamic characteristics of the turbine: the eccentrically mounted rotor should reduce the aerodynamic power to the rated power of 4 kW.

6.1.3 Batteries

The objective of the battery model is twofold:

- to estimate the state of charge SOC, electrical capacity and losses as a function of the charge and discharge current. This is required to calculate power flows in a system;
- to estimate the charge and discharge voltage as function of the SOC. This is required to calculate the effect of the battery voltage on the overall aerodynamic efficiency of the wind turbine.

The SOC is the amount of chemical energy stored in a battery. It is assumed that the maximum amount of chemical energy that can be stored in a battery is constant, which is equivalent to assuming a constant amount of chemical reactants and products. This may change if the battery ages, but is not considered in this simple approach.

When the battery is discharged, not all chemical energy is converted into electrical energy. Part of it is converted into heat in an irreversible chemical reaction. These losses strongly depend on the rate of discharge, i.e. the current. This is the reason for a strong dependency of the battery's electrical capacity (Amp-hours) on the rate of discharge or the total discharge time. Discharge at a high current will yield considerably less electric energy output than at a low current. The chemical energy stored in the battery is in both cases the same. This is visualized in a very simple model. In this model is assumed that losses are predominantly of an electrical nature, i.e. can be described by Ohms Law. Values of the battery electrical capacity (Amp-hours) as function of the discharge current are used to calculate an equivalent resistance R_{eq} which accounts for the losses, assuming a constant E_{chem}:

$$E_{chem} = E_{el} + E_{loss} \tag{6.20}$$

$$E_{el} = VI \tag{6.21}$$

$$E_{loss} = R_{eq} I^2 \tag{6.22}$$

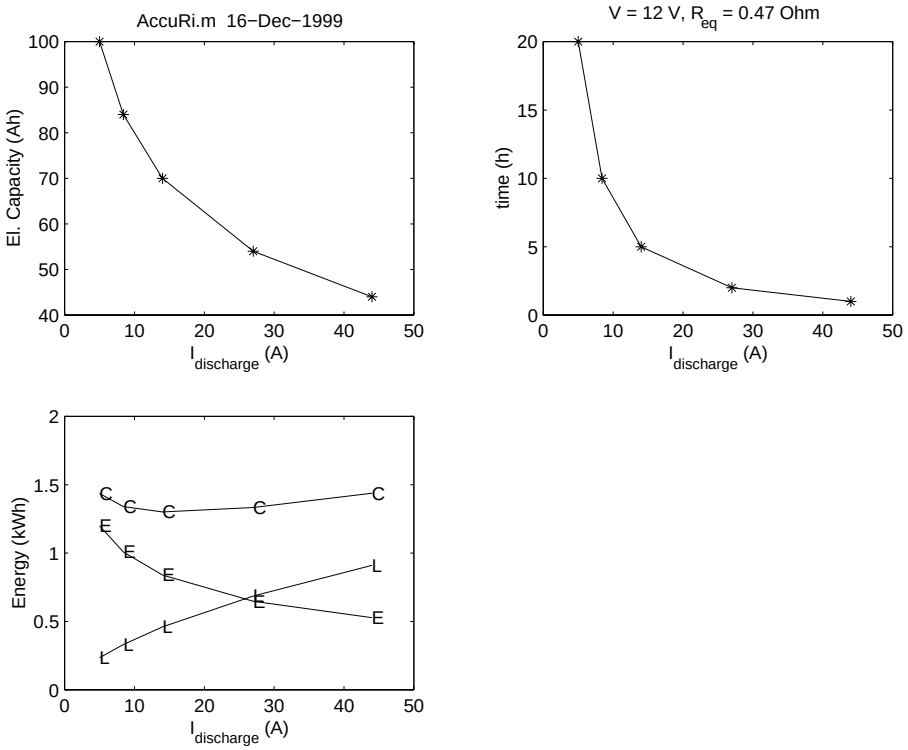

Figure 6.4 *Chemical Energy (C), Losses (L) and Electric Energy (E) as function of the discharge current*

Figure 6.4 gives an example based on Amp-hour ratings (from *Storage Batteries for Photovoltaic Power Systems*). A value of R_{eq} of 0.47 Ω gives a good result: the calculated chemical energy is almost constant. The chemical energy is the quantity associated with the state of charge (SOC).

For the batteries in the test system, the resistance can also be determined directly from measurements. Figure 5.11 give a value $R_{bat} = 0.18\Omega$.

From figure 6.4 can be concluded that, although the losses are proportional to the square of the discharge current, the total energy loss is almost proportional to the discharge current, due to the reduction in discharge time. The figure also shows that at high discharge currents the losses exceed the electrical output of the battery, which is an indication that battery losses are an important factor in a stand alone system and have to be included in a model that calculates system performance for a specific end user.

This simple model is used to estimate the losses for charging as well as discharging. Secondly, it can estimate the effect of the charge and discharge current on the battery voltage. This relation will be required if the battery voltage is an important factor in the estimation of the power performance of stand alone systems.

A model for the charge and discharge voltage found in [12] is used. It should be emphasized that the model is only indicative. The equations are derived empirically from manufacturer's data. Care should be taken in applications with batteries operating under transient conditions (as is the case in stand-alone systems).

$$V^0_{cell} = 2.094[1.0 - 0.001(T - 25)] \quad (6.23)$$

$$R_i = 0.150[1.0 - 0.020(T - 25)] * \frac{1}{6} \quad (6.24)$$

$$R_p^{disch} = \frac{0.189}{SOC} * \frac{1}{6} \quad (6.25)$$

$$V_{disch} = n_{cell}[V_{cell}^0 - \frac{I}{AH}(R_p^{disch} + R_i)] \quad (6.26)$$

$$R_p^{charge} = \frac{0.189}{1.142 - SOC} * \frac{1}{6} \quad (6.27)$$

$$V_{charge}^* = V_{cell}^0 + \frac{I}{AH}(R_p^{charge} + R_i) \quad (6.28)$$

$$dV_{gassing} = (SOC - 0.9)\ln(300\frac{I}{AH} + 1.0) * \frac{1}{6} \quad (6.29)$$

$$\text{if } V_{charge}^* > 2.29$$

$$dV_{gassing} = 0 \quad (6.30)$$

$$\text{if } V_{charge}^* < 2.29$$

$$V_{charge} = n_{cell}[V_{charge}^* + dV_{gassing}] \quad (6.31)$$

The charge and discharge voltage equations contain two terms responsible for the voltage change: one labelled polarisation resistance R_p and one internal R_i. However, they do not appear as an ordinary resistance since they are multiplied by the current divided by the Amp-hour rating. Since the Amp-hour rating is dependent on the (dis)charge current, the actual resistance therefore also depends on the (dis)charge current. In the charge equation an additional term appears for voltages above 2.29 V, labelled the gassing voltage $dV_{gassing}$. The equations for R_i, R_p and $dV_{gassing}$ in [12] suggest validity for a single cell. This gives unrealistic voltage values when applied to the battery conditions of figure 6.4: double or zero battery voltages. Assuming that the equations were intended for a 12 V battery, which explains the factors $\frac{1}{6}$, gives realistic results.

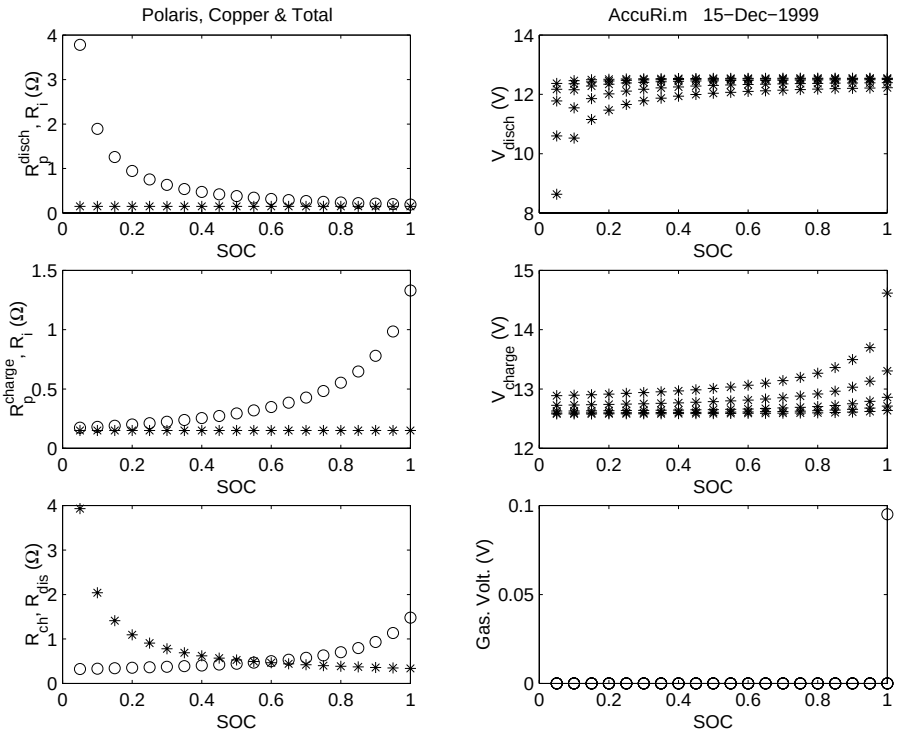

Figure 6.5 *Resistances, discharge and charge voltages for the battery and discharge currents of the previous figure (5, 8.5, 14, 27 & 44 A)*

Figure 6.5 gives the model results for the same discharge currents as used in figure 6.4. Compared to the equivalent resistance $R_{eq} = 0.47\Omega$, that was estimated on the basis of the assumption of constant chemical energy, the model calculates a value of $R_{ch} = R_{dis} = R_i + R_p = 0.5$ for a SOC of about 50%. This indicates the applicability of the model for the (quasi-steady state) estimation of the SOC and losses as well.

6.2 System model

6.2.1 Matching of turbine rotor and generator

For optimal aerodynamic operation of a turbine the rotor and generator have to be matched. This means that a more or less optimal curve of operation is chosen, where the aerodynamic power produced by the rotor balances the electrical power produced by the generator. A difference between aerodynamic and electric power will result in a change of speed and consequently in a different aerodynamic and electric power. It is the task of the turbine manufacturer to establish a good match between the aerodynamic and the electric power characteristics.

For a system with permanent magnet generator, diode bridge rectifier and batteries, the matching depends on the gearbox ratio or number of pole pairs, the field strength of the permanent magnets and the voltage of the batteries and the setpoint of the charge controller.

A Matlab program was made to match a turbine rotor and a permanent magnet generator. The program calculates the equilibrium conditions $P_{aero} = P_{el}$ for given rotor characteristics and electric power curve as function of the wind speed. The result is a power-wind speed curve for the system.

Figure 6.6 gives an example of the matching for 2 battery voltages. The battery voltage for upper part of the figure is $\frac{3}{4}$ of the voltage for the lower part. This shifts the generator curve (the dotted line) to the right: the turbine starts delivering power at a higher speed and the maximum electrical power is higher. The power-wind speed curve is also shifted. Figure 6.7 shows this in more detail. At lower wind speed the turbine with lower voltage produces more power, at higher wind speeds this is reversed. The fact that the change in voltage does not have a clear unidirectional effect on the power, indicates a less severe effect on the overall power performance. This will be verified by a statistical calculation.

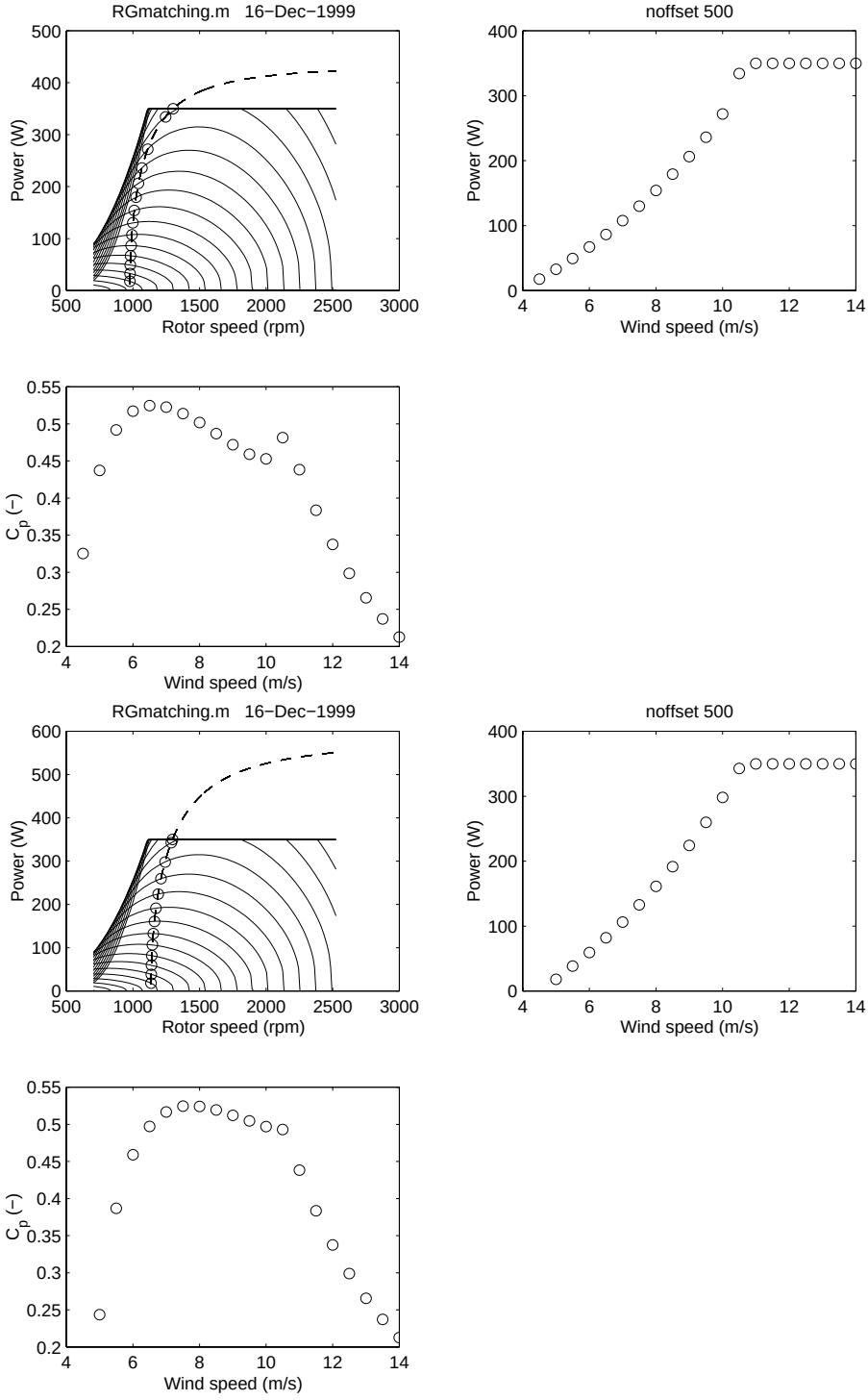

Figure 6.6 *Example of matching of rotor and generator for 2 battery voltages* $U_{dc,low}/U_{dc,high} = 3/4$

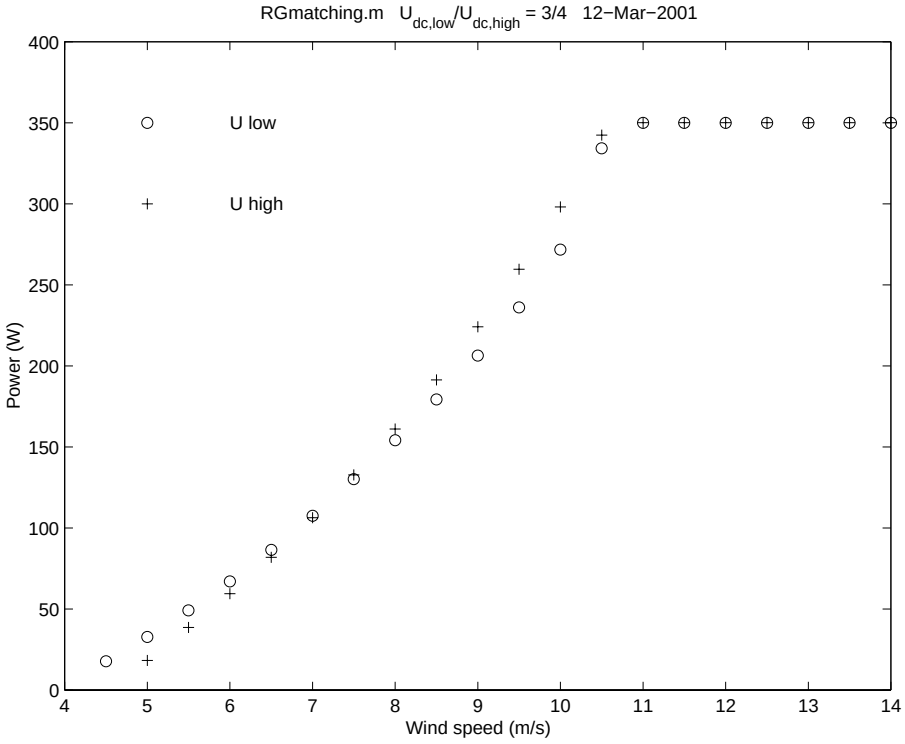

Figure 6.7 *P(v) curves for 2 battery voltages*

7. UNDERSTANDING REAL LOAD BEHAVIOUR: MEASUREMENTS

In this chapter the influence of a changing DC voltage on the power performance of autonomous systems with batteries will be analysed. The DC voltage depends on the state of charge of the batteries and even more strongly on the direction of the current, as demonstrated in chapter 5.

To evaluate the potential effect of the DC voltage, measurement series with a sample frequency of 4 Hz are used. The AC load in the measurements was variable and the power balance $P_{bat} = P_{gen} - P_{load} - P_{dump} - P_{losses}$ determined the direction and magnitude of the battery current. The measurement conditions are identical to a system under real load conditions: randomly changing AC load and randomly changing wind power. The range of operation of the DC voltage depends on the maximum discharge current (in the Fortis system 47 A, equivalent to 5.2 kW) and the set point of the dumpload controller. This results in a lower limit of about 112 V, the dumpload limits the DC voltage to 143 V.

The same measurement data (about 100 hours) as in chapter 5 is used. The measurements are corrected for temperature and pressure and averaged over 30 seconds. Next, the resulting data are binned against the DC voltage. Three bins were chosen: below 125 V, between 125 and 135 V and above 135 V. Finally, the data per voltage bin is binned a second time, now against the wind speed or the rotor speed. Different DC voltages will result in different P(V), P(N) and N(V) curves. The following figures and tables show the results.

In figure 7.1 the P(N) curves show a clear effect of the DC voltage. At a lower DC voltage, the turbine starts delivering power at a lower speed and the power is higher at low rotor speeds. This corresponds to the prediction in chapter 6. It was also predicted that the effect would reverse at high rotor speeds. Since the combination of high rotor speed and low DC voltage does not occur, this effect is not present in the measurements and can not be verified from the measurements. Since it does not occur under real load conditions, it is not relevant for the power performance, and will not be pursued any further. Table 7.1 lists the plotted data together with the number of data points per bin. Some of the high rotor speed bins have an unsufficient number of data to draw conclusions. In the middle and low speed bins the numbers are sufficient to be representative. In this range the difference in power between the low and high voltage condition is about 0.5 kW, which is substantial.

Figure 7.2 plots the power-wind speed curves from the same data. The wind speed bins have a width of 0.5 m/s, are centered on whole and half values but the result per bin will give the average wind speed per bin and not the bin center. This is particularly relevant for bins with a limited number of data.

The following observations are made:

- Below 5 m/s there is unsufficient data in the high voltage bin, which is logical since a high voltage is not likely to occur in combination with low wind speed. Any differences in the low region can be attributed to insufficient number of data.
- In the range from 5 to 8 m/s the amount of data is sufficient for all three voltage levels. In this range the differences in power for the 3 voltages are small.
- The range from 8 to 9.5 m/s also has sufficient data for all three voltage levels

and shows a slight increase of power with voltage: about 0.2 kW.

- Above 9.5 m/s the number of data in the low voltage bin is unsufficient and this goes for the medium voltage bin too above 10.5 m/s. Above this wind speed level it is not likely that the voltage will be in the two lower bins for a significant amount of time.

The general impression is that the effect of the DC voltage on the power curve **under real load conditions** therefore is relatively small. An argument to strengthen this conclusion could be the effect of the wind speed distribution on the actual energy production over a long period, which may further reduce the effect of any differences in P(V) curve at the low and high wind speed end. In the end it is this estimate that counts. This effect will be analysed in the next chapter.

It may come as a surprise that substantial differences in the power-rotor speed curve do not lead to significant differences in the power-wind speed curve. This can be explained by the strongly nonlinear behaviour of the rotor (see for instance figure 6.6). For the turbine under investigation, the $C_p(\lambda)$ curve is not particularly flat (see figure 5.8) and the effect of voltage on power performance is small. This may justify the conclusion that in many cases the effect of the DC voltage on the P(V) curve will not be very significant. This is an important argument for the recommendation of a simple method to determine the power performance of autonomous systems with batteries.

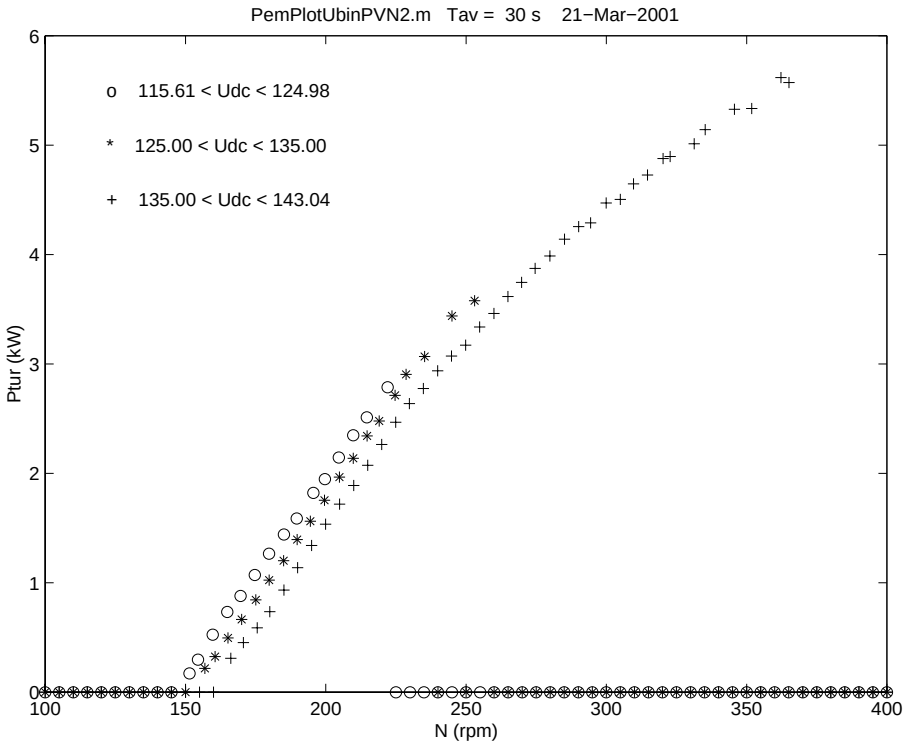

Figure 7.1 *Power-rotor speed curves for 3 DC voltage intervals*

Table 7.1 *Power-rotor speed data for 3 DC voltage intervals*

U<125			125<U<135			U>135		
N (rpm)	Pel (kW)	Nr. of data	N (rpm)	Pel (kW)	Nr. of data	N (rpm)	Pel (kW)	Nr. of data
145.000	0.0000	0	145.000	0.0000	0	145.000	0.0000	0
151.441	0.1714	214	150.000	0.0000	0	150.000	0.0000	0
154.468	0.2982	205	156.917	0.2175	3	155.000	0.0000	0
159.737	0.5238	104	160.542	0.3251	126	160.000	0.0000	0
164.951	0.7342	88	165.127	0.4960	321	166.186	0.3101	2
169.618	0.8788	106	170.004	0.6654	428	170.620	0.4527	33
174.700	1.0716	87	175.045	0.8431	435	175.562	0.5883	90
179.787	1.2662	68	179.827	1.0236	385	180.071	0.7353	257
185.081	1.4420	30	184.970	1.2011	319	185.071	0.9327	390
189.678	1.5869	32	189.800	1.3955	243	189.976	1.1378	466
195.560	1.8205	19	194.536	1.5630	143	194.982	1.3408	470
199.692	1.9459	18	199.528	1.7547	102	199.922	1.5362	402
204.663	2.1451	14	204.867	1.9656	46	204.921	1.7192	368
209.829	2.3487	6	209.792	2.1379	41	209.978	1.8899	396
214.599	2.5109	6	214.744	2.3429	13	214.978	2.0736	401
222.071	2.7870	1	219.039	2.4792	10	219.961	2.2640	416
225.000	0.0000	0	224.702	2.7136	17	224.914	2.4679	301
230.000	0.0000	0	228.648	2.9043	3	229.824	2.6374	239
235.000	0.0000	0	235.217	3.0675	3	234.796	2.7751	187
240.000	0.0000	0	240.000	0.0000	0	239.895	2.9379	168
245.000	0.0000	0	244.976	3.4388	2	244.842	3.0726	122
250.000	0.0000	0	250.000	0.0000	0	249.867	3.1717	114
255.000	0.0000	0	253.034	3.5784	1	254.861	3.3377	106
260.000	0.0000	0	260.000	0.0000	0	259.971	3.4614	87
265.000	0.0000	0	265.000	0.0000	0	264.947	3.6163	76
270.000	0.0000	0	270.000	0.0000	0	269.826	3.7461	55
275.000	0.0000	0	275.000	0.0000	0	274.625	3.8736	38
280.000	0.0000	0	280.000	0.0000	0	279.876	3.9869	36
285.000	0.0000	0	285.000	0.0000	0	285.082	4.1411	35
290.000	0.0000	0	290.000	0.0000	0	290.159	4.2556	29
295.000	0.0000	0	295.000	0.0000	0	294.417	4.2903	23
300.000	0.0000	0	300.000	0.0000	0	299.933	4.4718	14
305.000	0.0000	0	305.000	0.0000	0	305.014	4.5039	9
310.000	0.0000	0	310.000	0.0000	0	309.714	4.6468	12
315.000	0.0000	0	315.000	0.0000	0	314.671	4.7272	9
320.000	0.0000	0	320.000	0.0000	0	320.243	4.8775	9
325.000	0.0000	0	325.000	0.0000	0	322.743	4.8965	2
330.000	0.0000	0	330.000	0.0000	0	331.294	5.0130	2
335.000	0.0000	0	335.000	0.0000	0	335.217	5.1426	2
340.000	0.0000	0	340.000	0.0000	0	340.000	0.0000	0
345.000	0.0000	0	345.000	0.0000	0	345.634	5.3284	2
350.000	0.0000	0	350.000	0.0000	0	351.838	5.3358	1
355.000	0.0000	0	355.000	0.0000	0	355.000	0.0000	0
360.000	0.0000	0	360.000	0.0000	0	362.217	5.6185	1
365.000	0.0000	0	365.000	0.0000	0	365.124	5.5730	1
370.000	0.0000	0	370.000	0.0000	0	370.000	0.0000	0

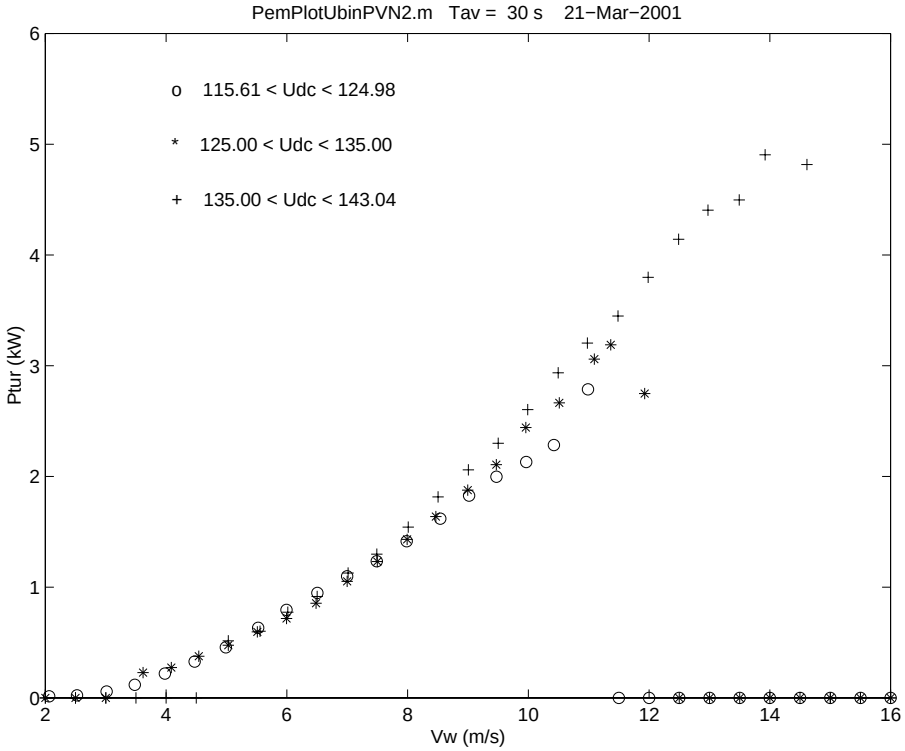

Figure 7.2 *Power-wind speed curves for 3 DC voltage intervals*

Table 7.2 *Power-wind speed data for 3 DC voltage intervals*

U<125			125<U<135			U>135		
Vw (m/s)	Pel (kW)	Nr. of data	Vw (m/s)	Pel (kW)	Nr. of data	Vw (m/s)	Pel (kW)	Nr. of data
2.063	0.0145	62	2.000	0.0000	0	2.000	0.0000	0
2.527	0.0234	170	2.500	0.0000	0	2.500	0.0000	0
3.014	0.0579	230	3.000	0.0000	0	3.000	0.0000	0
3.482	0.1180	191	3.617	0.2285	5	3.500	0.0000	0
3.978	0.2197	166	4.085	0.2740	25	4.000	0.0000	0
4.473	0.3283	87	4.542	0.3768	67	4.500	0.0000	0
4.989	0.4572	76	5.030	0.4763	184	5.030	0.5154	16
5.523	0.6332	79	5.512	0.5963	281	5.557	0.6020	93
5.995	0.7956	92	5.994	0.7176	399	6.015	0.7735	228
6.506	0.9471	104	6.483	0.8554	402	6.502	0.9160	362
6.998	1.0982	90	6.999	1.0520	344	7.014	1.1275	480
7.490	1.2344	56	7.499	1.2314	348	7.491	1.2987	450
7.983	1.4147	41	7.991	1.4322	283	8.011	1.5423	495
8.542	1.6200	24	8.469	1.6376	149	8.505	1.8147	523
9.021	1.8269	24	8.995	1.8769	92	9.007	2.0594	557
9.472	1.9974	18	9.468	2.1071	26	9.500	2.2996	585
9.962	2.1303	8	9.958	2.4422	19	9.989	2.6040	529
10.423	2.2835	5	10.514	2.6653	13	10.494	2.9365	390
10.988	2.7870	1	11.092	3.0597	1	10.977	3.2049	242
11.500	0.0000	0	11.365	3.1884	2	11.484	3.4490	221
12.000	0.0000	0	11.928	2.7492	1	11.984	3.7977	98
12.500	0.0000	0	12.500	0.0000	0	12.488	4.1422	66
13.000	0.0000	0	13.000	0.0000	0	12.974	4.4048	22
13.500	0.0000	0	13.500	0.0000	0	13.492	4.4978	6
14.000	0.0000	0	14.000	0.0000	0	13.923	4.9050	7
14.500	0.0000	0	14.500	0.0000	0	14.615	4.8161	1
15.000	0.0000	0	15.000	0.0000	0	15.000	0.0000	0

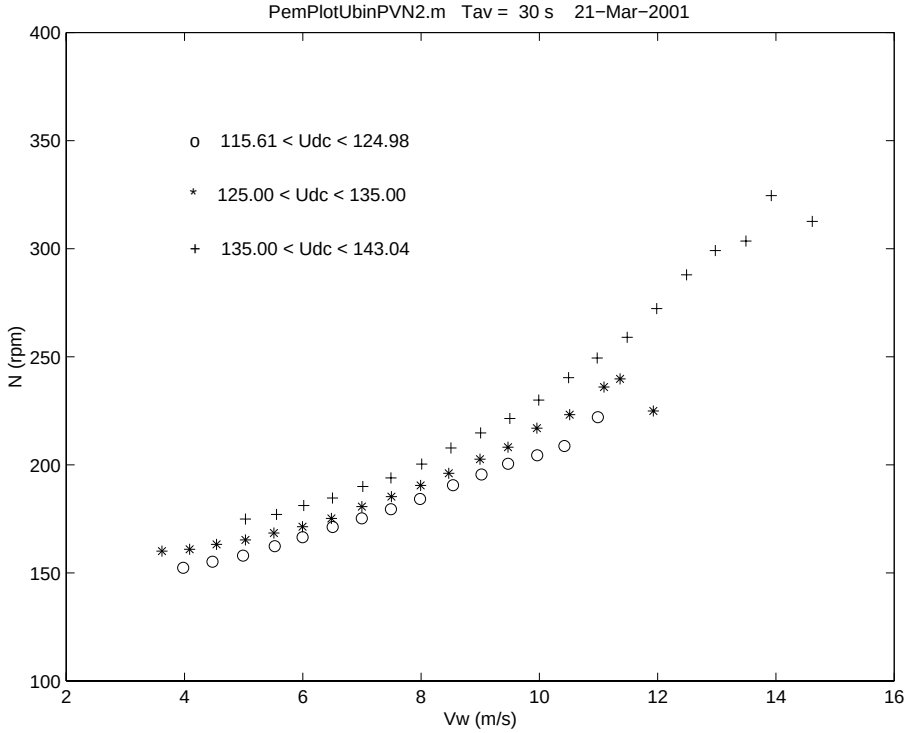

Figure 7.3 *Rotor speed- wind speed curves for 3 DC voltage intervals*

Figure 7.3 illustrates the effect of the voltage on the rotor speed at a given wind speed. A low voltage will reduce the rotor speed and vice versa. The speed differences are in the range of 20 to 40 rpm. These rotor speed differences are the cause of the different power-wind speed curves.

Table 7.3 *Rotor speed-wind speed data for 3 DC voltage intervals*

U<125			125<U<135			U>135		
Vw (m/s)	N (rpm)	Nr. of data	Vw (m/s)	N (rpm)	Nr. of data	Vw (m/s)	N (rpm)	Nr. of data
2.063	0.0000	62	2.000	0.0000	0	2.000	0.0000	0
2.527	0.8977	170	2.500	0.0000	0	2.500	0.0000	0
3.014	15.1512	230	3.000	0.0000	0	3.000	0.0000	0
3.482	81.8433	191	3.617	160.0880	5	3.500	0.0000	0
3.978	152.3744	166	4.085	160.9109	25	4.000	0.0000	0
4.473	155.2082	87	4.542	163.1824	67	4.500	0.0000	0
4.989	158.0215	76	5.030	165.2675	184	5.030	174.9314	16
5.523	162.3287	79	5.512	168.4591	281	5.557	177.0271	93
5.995	166.4832	92	5.994	171.3944	399	6.015	181.1593	228
6.506	171.2261	104	6.483	175.2315	402	6.502	184.6498	362
6.998	175.2273	90	6.999	180.6584	344	7.014	189.9872	480
7.490	179.4597	56	7.499	185.2875	348	7.491	193.9839	450
7.983	184.2052	41	7.991	190.4876	283	8.011	200.3638	495
8.542	190.5511	24	8.469	196.0869	149	8.505	207.8357	523
9.021	195.5413	24	8.995	202.6343	92	9.007	214.7671	557
9.472	200.4662	18	9.468	208.1789	26	9.500	221.4784	585
9.962	204.4238	8	9.958	216.9836	19	9.989	229.9903	529
10.423	208.7118	5	10.514	223.2160	13	10.494	240.3291	390
10.988	222.0712	1	11.092	236.0225	1	10.977	249.4200	242
11.500	0.0000	0	11.365	239.7378	2	11.484	259.0112	221
12.000	0.0000	0	11.928	224.9562	1	11.984	272.2762	98
12.500	0.0000	0	12.500	0.0000	0	12.488	287.8991	66
13.000	0.0000	0	13.000	0.0000	0	12.974	299.1475	22
13.500	0.0000	0	13.500	0.0000	0	13.492	303.5512	6
14.000	0.0000	0	14.000	0.0000	0	13.923	324.5755	7
14.500	0.0000	0	14.500	0.0000	0	14.615	312.6454	1
15.000	0.0000	0	15.000	0.0000	0	15.000	0.0000	0

Figure 7.4 gives the electrical losses in the medium voltage bin (125-135 V), binned against the electric power. The reason for choosing this voltage bin is that the dumpload is not in operation and the number of data in this bin is sufficient. The losses are caused by the rectifier. The losses in the generator windings, the cables and the batteries are not included in figure 7.4. These losses can be estimated from the stator and cable resistance and the battery internal resistance. The converter losses are small: about 2% of the rated power.

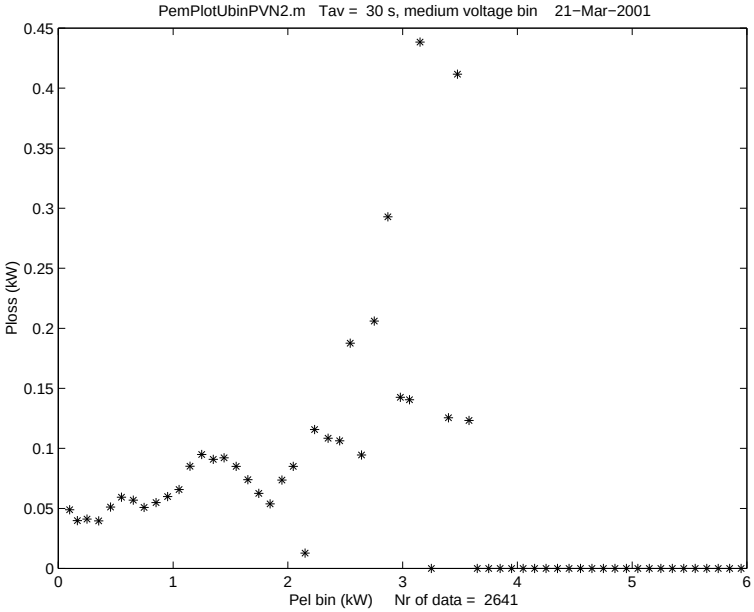

Figure 7.4 *Electrical losses in medium voltage bin (generator winding, cable and battery losses excluded)*

8. PREDICTION OF REAL LOAD PERFORMANCE

Models are used to estimate the average annual energy production of autonomous wind energy converter systems under various wind conditions. A distinction has to be made between the actually produced wind power and the power that can actually be used by a consumer. For grid connected systems the grid acts as an infinite buffer and all energy produced by the turbine is used by the consumers. This is generally not the case in autonomous systems: if the wind power exceeds the demand and the batteries are full, the power is dumped. This effect is influenced by the system lay-out (mainly the battery size) and the consumer demand pattern. For a standard power performance evaluation however, this effect is not taken into account.

Models to determine the power performance can either be statistical or time domain models. For power performance evaluation of grid connected systems only statistical models are used. To determine the amount of dumped power in an autonomous system with batteries, a time domain model is preferred, due to the difficulty to include the battery SOC in a statistical model [6, 3]. This type of model is sometimes referred to as logistic model, it estimates the system behaviour over a long period of time, for instance one year, by calculating the power balance at an interval of 1 hour or even better 10 or 1 minute. This type of model is especially useful to size the system components and to evaluate the effect of different control strategies on the amount of power the consumer can use. In the time domain model the consumer load pattern has to be specified. The amount of dumped and useful power depend on this pattern. For the user of the system, the results from time domain models are very relevant.

For the determination of the standard power performance of an autonomous system, the dumped power and power lost by charging and discharging are counted as produced power (though not actually used). In other words the battery size and losses are not taken into account: it is assumed to have an infinite size and zero losses. For this power performance evaluation, the statistical model is sufficient, but a time domain model can also be used. Figure 8.1 shows the item to be considered in the estimation of the energy output.

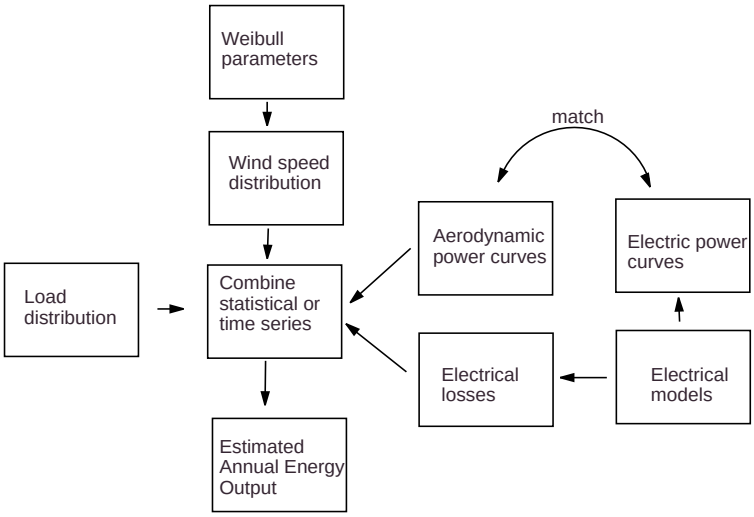

Figure 8.1 *Power Performance determination of Stand-Alone Systems*

8.1 Statistical power performance model

The statistical wind model is based on the Weibull distribution. The cumulative probability distribution $H(V)$ of the wind speed (for instance averaged over 10 minutes) is:

$$H(V_i) = Prob(V \leq V_i) \tag{8.1}$$

The probability density function is given by:

$$h(V) = Prob(V_{i-1} \leq V \leq V_i) \tag{8.2}$$

$$h(V) = \frac{H(V) - H(V - \Delta V)}{\Delta V} = \frac{dH}{dV} \tag{8.3}$$

The average wind speed is:

$$V_{av} = \lim_{T \to \infty} \int_0^T V(t)dt = \int_0^\infty Vh(V)dV \tag{8.4}$$

and the annual energy in the wind:

$$dE_{annual} = \frac{1}{2}\rho dA_r \int_0^\infty V^3 h(V)dV \tag{8.5}$$

The 10 minutes averaged wind speed is often described by a Weibull distribution:

$$H(V_i) = Prob(V \leq V_i) = 1 - exp(-[\frac{V_i}{A}]^k) \tag{8.6}$$

with k the shape factor and A the scale factor.

The probability density function of the Weibull distribution is:

$$h(V) = \frac{dH}{dV} = \frac{k}{A}(\frac{V}{A})^{k-1} exp(-[\frac{V}{A}]^k) \tag{8.7}$$

Using the gamma function a simple expression for the average wind speed depending on the shape and scale factor results:

$$\begin{aligned}
\Gamma(x) &= \int_0^\infty \zeta^{x-1} exp(-\zeta) d\zeta & (8.8)\\
\zeta &= (\frac{V}{A})^k & (8.9)\\
d\zeta &= k(\frac{V}{A})^{k-1}\frac{1}{A}dV & (8.10)\\
\overline{V_{annual}} &= \int_0^\infty V h(V) dV = & (8.11)\\
&= \int_0^\infty V \frac{k}{A}(\frac{V}{A})^{k-1} exp(-[\frac{V}{A}]^k) dV = & (8.12)\\
&= A\Gamma(1+\frac{1}{k}) & (8.13)\\
\Gamma(1+\frac{1}{k}) &\approx (0.568 + \frac{1.434}{k})^{1/k} \pm 0.5\% & (8.14)\\
E_{av} &= \frac{1}{2}\rho A_r (V^3)_{av} = \frac{1}{2}\rho A_r A^3 \Gamma(1+\frac{3}{k}) & (8.15)
\end{aligned}$$

Summarizing,
- the Weibull distribution is a mathematical fit to 10 min. average wind speed;
- the Weibull parameters k and A depend on the site;
- if only V_{av} is known take $k = 2$;
- the total annual wind energy of a site is proportional to $(V^3)_{av}$.

The Weibull distribution is the one of the two inputs for the statistical model of the power performance. The second input is the $P(V)$-curve of the wind turbine. The model calculates the produced electric power per wind speed bin and multiplies this with the number of hours of wind in this bin. This is summarised for totals over the period of evaluation.

Figure 8.2 gives an example for 2 battery voltages $U_{dc,low}/U_{dc,high} = 3/4$. The model does not include the battery model however: this is included in the time domain model only. The calculation did not include any losses either, for which is also referred to the time domain model. However, the result shows clearly that the effect of the battery voltage on the annual energy production is small: in this particular case with a considerable voltage difference only 4%. This is a second indication for the simplification of the performance models by excluding the effect of the battery voltage on the electricity production.

The electrical energy produced by a wind turbine is approximately proportional to $\overline{V_{annual}}$. This can be shown by using the performance models.

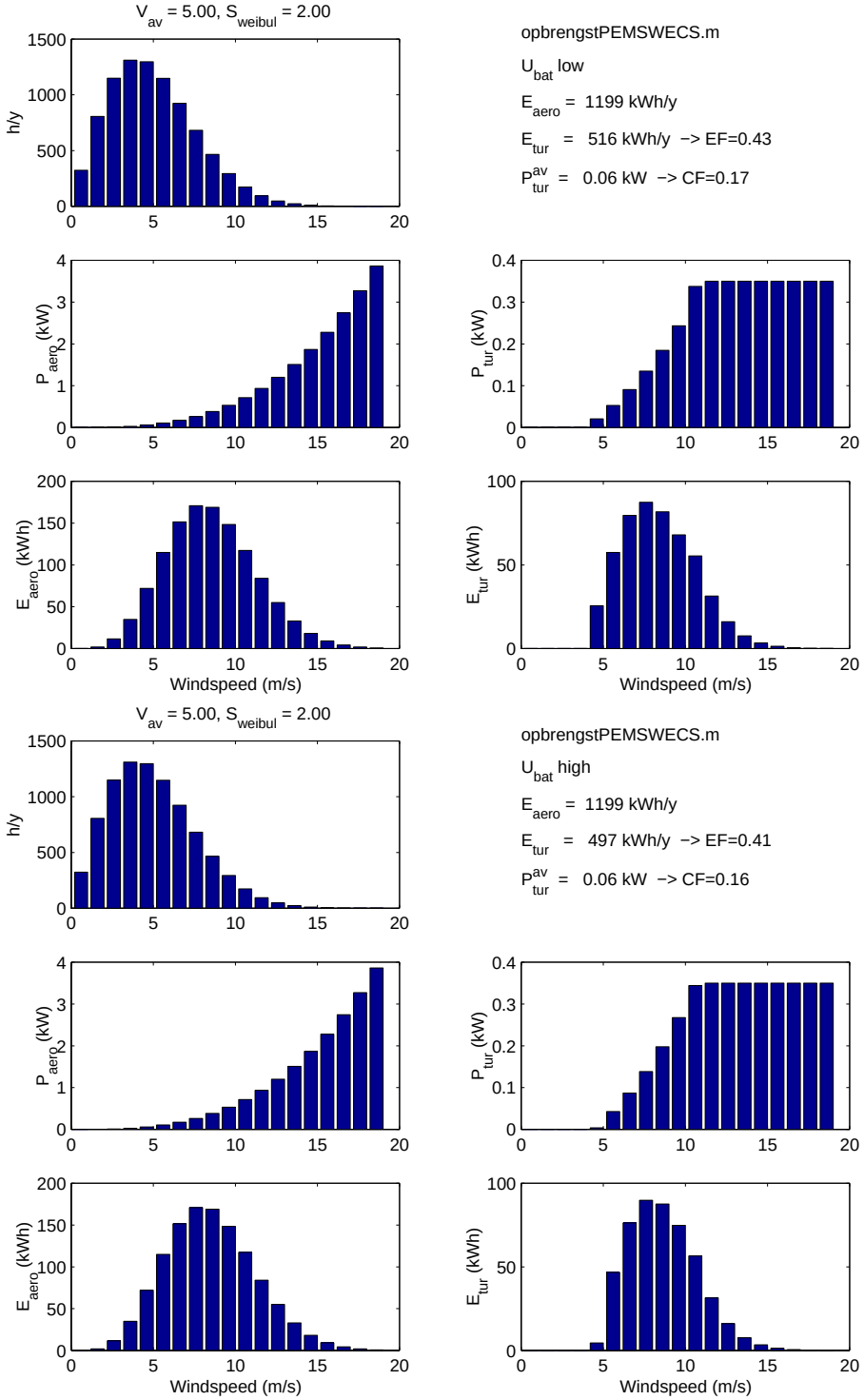

Figure 8.2 *Example of a statistical performance calculation for 2 battery voltages* $U_{dc,low}/U_{dc,high} = 3/4$

8.2 Time domain power performance model

For a time domain model a wind speed time series realisation which satisfies the Weibull distribution has to be made. A method is given by Kaminski [8]. A uniformly distributed random variable $u(t)$ between 0 and 1 is mapped to a random variable $V_w(t)$ which satisfies the Weibull distribution:

$$V_w(t) = A \cdot [-\ln(1 - u(t))]^{\frac{1}{k}} \tag{8.16}$$

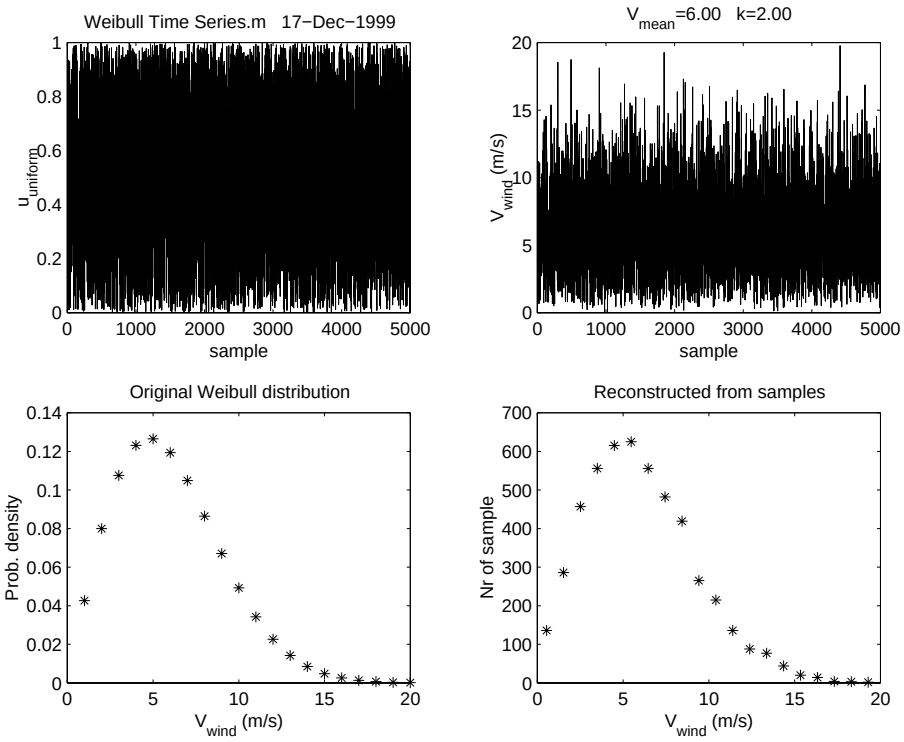

Figure 8.3 *A realisation of a Weibull time series*

Figure 8.3 shows a result. The time domain model calculates the actual load flow in a system instead of the probability of a certain system state. The component models only determine the power into or out of a component and the rest is administration. Checks are required to determine:

- if the turbine power can supply the load;
- if the batteries are full or empty.

The time domain model includes:

- the P(V) curve;
- batteries SOC and losses;

The equations of the time domain model:

$$P_{dif} = P_{tur} - P_{load} \tag{8.17}$$

$$\text{if } P_{dif} < 0 \quad \text{and} \quad \text{if } SOC > SOC_{min} \longrightarrow \text{Discharging}: \tag{8.18}$$

$$I_{bat} = \frac{P_{dif}}{U_{bat}} \tag{8.19}$$

$$P_{bat}^{los} = R_i I_{bat}^2 \tag{8.20}$$

$$E_{bat}^{out} = \Delta t(-P_{dif} + P_{bat}^{los}) \tag{8.21}$$

$$E_{bat}^{chem}(t + \Delta t) = E_{bat}^{chem}(t) - E_{bat}^{out} \tag{8.22}$$

$$SOC(t + \Delta t) = \frac{E_{bat}^{chem}(t + \Delta t)}{C_{bat}} \tag{8.23}$$

$$P_{short} = 0 \tag{8.24}$$
$$P_{dump} = 0 \tag{8.25}$$

$$\text{if } P_{dif} < 0 \quad \text{and} \quad \text{if } SOC < SOC_{min} \longrightarrow \text{Shortage :} \tag{8.26}$$
$$E_{bat}^{chem}(t+\Delta t) = E_{bat}^{chem}(t) \tag{8.27}$$
$$SOC(t+\Delta t) = SOC(t) \tag{8.28}$$
$$P_{short} = -P_{dif} \tag{8.29}$$
$$P_{dump} = 0 \tag{8.30}$$

$$\text{if } P_{dif} > 0 \quad \text{and} \quad \text{if } SOC < SOC_{max} \longrightarrow \text{Charging :} \tag{8.31}$$
$$I_{bat} = \frac{P_{dif}}{U_{bat}} \tag{8.32}$$
$$P_{bat}^{los} = R_i I_{bat}^2 \tag{8.33}$$
$$E_{bat}^{in} = \Delta t(P_{dif} - P_{bat}^{los}) \tag{8.34}$$
$$E_{bat}^{chem}(t+\Delta t) = E_{bat}^{chem}(t) - E_{bat}^{in} \tag{8.35}$$
$$SOC(t+\Delta t) = \frac{E_{bat}^{chem}(t+\Delta t)}{C_{bat}} \tag{8.36}$$
$$P_{short} = 0 \tag{8.37}$$
$$P_{dump} = 0 \tag{8.38}$$

$$\text{if } P_{dif} > 0 \quad \text{and} \quad \text{if } SOC > SOC_{max} \longrightarrow \text{Dumping :} \tag{8.39}$$
$$E_{bat}^{chem}(t+\Delta t) = E_{bat}^{chem}(t) \tag{8.40}$$
$$SOC(t+\Delta t) = SOC(t) \tag{8.41}$$
$$P_{short} = 0 \tag{8.42}$$
$$P_{dump} = P_{dif} \tag{8.43}$$

Figure 8.4 gives a result of the time domain model.

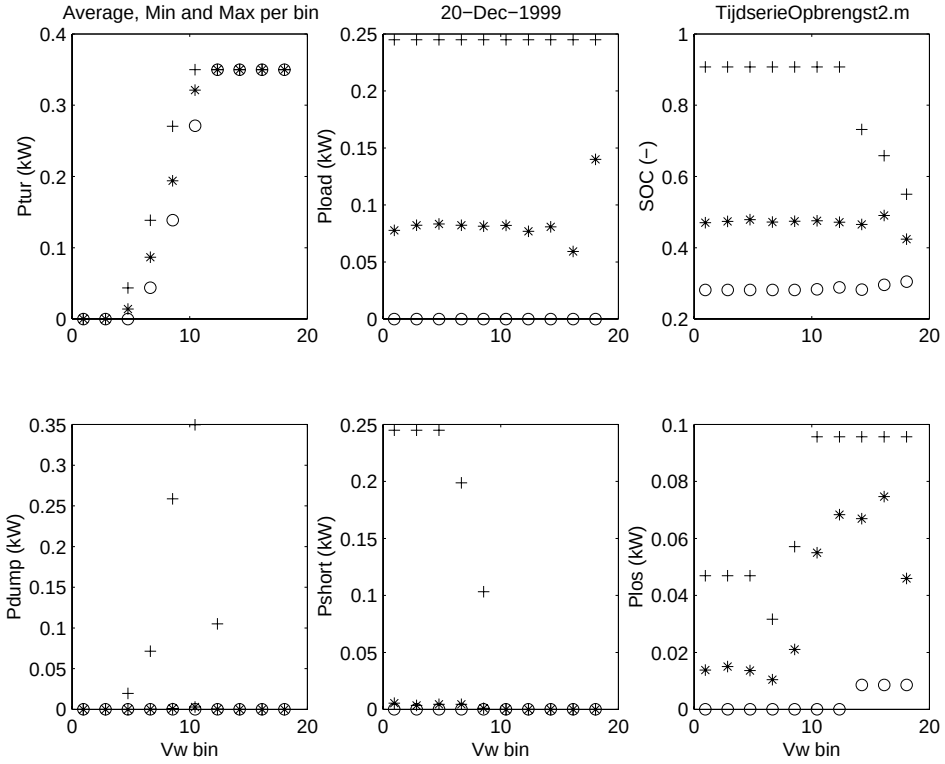

Figure 8.4 *Binned results of a time series performance calculation*

8.3 Power performance for different voltage levels

Based on the measured power curves for three DC voltage levels, presented in chapter 7, the annual average energy production is estimated for the wind speed range available for all three levels: 5 to 11 m/s. In this region it is likely that all three voltage levels can occur and it is also the region which is most important from an energy production point of view.

The differences in the power curves found in chapter 7 are small, and it will now be checked if the differences are magnified by the wind speed distribution. Figure 8.5 to 8.7 give the results for a Weibull distribution with average wind speeds of 5, 6 and 7 m/s and a shape factor of 2. Table 8.1 shows the cumulative results. The maximum deviations are 7-10%. This is the upper limit, under real conditions the value listed under $allU$ are expected. The differences, especially the $allU$ values compared to the upper limit, are relatively small. Therefore, there seems to be no justification for a complicated measurement procedure to take the effect of DC voltage variations into account for the estimation of the average annual energy production of autonomous WECS with batteries. It is recommended to perform the measurements under random load conditions, implying randomly changing voltages, and make no correction for these changes.

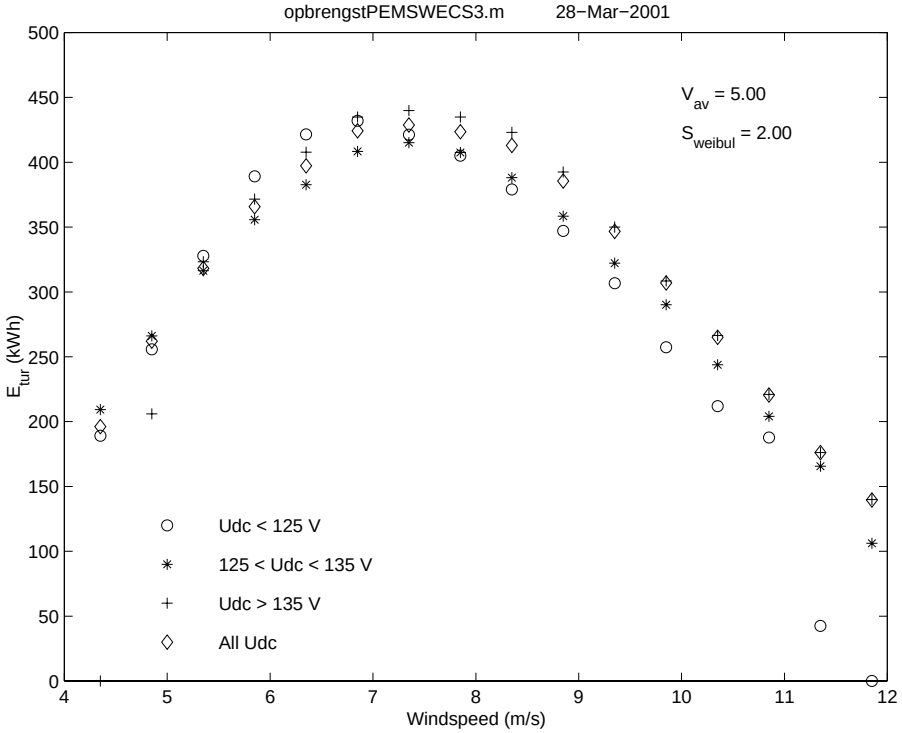

Figure 8.5 *Energy production for 3 DC voltage levels versus all data: Vav =5 m/s, k=2*

Table 8.1 *Annual production in wind speed interval 5-11 m/s*

Weibull parameters			
$V_{w,av}$	5	6	7
k	2	2	2
Annual energy production E (kWh/y)			
$U < 125V$	4087	5359	5959
$125 < U < 135V$	4093	5455	6128
$U > 135V$	4374	5849	6582
$allU$	4296	5753	6482
Deviations			
$\frac{E_{U>135}-E_{U<125}}{E_{U<125}}$	7%	9%	10%
$\frac{E_{U>135}-E_{allU}}{E_{allU}}$	2%	1.5%	1.5%

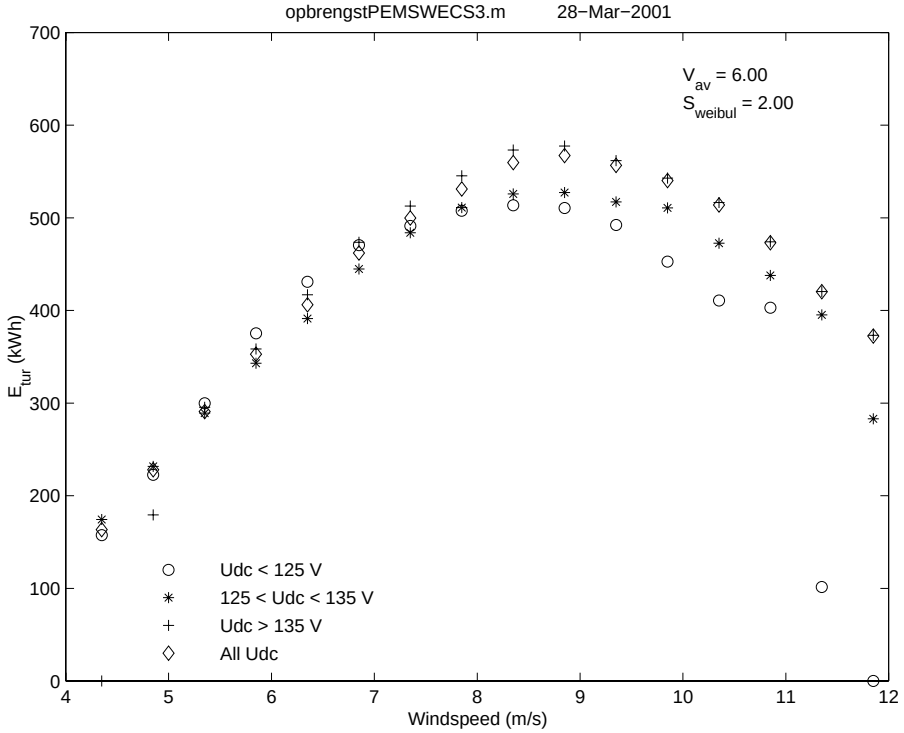

Figure 8.6 *Energy production for 3 DC voltage levels versus all data: Vav =6 m/s, k=2*

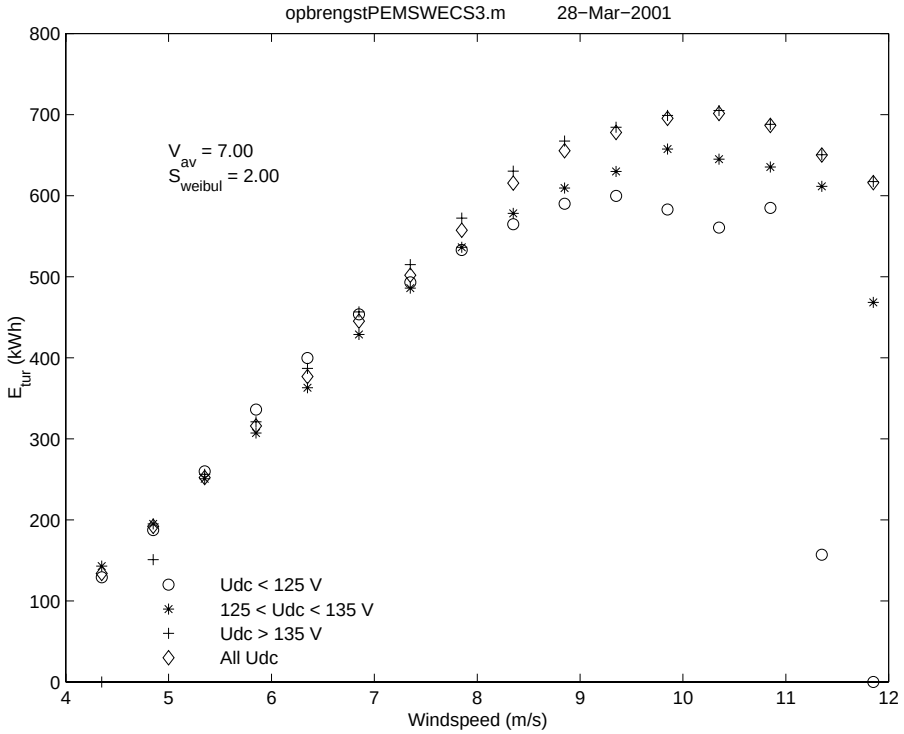

Figure 8.7 *Energy production for 3 DC voltage levels versus all data: Vav =7 m/s, k=2*

9. CONCLUSIONS AND RECOMMENDATIONS

This report describes measurements and simulations to determine a method for the power performance evaluation of autonomous wind turbine systems. The method applies to small systems, in the range of a few 100 W to 10 kW, equipped with a permanent magnet generator, a diode rectifier and batteries. The analysis concentrates on two aspects:

- the choice of the pre-averaging time for the power curve determination;
- the effect of the load on the power-wind speed curve of the turbine.

An estimate of the optimal pre-averaging time was determined by calculating the transfer function $\mathrm{d}P_{\mathrm{el}}/\mathrm{d}V_{\mathrm{w}}$. A value of 30 seconds appeared to be a good choice for the 4 kW system that was investigated. This choice was verified by comparing the power curves for pre-averaging times of 10, 30, 60, 120, 300 and 600 s. The differences that were found were small or could be explained by an insufficient number of data in some of the bins.

With regard to the effect of the load on the power performance it was shown that, although the influence of the load on the DC voltage is substantial (a 30% variation is not unusual) the effect on the power-wind speed curve is relatively small. The effect on the annual averaged energy production, although dependent on the wind regime, is also small: in the range of 5%. This justifies a simplified method for the determination of the power-wind speed curve for systems that fulfill the conditions in the measurements.

Recommendations

Power performance measurements for autonomous WECS with batteries:

- required measurements:
  - wind speed and direction;
  - electric power at generator terminals or at rectifier (depending on location of dumpload);
  - ambient temperature and pressure;
- optional measurements:
  - DC voltage and current;
  - turbine rotational speed;
  - yaw angle;
- use a sample frequency of 2 Hz or higher;
- save raw 2 Hz data for later reference;

Measurement conditions for systems with permanent magnet generator, diode rectifier and charge controller directly connected to the batteries or through a downchopper:

- consult the manufacturer or perform a scoping measurement to quantify the variation, due to load changes, of the DC voltage at the diode rectifier;
- if the voltage deviations are 30% or less, voltage changes need not be taken into account in the power performance measurement and evaluation procedure;
- if voltage variations are not taken into account, take measurements for the power-wind speed curve under random load conditions, comparable to end user conditions;
- if the voltage deviations exceed 30%:
  – either include voltage measurement in the data acquisition and bin measurements against 3 voltage levels and evaluate the effect on the power performance,

– or measure power-wind speed curves at the two extreme values of the DC voltage and evaluate the effect on the power performance.

Evaluation of measurements:

- use a pre-averaging time of 30 seconds for systems with a rotor diameter of less than 6 m and 60 seconds for systems up to 10 m diameter;
- perform a pressure and temperature correction.

REFERENCES

[1] K. Bamborough, W. Richmond, and H. Piggot. Experience with a 3.6 kw aerogenerator at a remote highland school. In *EWEC 91*, Amsterdam, 1991.

[2] International Electrotechnical Commission. IEC standard: Rotating electrical machines; part 10: Conventions for description of synchronous machines. Technical Report Publication 34-10, IEC, Geneve, 1975.

[3] D. Infield (ed.). Engineering design tools for wind diesel systems. Technical Report RAL-94-006, RAL, 1994.

[4] IT Power et.al. Development of methodology for the standardisation of performance claims for wind turbine systems. Technical Report ETSU W/52/00523/REP, IT Power, 2000. Draft Methodology.

[5] A.C. Hansen and T.E. Hausfeld. Frequency response matching to optimize wind-turbine test data correlation. *Transactions of the ASME*, pages 246, Vol. 108, 1986.

[6] R. Hunter and G. Elliot (ed.). *Wind-Diesel Systems*. Cambridge University Press, Cambridge, 1994.

[7] R. Hunter, G. Skivington, and I. Ravey. Performance evaluation methodologies for small wind energy conversion systems. In *EWEC 1997*, Dublin, 1997.

[8] F.C. Kaminsky, R.H. Kirchhoff, C.Y. Syu, and J.F. Manwell. A comparison of alternative approaches for the synthetic generation of a wind speed time series. In *Ninth ASME Wind Energy Symposium*, New Orleans, 1990.

[9] J. Kuikman. Instructions for assembly of the Fortis Montana 4000. Technical Report -, Fortis Windenergy, 1999.

[10] P.H. Mellor, F.B. Chaaban, and K.J. Binns. Estimation of parameters and performance of rare-earth permanent-magnet motors avoiding measurement of load angle. *IEE Proceedings-B, Vol. 138, No. 6, November 1991*, pages 322–330.

[11] A. Miedema and A. Loorbach. Generator windmolen. Technical Report ELVE-4, Hanze Hogeschool Groningen, 1999.

[12] NN. *Storage systems for Photovoltaic Power Systems*. NN, NN, 00.

[13] J. Perahia and C.V. Nayar. Model and simulation of a wind turbine powered permanent magnet alternator battery charging system. *Wind Engineering Vol. 19 No. 6*, page 303, 1995.

[14] D.J.J Schotvanger. Kleine windturbine Tocardo 4500. Technical Report E 49-EE-96, Hogeschool Alkmaar, 1996.

[15] V.A.P. van Dijk and E.A Alsema. SOMES Version 3.0: Technical reference manual. Technical Report W 92009, Dept. of Science,Technology and Society, University of Utrecht, March 1992.

APPENDIX A. PHOTOS OF TEST SYSTEM

Figure A.1 *Fortis turbine installed at ECN testsite*

Figure A.2 *Yaw measurement equipment*

Figure A.3 *Turbine switch, rectifier control box and measurement transducers*

Figure A.4 *Data acquistion system*

Figure A.5 *Sunpower PV UP 5000 Inverter*

Figure A.6 *Binary resistor bank acting as simulated load*

Figure A.7 *Batteries*

APPENDIX B. MEASUREMENT FORTIS MONTANA GENERATOR PARAMETERS

B.1 Introduction

The *Hanze Hogeschool Groningen* performed a number of measurements on the Fortis Montana Permanent Magnet generator to determine the characteristics [11]. This appendix first lists these measurements and subsequently estimates the most relevant machine parameters from these measurements:

- the open circuit flux Ψ_f;
- the stator resistance R_a and synchronous inductance L_s.

These parameters are used to calculate the stator voltage and current phasor and the power of the permanent magnet generator under loaded conditions.

The general characteristics of the permanent magnet generator of the Fortis Montana turbine [9] are listed in table B.1.

Table B.1 *Fortis Montana Generator*

Type	brushless permanent magnet
Rated power	4000 W
Max. power	4500 W
Nr. of pole pairs	9
Rated speed	300 rpm
Max. speed	420 rpm
Voltage DC	24 or 120 V
Frequency	0-70 Hz

The *Hanze Hogeschool Groningen* performed the following measurements:

1. DC voltage and current to determine the stator resistance;
2. open circuit voltage at a number of speeds;
3. short circuit current at a number of speeds;
4. voltage and current with the machine loaded with a number of resistors;
5. voltage and current with the machine loaded with a diode rectifier.

B.2 Stator resistance measurement

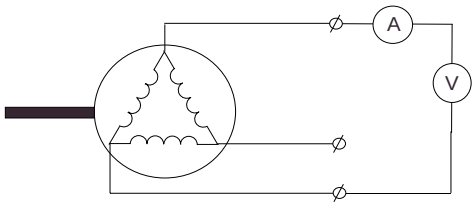

Figure B.1 *Stator resistance measurement*

The stator resistance was measured using a DC voltage source. A voltage of 1.4945 V resulted in a current of 0.9 A. This gives the resistance of the stator coil:

- for delta connection of generator phases: $R_a = 1.5\frac{1.4945}{0.9} = 2.49\Omega$;
- for star connection: $R_a = 0.83\Omega$.

B.3 Open circuit measurement

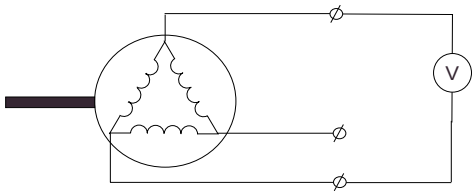

Figure B.2 *Open circuit measurement*

The open circuit voltage was measured at 5 rotor speeds. Assuming the generator is delta-connected the measured voltage is the phase voltage (see figure B.2).

Table B.2 *Open circuit voltage measurement*

n (rpm)	f (Hz)	E_{eff} (V)
10.00	1.50	2.00
20.00	3.00	12.50
50.00	7.50	30.50
200.00	30.00	123.00
300.00	45.00	182.60

From the open circuit measurements the effective open circuit flux per phase is calculated:

- for delta connection of generator phases: $\Psi_f = \frac{E}{\omega} = 0.652$ Vs;
- for star connection: $\Psi_f = \frac{E}{\omega\sqrt{3}} = 0.376$ Vs.

B.4 Short circuit measurement

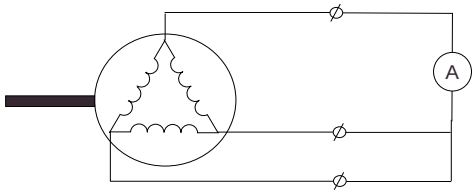

Figure B.3 *Short circuit measurement*

The short circuit current is measured at 5 rotor speeds (see figure B.3 and table B.3).

Table B.3 *Short circuit measurement*

n (rpm)	$I_{sc,eff}$ (A)
7.10	3.10
14.20	6.00
27.00	10.00
38.40	15.00
59.40	20.00

B.5 Estimation of the synchronous inductance

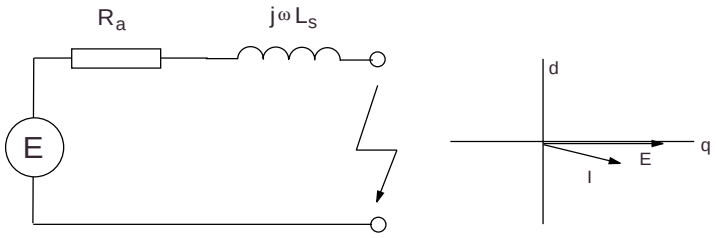

Figure B.4 *Simplified Permanent Magnet generator circuit representation*

The synchronous inductance is estimated from the short circuit measurements in B.4. A simplified representation of a permanent magnet generator is used for the estimation (see figure B.4). Compared to a model found in literature [10], this representation neglects the stator core loss R_c and assumes equal inductances in the direct and quadrature direction. Comparison of the results of the model with the load measurements will show whether these simplifications are justified. The equations for the short circuit are:

$$E = R_a\vec{I} + j\omega L_s\vec{I} \quad \text{(B.1)}$$
$$= R_a(I_q + jI_d) + j\omega L_s(I_q + jI_d) \quad \text{(B.2)}$$

Splitting in real and imaginary parts:

$$E = R_aI_q - \omega L_sI_d \quad \text{(B.3)}$$
$$0 = R_aI_d + \omega L_sI_q \quad \text{(B.4)}$$

Assuming angle γ between current and EMF phasor:

$$I_d = I\sin\gamma \quad \text{(B.5)}$$
$$I_q = I\cos\gamma \quad \text{(B.6)}$$

Which gives 2 equations with L_s and γ to be calculated:

$$E = R_aI\cos\gamma - \omega L_sI\sin\gamma \quad \text{(B.7)}$$
$$0 = R_aI\sin\gamma + \omega L_sI\cos\gamma \quad \text{(B.8)}$$

The following synchronous inductance values are found:

Table B.4 *Synchronous inductance short circuit measurement*

n (rpm)	$I_{sc,eff}$ (A)	L_s (H) Δ	L_s (H) Y
7.10	3.10	no convergence	no convergence
14.20	6.00	0.0285	0.0095
27.00	10.00	0.0564	0.0188
38.40	15.00	0.0306	0.0102
59.40	20.00	0.0348	0.0116

Except for the value for 10 A the result is reasonably consistant. A value of 0.03 H will be assumed for calculation of the loaded generator.

B.6 Resistive load measurement

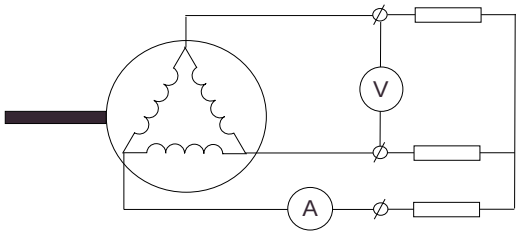

Figure B.5 *Resistive load measurement*

Table B.5 *Load measurement for 7 resistors and 4 rotational speeds (50, 100, 200 and 300 rpm)*

Nr.	U_{50} (V)	I_{50} (A)	U_{100} (V)	I_{100} (A)	U_{200} (V)	I_{200} (A)	U_{300} (V)	I_{300} (A)
1	29.50	0.27	60.10	0.56	120.70	1.12	180.80	1.65
2	29.00	0.52	59.60	1.05	119.30	2.10	177.80	3.12
3	28.90	0.74	59.00	1.50	117.40	2.98	175.00	4.55
4	28.50	0.91	58.00	1.90	115.50	3.80	171.10	5.75
5	28.30	1.13	57.50	2.35	114.00	4.65	168.30	6.94
6	28.40	1.26	58.00	2.60	112.10	5.60	164.90	8.16
7	28.20	1.44	57.50	2.96	110.60	6.40	161.70	9.34

The resistors used in the measurement 1-7 are calculated in table B.6.

Table B.6 *Load measurement resistances*

Nr.	1	2	3	4	5	6	7
R_m (Ω)	108.4811	56.5820	39.0612	30.4991	24.5698	21.2684	18.4007

B.7 Comparison of model results with load measurements

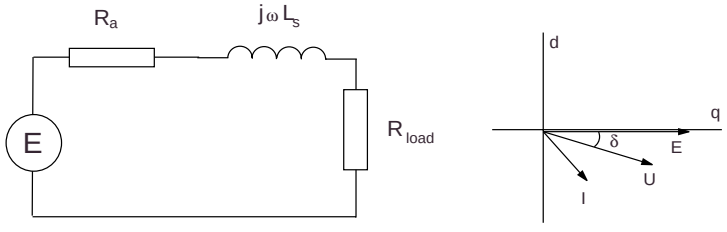

Figure B.6 *Permanent Magnet generator circuit with resistive load*

Based on the equivalent circuit of figure B.6 the following equations are used to calculate the generator voltage and current phasor and the power for the conditions in the loaded measurements listed in table B.5:

$$
\begin{aligned}
R_{eq} &= R_a + R_{load} && \text{(B.9)}\\
E &= -\omega L_s I_d + R_{eq} I_q && \text{(B.10)}\\
0 &= \omega L_s I_q + R_{eq} I_d && \text{(B.11)}\\
U_d &= R_{load} I_d && \text{(B.12)}\\
U_q &= R_{load} I_q && \text{(B.13)}\\
\delta &= -\arctan \frac{U_d}{U_q} && \text{(B.14)}\\
P_g &= 3(U_d I_d + U_q I_q) && \text{(B.15)}\\
P_{load} &= 3 \cdot R_{load} I^2 && \text{(B.16)}\\
P_{loss} &= 3 \cdot R_{loss} I^2 && \text{(B.17)}\\
& && \text{(B.18)}
\end{aligned}
$$

The value of the load resistor depends on the connection chosen for the generator phases:

- $R_{load} = 3R_m$ (generator delta);
- $R_{load} = R_m$ (generator star).

Figure B.7 compares the calculated power (*) with the measured values (+). The differences are small. Figure B.8 compares the value of the stator reactance X_s to the resitor values R_{eq}. Only at the highest speed and the highest load the X_s value approaches the resistance. This explains the insensitivity of the power to the value of the stator reactance. Figure B.9 compares calculated and measured terminal voltages. The small differences could be explained by the measurement accuracy. At the highest load the stator losses amount to around 10%. The maximum load angle reached is 18 degrees. In figure B.12 and B.13 the location of the voltage and current phasors are given for the measured rotor speeds and loads.

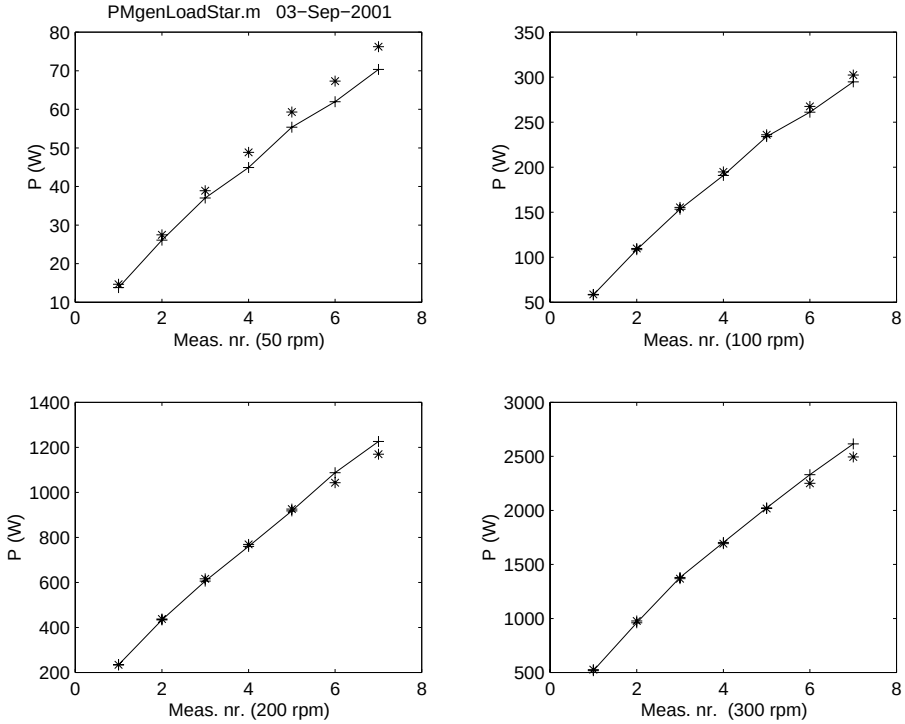

Figure B.7 *Resistive load measurements (+) and model results (*)*

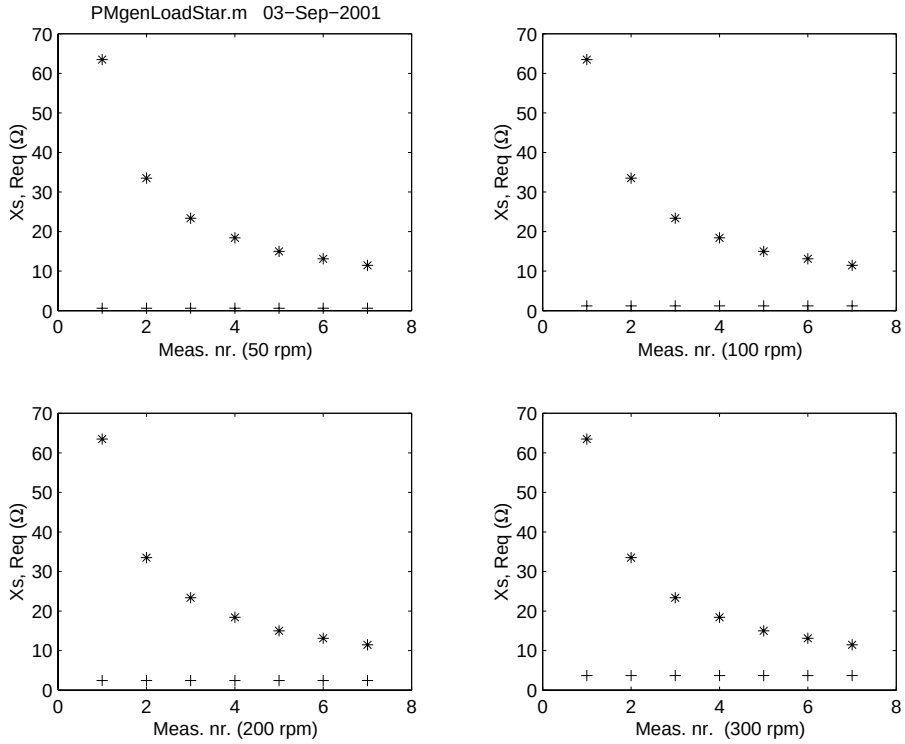

Figure B.8 *Stator reactance (+) and resistive load (*)*

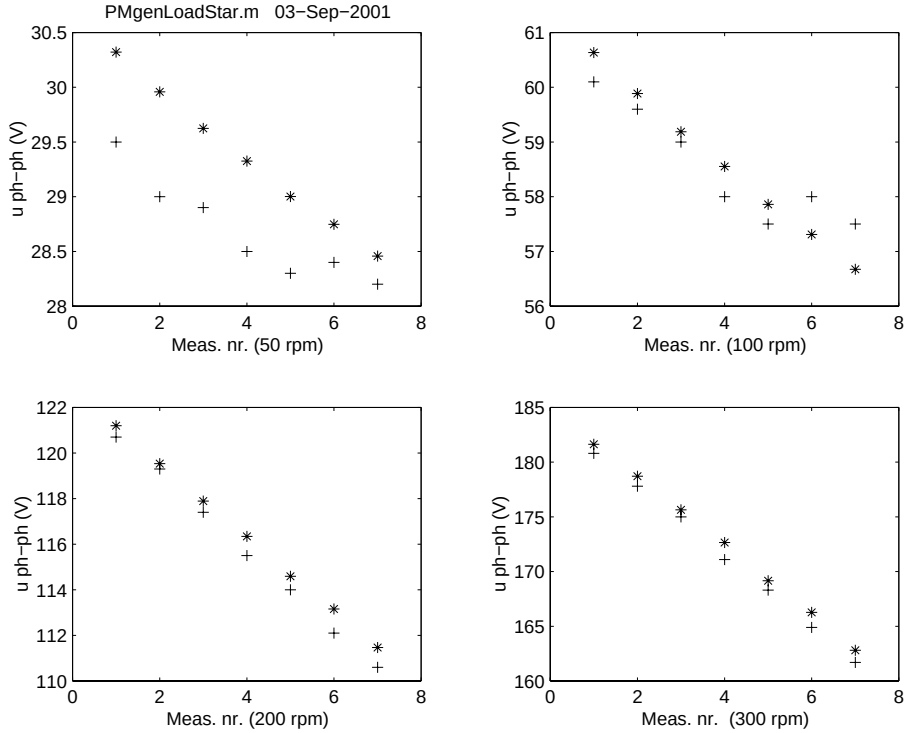

Figure B.9 *Stator voltages measured (+) and model results (*)*

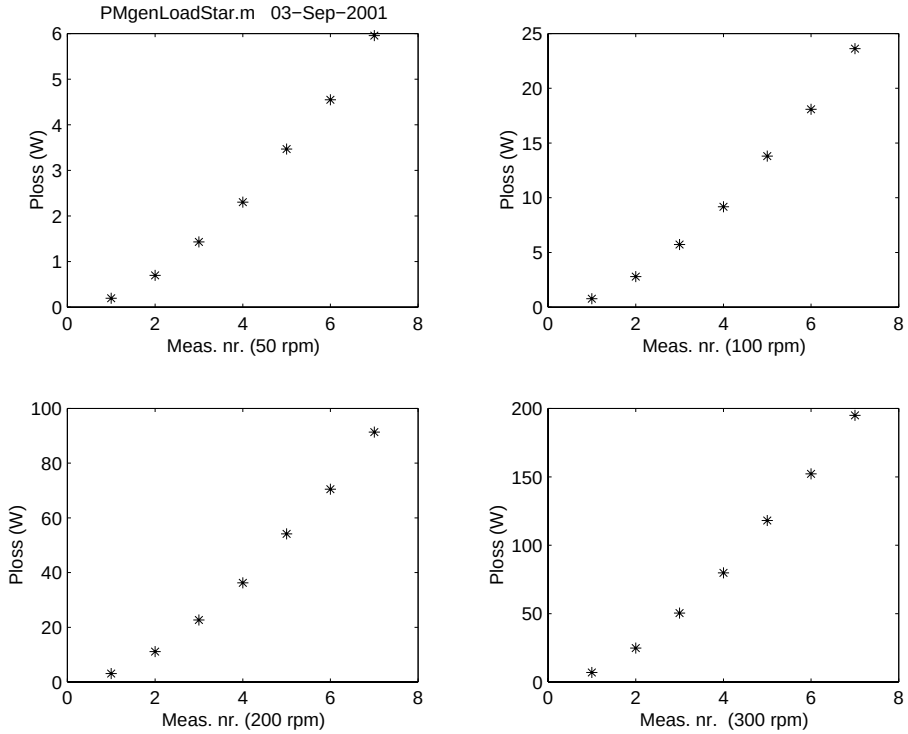

Figure B.10 *Stator losses*

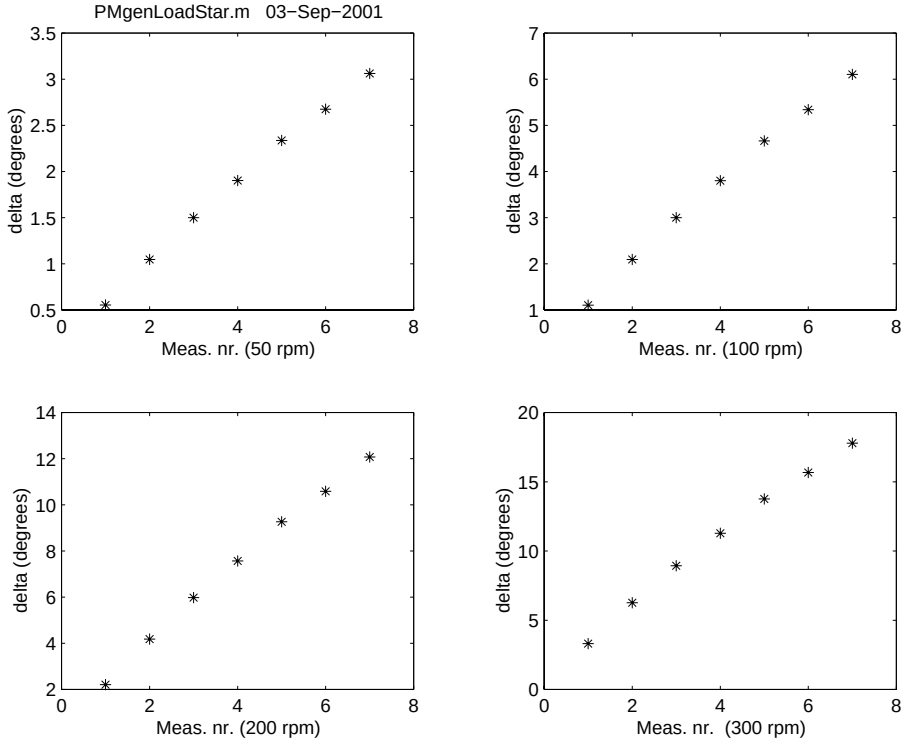

Figure B.11 *Load angle*

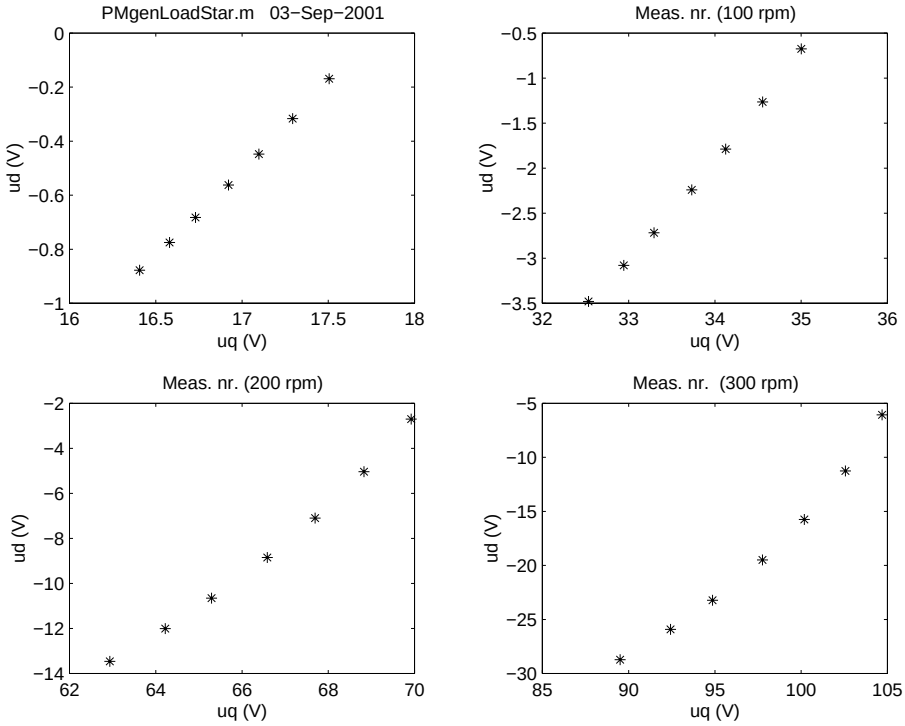

Figure B.12 *Voltage phasors*

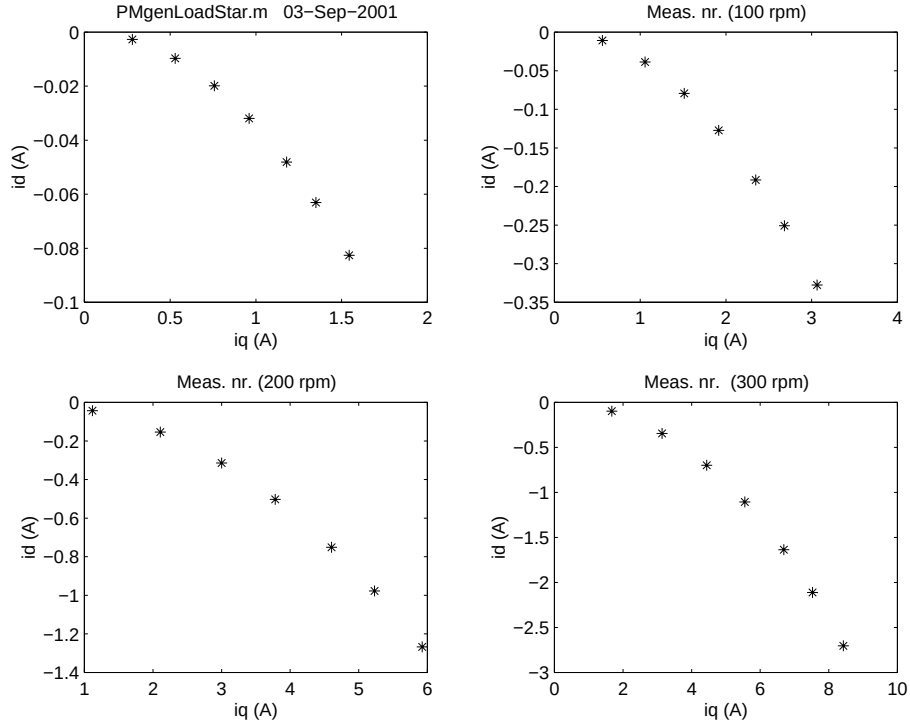

Figure B.13 *Current phasors*

APPENDIX C. MATLAB PROGRAMS

C.1 Estimation of L_s

```
% ParPMscStar.m
%
% 02-03-00 PEMSWECS
% berekent Xs
% uit de kortsluitmetingen voor de Montana PM generator
% probleem is dat er mogelijk verzadiging optreedt
% waardoor E0 en Xd of Xq niet meer constant zijn
% zie de paper van Mellor
%
% GA UIT VAN ZOWEL DE GENERATOR ALS DE LOAD IN STER

clear
% de statorweerstand met generator in STER
Ra=0.83
root3=sqrt(3);

% kortsluitmeting:
% aanname dat generator in ster is aangesloten
% in meetrapport staat de generator in driehoek getekend
% converteer spanning en stroom alsof de generator in ster staat
% dat maakt de aansluiting op een ster belasting eenvoudig
%
% Tussen waarden Ra en Ls ster of driehoek zit FACTOR 3
%
% effectieve waarden kortsluitstroom:
Imeet=[3.1 6 10 15 20];
Ia=Imeet;
% in ster gaat de gemeten stroom door elke fase
ntur=[7.1 14.2 27 38.4 59.4];
pp=9;
w=2*pi*pp*ntur/60;
% de gemeten open klemspanning was de gekoppelde waarde, effectief
% daarom correctie met root3:
E0=w*0.652/root3;

% Poging 2: nu zit 't hoekverschil er wel in
% de core verliezen zijn verwaarloosd
% alleen de rotorweerstand doet mee
% en Ld=Lq genomen

% vergelijkingen:
% E0=Ra*I*cos(gamma) -w*Ls*I*sin(gamma)
%  0=Ra*I*sin(gamma) +w*Ls*I*cos(gamma)
%
% gamma is de hoek tussen E0 en I
% varieer gamma totdat de waarde van Ls in beide
% vergelijkingen gelijk:

clf

gammax=85;
gammin=5;
gamneg=[-gammax:1:-gammin];
gampos=[gammin:1:gammax];
gamma=[gamneg gampos]*pi/180;
sg=size(gamma);
sg2=sg(2)
nulvec=zeros(1,sg2);

%[initialisatie:
% maak lege matrix (geen nullen)
% matrix is leeg door 2e dimensie 0 te kiezen
% waarin de uitvoer geschreven wordt:
MLs=zeros(sg2,0);
% plak de vectoren vervolgens aan de matrix

for n=1:5
In=Ia(n)
wn=w(n)
nn=ntur(n)
E0n=E0(n)

for n=1:sg2
Ls1(n)=-(E0n-Ra*In*cos(gamma(n)))/(wn*In*sin(gamma(n)));
Ls2(n)=-Ra*In*sin(gamma(n))/(wn*In*cos(gamma(n)));
end
gamdeg=gamma*180/pi;
Lsdif=Ls1-Ls2

%[paste naar matrix:
```

```
MLs=[MLs gamdeg' 1000*Lsdif' Ls1'];

subplot(211),plot(gamdeg,Lsdif,gamdeg,nulvec)
title(sprintf('Estim. Ls from short circuit test I=%3.3f, n=%3.3f ',In,nn))
xlabel('Current angle (degrees)')
ylabel('Ls1-Ls2')
subplot(212),plot(gamdeg,Ls1)
xlabel('Current angle (degrees)')
ylabel('Ls (H)')
 pause
end

fid = fopen('tabel.tex','w');
fprintf(fid,'/t%2.1f/t%2.1f/t%2.4f/t%2.1f/t%2.1f/t%2.4f/t%2.1f/t%2.1f/t
%2.4f/t%2.1f/t%2.1f/t%2.4f/t%2.1f/t%2.1f/t%2.4f ///n',MLs')
fclose(fid);
```

C.2 Calculation of measurements with resistive load

```
% PMgenLoadStar.m
%
% narekenen van de belaste metingen uitgevoerd door
% Hogeschool Groningen (Miedema en Loorbach)
% aan de Fortis Montane Generator voor PEMSWECS
%
% berekend eerst de belastingsweerstanden uit gemeten U en I
% vervolgens wordt de equivalente weerstand bepaald
% (ster-driehoek schakeling van load-generator)
% en opgeteld bij de statorweerstand
% daarna worden de machinevergelijkingen opgelost
% voor id, iq, ud en uq
% maakt plaatjes van P, Ploss, Xs, Req, us, cosphi, delta,
  ud-uq en id-iq
% voor de gemeten toerentallen: 50, 100, 200 en 300 rpm
%
% de MACHINEVERGL. STAAN IN MODELEQ.M
%
% PMgenLoadStar.m   : ga uit van generatormodel in STER
%                   parameters zijn de fasewaarden in ster
%                   belasting ook in STER
clear
clf
filenaam='PMgenLoadStar.m';
fig_to_printer=0;
fig_to_file=1;
root3=sqrt(3);
ntur=[50 100 200 300];
% de meetwaarden waaruit de weerstand wordt berekend:
% n=50 rpm, 7 weerstandswaarden:
u50=[29.5 29.0 28.9 28.5 28.3 28.4 28.2];
i50=[0.27 0.52 0.74 0.91 1.13 1.26 1.44];
% belasting in ster,
% i is de EFFECTIEVE stroom door elke belastingsweerstand,
% u is de GEKOPPELDE EFFECTIEVE spanning over 2 weerstanden
% P=root3*Ub*Ib
P50=root3*u50.*i50;
% n=100 rpm:
u100=[60.1 59.6 59.0 58.0 57.5 58.0 57.5];
i100=[0.56 1.05 1.50 1.90 2.35 2.60 2.96];
P100=root3*u100.*i100;
% n=200 rpm:
u200=[120.7 119.3 117.4 115.5 114.0 112.1 110.6];
i200=[1.120 2.100 2.980 3.800 4.650 5.600 6.400];
P200=root3*u200.*i200;
% n=300 rpm:
u300=[180.8 177.8 175.0 171.1 168.3 164.9 161.7];
i300=[1.650 3.120 4.550 5.750 6.940 8.160 9.340];
P300=root3*u300.*i300;
nr=[1:7];
subplot(221),plot(nr,P50)
xlabel('meting nr')
ylabel('P (W)')
title(sprintf('%s   %s',filenaam,date))
subplot(222),plot(nr,P100)
xlabel('meting nr')
ylabel('P (W)')
title('<<< 50 rpm,  deze 100 rpm')
subplot(223),plot(nr,P200)
xlabel('meting nr')
ylabel('P (W)')
title('boven 50 rpm,  onder 200 rpm')
subplot(224),plot(nr,P300)
xlabel('meting nr')
ylabel('P (W)')
```

```
title('boven 100 rpm,  onder 300 rpm')
% de u's zijn de gekoppelde waarden:
% de spanning over 1 weerstand is 1/root3 maal de gekoppelde
  waarde:
r50 =u50./(root3*i50)
r100=u100./(root3*i100)
r200=u200./(root3*i200)
r300=u300./(root3*i300)
P50ch=3*r50.*i50.*i50;
P100ch=3*r100.*i100.*i100;
P200ch=3*r200.*i200.*i200;
P300ch=3*r300.*i300.*i300;
MR=[r50' r100' r200' r300']
for n=1:7
   % in de meting is de weerstand in ster geschakeld:
   % generatormodel ook in STER
   Rload(n)=mean(MR(n,:))
end
% statorfaseweerstand generator
Ra=0.83*ones(1,7);
pp=9;
w=2*pi*pp*ntur/60;
% E de EFFECTIEVE GENERATORFASE WAARDE:
E=w*0.652/root3;
% statorfaseimpedantie generator
Ls=0.013;
Xs=w*Ls;
Reg=Ra+Rload
% P = 3*Ifase*Ufase
% 50 rpm:
Xsn=Xs(1);
En=E(1);
label='50';
modeleq
% 100 rpm:
Xsn=Xs(2);
En=E(2);
label='100';
modeleq
% 200 rpm:
Xsn=Xs(3);
En=E(3);
label='200';
modeleq
% 300 rpm:
Xsn=Xs(4);
En=E(4);
label='300';
modeleq
nr=[1:7];
subplot(221),plot(nr,P50,nr,P50ch,'+',nr,P50mod,'*')
xlabel('Meas. nr. (50 rpm)')
ylabel('P (W)')
title(sprintf('%s   %s',filenaam,date))
subplot(222),plot(nr,P100,nr,P100ch,'+',nr,P100mod,'*')
xlabel('Meas. nr. (100 rpm)')
ylabel('P (W)')
%title('left: 50 rpm,  below: 100 rpm')
subplot(223),plot(nr,P200,nr,P200ch,'+',nr,P200mod,'*')
xlabel('Meas. nr. (200 rpm)')
ylabel('P (W)')
%title('TOP: 50 rpm,  BOTTOM: 200 rpm')
subplot(224),plot(nr,P300,nr,P300ch,'+',nr,P300mod,'*')
xlabel('Meas. nr.  (300 rpm)')
ylabel('P (W)')
%title('TOP: 100 rpm, BOTTOM: 300 rpm')
pause
if fig_to_printer==1
print
end
if fig_to_file==1
print -deps D:/1_PEMSWECS/Figures/PMgenLoad.eps
end
% stop
subplot(221),plot(nr,P50loss,'*')
xlabel('Meas. nr. (50 rpm)')
ylabel('Ploss (W)')
title(sprintf('%s   %s',filenaam,date))
subplot(222),plot(nr,P100loss,'*')
xlabel('Meas. nr. (100 rpm)')
ylabel('Ploss (W)')
%title('left: 50 rpm,  below: 100 rpm')
subplot(223),plot(nr,P200loss,'*')
xlabel('Meas. nr. (200 rpm)')
ylabel('Ploss (W)')
%title('TOP: 50 rpm,  BOTTOM: 200 rpm')
subplot(224),plot(nr,P300loss,'*')
xlabel('Meas. nr.  (300 rpm)')
ylabel('Ploss (W)')
%title('TOP: 100 rpm, BOTTOM: 300 rpm')
```

```
pause
if fig_to_printer==1
print
end
if fig_to_file==1
print -deps D:/1_PEMSWECS/Figures/PMgenLoss.eps
end
subplot(221),plot(nr,Xs50,'+',nr,Req50,'*')
xlabel('Meas. nr. (50 rpm)')
ylabel('Xs, Req (/Omega)')
title(sprintf('%s   %s',filenaam,date))
subplot(222),plot(nr,Xs100,'+',nr,Req100,'*')
xlabel('Meas. nr. (100 rpm)')
ylabel('Xs, Req (/Omega)')
%title('left: 50 rpm,  below: 100 rpm')
subplot(223),plot(nr,Xs200,'+',nr,Req200,'*')
xlabel('Meas. nr. (200 rpm)')
ylabel('Xs, Req (/Omega)')
%title('TOP: 50 rpm,  BOTTOM: 200 rpm')
subplot(224),plot(nr,Xs300,'+',nr,Req300,'*')
xlabel('Meas. nr.  (300 rpm)')
ylabel('Xs, Req (/Omega)')
%title('TOP: 100 rpm, BOTTOM: 300 rpm')
pause
if fig_to_printer==1
print
end
if fig_to_file==1
print -deps D:/1_PEMSWECS/Figures/PMgenLoadx.eps
end
% u  = meting, gekoppelde spanning cq. driehoek
% us = berekening, fasespanning in ster
%      daarom maal root3
subplot(221),plot(nr,u50,'+',nr,us50*root3,'*')
xlabel('Meas. nr. (50 rpm)')
ylabel('u ph-ph (V)')
title(sprintf('%s   %s',filenaam,date))
subplot(222),plot(nr,u100,'+',nr,us100*root3,'*')
xlabel('Meas. nr. (100 rpm)')
ylabel('u ph-ph (V)')
%title('left: 50 rpm,  below: 100 rpm')
subplot(223),plot(nr,u200,'+',nr,us200*root3,'*')
xlabel('Meas. nr. (200 rpm)')
ylabel('u ph-ph (V)')
%title('TOP: 50 rpm,  BOTTOM: 200 rpm')
subplot(224),plot(nr,u300,'+',nr,us300*root3,'*')
xlabel('Meas. nr.  (300 rpm)')
ylabel('u ph-ph (V)')
%title('TOP: 100 rpm, BOTTOM: 300 rpm')
pause
if fig_to_printer==1
print
end
if fig_to_file==1
print -deps D:/1_PEMSWECS/Figures/PMgenLoadu.eps
end

subplot(221),plot(nr,cosphi50,'*')
xlabel('Meas. nr. (50 rpm)')
ylabel('cosphi (-)')
title(sprintf('%s   %s',filenaam,date))
subplot(222),plot(nr,cosphi100,'*')
xlabel('Meas. nr. (100 rpm)')
ylabel('cosphi (-)')
%title('left: 50 rpm,  below: 100 rpm')
subplot(223),plot(nr,cosphi200,'*')
xlabel('Meas. nr. (200 rpm)')
ylabel('cosphi (-)')
%title('TOP: 50 rpm,  BOTTOM: 200 rpm')
subplot(224),plot(nr,cosphi300,'*')
xlabel('Meas. nr.  (300 rpm)')
ylabel('cosphi (-)')
%title('TOP: 100 rpm, BOTTOM: 300 rpm')
pause
if fig_to_printer==1
print
end
if fig_to_file==1
print -deps D:/1_PEMSWECS/Figures/PMgenLoadCosFi.eps
end

subplot(221),plot(nr,delta50*180/pi,'*')
xlabel('Meas. nr. (50 rpm)')
ylabel('delta (degrees)')
title(sprintf('%s   %s',filenaam,date))
subplot(222),plot(nr,delta100*180/pi,'*')
xlabel('Meas. nr. (100 rpm)')
ylabel('delta (degrees)')
%title('left: 50 rpm,  below: 100 rpm')
subplot(223),plot(nr,delta200*180/pi,'*')
```

```
xlabel('Meas. nr. (200 rpm)')
ylabel('delta (degrees)')
%title('TOP: 50 rpm,  BOTTOM: 200 rpm')
subplot(224),plot(nr,delta300*180/pi,'*')
xlabel('Meas. nr.  (300 rpm)')
ylabel('delta (degrees)')
%title('TOP: 100 rpm, BOTTOM: 300 rpm')

pause
if fig_to_printer==1
print
end
if fig_to_file==1
print -deps D:/1_PEMSWECS/Figures/PMgenDelta.eps
end

subplot(221),plot(iq50,id50,'*')
title('Meas. nr. (50 rpm)')
xlabel('iq (A)')
ylabel('id (A)')
title(sprintf('%s   %s',filenaam,date))
subplot(222),plot(iq100,id100,'*')
title('Meas. nr. (100 rpm)')
xlabel('iq (A)')
ylabel('id (A)')
%title('left: 50 rpm,  below: 100 rpm')
subplot(223),plot(iq200,id200,'*')
title('Meas. nr. (200 rpm)')
xlabel('iq (A)')
ylabel('id (A)')
%title('TOP: 50 rpm,  BOTTOM: 200 rpm')
subplot(224),plot(iq300,id300,'*')
title('Meas. nr.  (300 rpm)')
xlabel('iq (A)')
ylabel('id (A)')
%title('TOP: 100 rpm, BOTTOM: 300 rpm')
pause
if fig_to_printer==1
print
end
if fig_to_file==1
print -deps D:/1_PEMSWECS/Figures/PMgenidiq.eps
end

subplot(221),plot(uq50,ud50,'*')
title('Meas. nr. (50 rpm)')
xlabel('uq (V)')
ylabel('ud (V)')
title(sprintf('%s   %s',filenaam,date))
subplot(222),plot(uq100,ud100,'*')
title('Meas. nr. (100 rpm)')
xlabel('uq (V)')
ylabel('ud (V)')
%title('left: 50 rpm,  below: 100 rpm')
subplot(223),plot(uq200,ud200,'*')
title('Meas. nr. (200 rpm)')
xlabel('uq (V)')
ylabel('ud (V)')
%title('TOP: 50 rpm,  BOTTOM: 200 rpm')
subplot(224),plot(uq300,ud300,'*')
title('Meas. nr.  (300 rpm)')
xlabel('uq (V)')
ylabel('ud (V)')
%title('TOP: 100 rpm, BOTTOM: 300 rpm')
pause
if fig_to_printer==1
print
end
if fig_to_file==1
print -deps D:/1_PEMSWECS/Figures/PMgenuduq.eps
end

tabLoad=[u50' i50' u100' i100' u200' i200' u300' i300']
fid = fopen('tabLoad.tex','w');
fprintf(fid,' %3.2f & %3.2f & %3.2f & %3.2f & %3.2f & %3.2f & ...
  %3.2f & %3.2f  /////n',tabLoad')
fclose(fid);
```

C.2.1 Model subroutine

```
% modeleq.m
% calculates the current and power for the
```

```
% PM generated loaded with resistors

% equivalent impedance:
F=Xsn*Xsn*ones(1,7)+Req.*Req;

% EFFECTIEVE GENERATOR PHASE CURRENT:
iq=En*Req./F;
id=-Xsn*iq./Req;
is2=id.*id+iq.*iq;
is=sqrt(is2);

% output power
Pload=3*Rload.*is2;

% loss in stator
Ploss=3*Ra.*is2;

% EFFECTIVE PHASE VOLTAGE and load angle:
ud=Rload.*id;
uq=Rload.*iq;
us=sqrt(ud.*ud+uq.*uq)
delta=-atan2(ud,uq);

% current angle:
eta=-atan2(id,iq);

% power factor:
phi=eta-delta;
cosphi=cos(phi)

% output to labeled variables:
% the label is changed each time this files is evaluated
% P...mod:
eval(['P' label 'mod=Pload']);
% P...loss:
eval(['P' label 'loss=Ploss']);
% Xs...:
eval(['Xs' label '=Xsn']);
% Req...:
eval(['Req' label '=Req']);
% us...:
eval(['us' label '=us']);
% is...:
eval(['is' label '=is']);
% delta...:
eval(['delta' label '=delta']);
% phi...:
eval(['phi' label '=phi']);
% cosphi...:
eval(['cosphi' label '=cosphi']);
% ud...:
eval(['ud' label '=ud']);
% uq...:
eval(['uq' label '=uq']);
% id...:
eval(['id' label '=id']);
% iq...:
eval(['iq' label '=iq']);
```

C.3 Calculation of Permanent Magnet generator with diode rectfier

```
% STEADY STATE SYNCHRONE MACHINE MODEL WITH DIODE RECTIFIER
% calculates voltages, currents and power as function of generator
  speed
% for scoping calculations PEMSWECS
%
% VERSIE 1A:      spanningscoordinatenstelsel !!!
%                 DC voltage constant
%                 no internal battery resistance
% 991214:         vergl. gewijzigd,
%                 nu is delta wel de load angle
%
% input:          n, ifh (of Psi_fh voor PMgen), Udc
% parameters:   ra=0, lq, ld, npp
%                 dit staat per machine in smparameters
%
% VERSIE 2: aangepast voor Fortis Montana
%           in de metingen worden de effectieve waarden gebruikt
%           eerst omgerekend naar ster model van zowel generator als
            load
%           dit model rekent met topwaarden -> Phi_fh in model root2
            maal zo hoog
```

```
%
clear
smparameters   % het Matlab path moet goed staan: Pathbrowser-Add to path
               % deze staat in MACHINEKAR (ER MOET MAAR EEN
                 smparameter.m ZIJN!)
filenaam='FortisPMdiode.m'
fig_to_printer=0;
fig_to_file=0;
facgr=180/pi;
root2 =sqrt(2.0);
root3 =sqrt(3.0);
root32=root3/root2;

ra=0;
% Ingangsvariabelen:
 Phi_fh=root2*0.652/root3;
% root3 omdat gemeten waarde de gekoppelde is
% dit model rekent met topwaarden -> Phi_fh in model root2 maal zo hoog
% amplitudeinvariante trafo want 't is de fasewaarde,
% dus factor 3/2 in vermogens
% Accuspanning, of beter de tussenkringspanning, dit ziet de diodebrug
Uvec=[110 125 143];
% toerentalbereik generatoras in rpm
ntur=[100:1:400];
% maak lege vectoren (ook ggen nullen) waarin de uivoer geschreven wordt:
% voor elke Udc uit Uvec een nieuwe kolom
su=size(Uvec)
numax=su(2);
sn=size(ntur)
nstep=sn(2)
pelkWvec=zeros(nstep,0);
pelDCkWvec=zeros(nstep,0);
deltagrvec=zeros(nstep,0);
etopvec=zeros(nstep,0);
itopvec=zeros(nstep,0);
utopvec=zeros(nstep,0);
udcvec=zeros(nstep,0);
checkvec=zeros(nstep,0);
Idcvec=zeros(nstep,0);
Idc2vec=zeros(nstep,0);
f=ntur*npp/60;
w=f*2*pi;
etop=w*Phi_fh;
for nu=1:numax             % loop voor de DC spanning
Udc=Uvec(nu);
utop=pi*Udc/(3*root3);     % fasespanning, zie paper Martin & JandeB
                           % nu volgt berekening op basis van
                             spanningscoordinaten
                           % voor varierend toerental:
for nn=1:nstep
if etop(nn) > utop
cosdelta=utop/etop(nn);
% blijkbaar moet E groter zijn dan Utop (overbekrachtiging)
% lijkt logisch ivm inductieve karakter stator
delta(nn)=acos(cosdelta);
itop(nn)=etop(nn)*sin(delta(nn))/(w(nn)*lq);
      % controle dmv vergelijking voor Ig uit artikel Martin/Jan:
      % alleen voor symetrische rotor!
      Idc(nn)=pi*Psi_fh*sqrt(1-utop*utop/(etop(nn)*etop(nn)))/(2*root3*lq);
% was Idc(nn)=pi*lafd*ifh*sqrt(1-utop*utop/(etop(nn)*etop(nn)))/(2*root3*lq);
      % moet hier ld staan of la (combinatie van ld en lq)?
Idc2(nn)=pi*itop(nn)/(2*root3);
% amplitudeinvariant:
pel(nn)=3*utop*itop(nn)/2;
% vermogensinvariant:
% pel(nn)=utop*itop(nn);
pelDC(nn)=Udc*Idc2(nn);
      check(nn)=pel(nn)/pelDC(nn);
else
delta(nn)=0;
itop(nn)=0;
   Idc(nn)=0;
Idc2(nn)=0;
pel(nn)=0;
pelDC(nn)=0;
check(nn)=0;
end
end
pelkW=pel/1000;
pelDCkW=pelDC/1000;
deltagr=delta*180/pi;
% uitvoervariabelen: vul een matrix
pelkWvec=[pelkWvec pelkW'];
pelDCkWvec=[pelDCkWvec pelDCkW'];
checkvec=[checkvec check'];
deltagrvec=[deltagrvec deltagr'];
itopvec=[itopvec itop'];
etopvec=[etopvec etop'];
utopvec=[utopvec utop*ones(nstep,1)];
udcvec=[udcvec Uvec(nu)*ones(nstep,1)];
```

```
Idcvec=[Idcvec Idc'];
Idc2vec=[Idc2vec Idc2'];
end                                     % van spannings-loop nu
                                        % nu volgen de plaatjes:
%-----------------------------------------------------------------------
%  vaste aantal plots:
clf
subplot(221),plot(ntur,pelkWvec(:,1),ntur,pelkWvec(:,2),ntur,...
    pelkWvec(:,3))
ylabel('P_e_l (kW)')
xlabel('n (rpm)')
title(sprintf('%s (PM+Diode)',naam))
xl=330;
text(xl,4.5,'H')
text(360,4.1,'M')
text(xl,3.8,'L')
xl=250;
yl=1.5;
dy=0.4;
text(xl,yl,'H = 143 V')
text(xl,yl-dy,'M = 125 V')
text(xl,yl-2*dy,'L = 110 V')
subplot(223),plot(ntur,itopvec(:,1),ntur,itopvec(:,2),ntur,itopvec(:,3))
ylabel('i_t_o_p (A)')
xlabel('n (rpm)')
subplot(222),plot(ntur,etopvec(:,1),ntur,udcvec(:,1),'.',ntur,...
      udcvec(:,2),'.',ntur,udcvec(:,3),'.')
ylabel('E_t_o_p, U_d_c (V)')
xlabel('n (rpm)')
title(sprintf('%s %s',filenaam,date))
subplot(224),plot(ntur,deltagrvec(:,1),ntur,deltagrvec(:,2),ntur,...
     deltagrvec(:,3))
ylabel(' delta (deg) --')
xlabel('n (rpm)')

pause
if fig_to_printer==1
print
end
if fig_to_file==1
print -deps D:/1_PEMSWECS/Figures/FortisPMdiode.eps
end
%-----------------------------------------------------------------------

%-----------------------------------------------------------------------
%  aantal plots variabel:
nu_plots=0
if nu_plot==1
clf

for nu=1:numax
subplot(221),plot(ntur,pelkWvec(:,nu),ntur,pelDCkWvec(:,nu),'--')
hold on
ylabel('P_e_l (kW)')
xlabel('n (rpm)')
title(sprintf('%s (PM+Diode)',naam))
subplot(223),plot(ntur,itopvec(:,nu))
hold on
ylabel('i_t_o_p (A)')
xlabel('n (rpm)')
%subplot(222),plot(ntur,etopvec(:,nu),ntur,udcvec(:,nu),'.',ntur,...
     utopvec(:,nu),'--')
subplot(222),plot(ntur,etopvec(:,nu),ntur,udcvec(:,nu),'.')
hold on
ylabel('E_t_o_p, U_d_c (V)')
xlabel('n (rpm)')
title(sprintf('%s %s',filenaam,date))
subplot(224),plot(ntur,deltagrvec(:,nu),'--')
hold on
ylabel(' delta (deg) --')
xlabel('n (rpm)')
end % of nu loop
pause
if fig_to_printer==1
print
end
if fig_to_file==1
print -deps D:/1_PEMSWECS/Figures/FortisPMdiode.eps
end
end  % of nu_plots
%-----------------------------------------------------------------------
moreplots=0;
if moreplots==1
clf
for nu=1:numax
subplot(321),plot(ntur,pelkWvec(:,nu),ntur,pelDCkWvec(:,nu),'--')
hold on
ylabel('P_e_l (kW)')
xlabel('n (rpm)')
title(sprintf('%s (PM+Diode)',naam))
```

```
%subplot(322),plot(ntur,etopvec(:,nu),ntur,udcvec(:,nu),'.',ntur,...
  utopvec(:,nu),'--')
subplot(322),plot(ntur,etopvec(:,nu),ntur,udcvec(:,nu),'.')
hold on
ylabel('E_t_o_p, U_d_c (V)')
xlabel('n (rpm)')
title(sprintf('%s %s',filenaam,date))
subplot(323),plot(ntur,itopvec(:,nu),ntur,deltagrvec(:,nu),'--')
hold on
ylabel('i_t_o_p (A), delta (deg) --')
xlabel('n (rpm)')
subplot(324),plot(ntur,checkvec(:,nu))
hold on
ylabel('Pdc1/Pdc2')
xlabel('n (rpm)')
subplot(325),plot(ntur,Idcvec(:,nu),ntur,Idc2vec(:,nu))
hold on
ylabel('Idc, IdcMartin')
xlabel('n (rpm)')
subplot(326),plot(ntur,pelkWvec(:,nu)./ntur')
hold on
ylabel('PelkW/ntur')
xlabel('n (rpm)')
end
pause
checkvec(nstep,1)
clf
nu=3
plot(ntur,pelkWvec(:,nu),ntur,pelDCkWvec(:,nu),'--')
hold on
ylabel('P_e_l (kW)')
xlabel('n (rpm)')
title(sprintf('%s (PM+Diode)',naam))
% gtext('Udc = 110 and 143 V')
end % moreplots
```

C.4 Bin routine

```
%        binANDplot.m
%
% Doel:  bint een vector Y tegen een vector X
%        plot evtl. ter controle de waarden per bin
%        berekend gemiddelde, min en max per bin
%
% input: nb   = aantal bins
%        Xb   = vector met de bingrenzen
%               bijv. [0 1 2 3 4 ... 10]
%        X    = de variabele waartegen gebind wordt
%        Y    = de te binnen variabele
%        np   = lengte van de X en Y vectoren (geen input)
%        Ys   = string met naam van de gebinde var
%                (voor uitvoer naar var)
%        filenaam  = naam van de file die X en Y berekent
%                    wordt gebruikt in title van plots
%        VARIABLES = tekst-string met naam van
%                    gebinde var (Y) en de onafh var (X)
% bijv:
%        nb       =2;
%        Xb       =[0 5 10];
%        X        =[1 2 5 3 7 6 4 8 9 3 2];
%        Y        =[4 2 3 5 6 3 2 8 9 8 3];
%        Ys       ='Pel';
%        filenaam='binAnDplot.m'
%        VARIABLES='TURB POWER against WINDSPEED'
%
% output: Yb_n(i) = vector met waarden die vallen in Xb(n)
%         Xb_n(i) = vectoren met waarden X die vallen in Xb(n)
%
%         YbAv    = gemiddelde Y per bin
%         YbMin   = minimum    Y per bin
%         YbMax   = maximum    Y per bin
%         XbAv    = gemiddelde X per bin
%
% plots: Yb waarden per bin
%        average, min and max Y per bin
%
showfig=1;
test=0;
localfilenaam='binANDplot.m';

if test==1
   % testen zonder input waarden
   nb=2;
   Xb=[0 5 10];
```

```
   X =[1 2 5 3 7 6 4 8 9 3 2];
   Y=[4 2 3 5 6 3 2 8 9 8 3];
   plot(X,Y,'*')
   pause
end

% legen bins:
clear Yb*
% maak bins met size 0:
for n2=1:nb
   eval(['Yb',int2str(n2),'=[];']);
   eval(['Xb',int2str(n2),'=[];']);
end

% bereken aantal datapunten np:
temp=size(X)
if temp(1)>1
   np=temp(1)
elseif temp(2)>1
   np=temp(2)
else
   warning('aantal datapunten np niet > 1')
   stop
end

% het binnen:
for n1=1:np
   for n2=1:nb
      if X(n1)>=Xb(n2) & X(n1)<Xb(n2+1)
         % zet de waarde van Y in vectoren Yb
         % de Yb's hebben een ongelijke lengte!
         eval(['Yb',int2str(n2),'=[Yb',int2str(n2),' Y(n1)];']);
         % zet ook de X waarden in vectoren om later te middelen:
         eval(['Xb',int2str(n2),'=[Xb',int2str(n2),' X(n1)];']);
      end
      if n2==nb & X(n1)==Xb(n2+1)
         % alleen een waarde die op laatste bingrens valt
         % wordt bij onderliggende bin geteld
         eval(['Yb',int2str(n2),'=[Yb',int2str(n2),' Y(n1)];']);
         eval(['Xb',int2str(n2),'=[Xb',int2str(n2),' X(n1)];']);
      end
   end
   if  X(n1)>Xb(nb+1)
      % X buiten bereik:
      warning('X buiten bereik:')
      relpowerlevel=X(n1)
   end
end

if showfig==1
% plots van de inhoud van elke bin:
star='*';
for n2=1:nb
   % controleer per bin of er iets in zit
   eval(['sY=size(Yb',int2str(n2),');']);
   if sY(1)>0
   eval(['subplot(',int2str(nb/2),',2,',int2str(n2),'),...
plot(Yb' int2str(n2)  ',star)']);
   % de Yb's hebben een ongelijke lengte!
   % niet als matrix te plotten!
   xlabel('Nr')
   ylabel(sprintf('Y bin= %i',n2))
   if n2==1
      title(sprintf('%s',VARIABLES))
   end
   if n2==2
      title(sprintf('%s    %s',localfilenaam,date))
   end
   end
end
pause
end % of showfig

% voor latere plots buiten binANDplot:
%
% calculate average Y per bin
% de lengte van de Yb_i's is verschillend, dus
YbAv=zeros(1,nb);
% waarden halverwege de x-bins voor plots:
XbAv=Xb+(Xb(2)-Xb(1))/2;
% de gemiddelde waarden van de variabele X
% waartegen gebint wordt
% worden ook berekend
for n2=1:nb
   % controleer per bin of er iets in zit
   eval(['sY=size(Yb',int2str(n2),');']);
   if sY(1)>0
      eval(['YbAv(n2)  = mean(Yb' int2str(n2) ');'])
      eval(['YbMin(n2) = min(Yb' int2str(n2) ');'])
      eval(['YbMax(n2) = max(Yb' int2str(n2) ');'])
```

```
      eval(['YbStd(n2) = std(Yb' int2str(n2) ');'])
      eval(['XbAv(n2)  = mean(Xb' int2str(n2) ');'])
      eval(['XbStd(n2) = std(Xb' int2str(n2) ');'])
      YbSize(n2)=sY(2);
   else
      YbAv(n2)=0;
      YbMin(n2)=0;
      YbMax(n2)=0;
      YbStd(n2)=0;
      XbStd(n2)=0;
      YbSize(n2)=0;
   end
end

clf
```

C.5 Estimation of transfer function

```
% Transferfunction from wind to power
% from Pemswecs data
%
% PemTransferFun.m

loaddata=0;

if loaddata==1
clear
eval(['load ' dir '/' meetfile '.dat -ascii'])
eval(['data=' meetfile ';']);

t=data(:,1);
Vw1=data(:,2);
Vw2=data(:,3);
Vd=data(:,4);
Pair=data(:,5);
Precip=data(:,6);
Temp=data(:,7);
Pgen=data(:,8)/1000;
Udc=data(:,9);
Idc=data(:,10);
N=data(:,11);
Yaw=data(:,12);
Iac=data(:,13);
Pac=data(:,14)/1000;
Pbat=Udc.*Idc/1000;

dt=t(8)-t(7);
meetfreq=1/dt
st=size(t);
meettijd=st(1)*dt
meetinterval=dt
tmin=t/60;

samplefreq=meetfreq;
end

progfile='PemTransferFun.m';
print2eps=1;
Vw_to_P=1;
N_to_P=1;

dir='D:/1_Pemswecs/Meetdata/Meetfiles';
meetfile='jan30';
plotdir='D:/1_Pemswecs/Meetdata/TransferFun';

% aantal punten NFFT voor de FFT bepaald de minimale freq
% NFFT moet een veelvoud van 2 zijn
% samplefreq bepaald de maximale freq:
% fmax=0.5*samplefreq=16Hz
% fmin=samplefreq/NFFT

NFFT=64*samplefreq;
NFFT=64*32;
NFFT=16*32;
NFFT=8*8*32;
NFFT=4*8*32;
NFFT=2*8*32;
sflabel=num2str(samplefreq,2);
nfftlabel=int2str(NFFT);


if Vw_to_P==1
[Txy f]=tfe(Vw1,Pgen,NFFT,samplefreq,'mean')
```

```
magTxy=abs(Txy);
angTxy=angle(Txy)*180/pi;

% in db:
magTxy_db=20*log10(magTxy);
clf
subplot(121),semilogx(f,magTxy_db)
xlabel('frequency (Hz)')
ylabel('|Pel/Vw| (db)')
% title(sprintf('%s  samplefreq= %s Hz,  Nr of FFT points= %s   %s',
  progfile,sflabel,nfftlabel,meetfile))
title(sprintf('%s  samplefreq= %s Hz,',progfile,sflabel))
axis([1e-3 1e1 -70 0]);
subplot(122),semilogx(f,angTxy);
xlabel('frequency (Hz)')
ylabel('angle(Pel/Vw) (degrees)')
% title(sprintf('%s  samplefreq= %s Hz,  Nr of FFT points= %s   %s',
progfile,sflabel,nfftlabel,meetfile))
title(sprintf('  Nr of FFT points= %s   %s',nfftlabel,meetfile))
pause

% loglog
clf
subplot(121),loglog(f,magTxy)
xlabel('frequency (Hz)')
ylabel('|Pel/Vw| (kWs/m)')
% title(sprintf('%s  samplefreq= %s Hz,  Nr of FFT points= %s   %s',
progfile,sflabel,nfftlabel,meetfile))
title(sprintf('%s  samplefreq= %s Hz,',progfile,sflabel))
axis([1e-3 1e0 1e-4 1e0]);
%subplot(122),semilogx(f,unwrap(angTxy));
subplot(122),semilogx(f,angTxy);
xlabel('frequency (Hz)')
ylabel('angle(Pel/Vw) (degrees)')
% title(sprintf('%s  samplefreq= %s Hz,  Nr of FFT points= %s   %s',
progfile,sflabel,nfftlabel,meetfile))
title(sprintf('  Nr of FFT points= %s   %s',nfftlabel,meetfile))
axis([1e-3 1e0 -200 200]);
pause

if print2eps==1
   eval(['print -deps ' plotdir '/PemTransferFun_PV_' meetfile '.eps']);
end

end % Vw_to_P

if N_to_P==1
[Txy f]=tfe(N,Pgen,NFFT,samplefreq,'mean')

magTxy=abs(Txy);
angTxy=angle(Txy)*180/pi;

% in db:
magTxy_db=20*log10(magTxy);
clf
subplot(121),semilogx(f,magTxy_db)
xlabel('frequency (Hz)')
ylabel('|Pel/N| (db)')
% title(sprintf('%s  samplefreq= %s Hz,  Nr of FFT points= %s   %s',
progfile,sflabel,nfftlabel,meetfile))
title(sprintf('%s  samplefreq= %s Hz,',progfile,sflabel))
% axis([1e-3 1e1 -70 0]);
subplot(122),semilogx(f,angTxy);
xlabel('frequency (Hz)')
ylabel('angle(Pel/N) (degrees)')
% title(sprintf('%s  samplefreq= %s Hz,  Nr of FFT points= %s   %s',
progfile,sflabel,nfftlabel,meetfile))
title(sprintf('  Nr of FFT points= %s   %s',nfftlabel,meetfile))
pause

% loglog
clf
subplot(121),loglog(f,magTxy)
xlabel('frequency (Hz)')
ylabel('|Pel/N| (kWs/m)')
% title(sprintf('%s  samplefreq= %s Hz,  Nr of FFT points= %s   %s',
progfile,sflabel,nfftlabel,meetfile))
title(sprintf('%s  samplefreq= %s Hz,',progfile,sflabel))
axis([1e-3 1e0 1e-6 1e-2 ]);
%subplot(122),semilogx(f,unwrap(angTxy));
subplot(122),semilogx(f,angTxy);
xlabel('frequency (Hz)')
ylabel('angle(Pel/N) (degrees)')
% title(sprintf('%s  samplefreq= %s Hz,  Nr of FFT points= %s   %s',
progfile,sflabel,nfftlabel,meetfile))
title(sprintf('  Nr of FFT points= %s   %s',nfftlabel,meetfile))
axis([1e-3 1e0 -200 200]);

if print2eps==1
```

```
   eval(['print -deps ' plotdir '/PemTransferFun_PN_' meetfile '.eps']);
end
end % N_to_P
```

C.6 Power performance estimation

```
% Opbrengstberekening voor Small WT (tbv PEMSWECS)
%
% vergelijkt de invloed van de DC spanning op de opbrengst
% 1. voer P(V) curve in als tabel
% 2. kies Weibull parameters
% 3. bereken Weibull verdeling voor te kiezen interval
% 4. interpoleer P(V) voor de uitvoervector van de Weibull
     berekening
% 5. bereken energieopbrengst
%
clear

rho=1.225;
D=5;
Prated=4;

v_mean=7;
s_weib=2;

% laad de P(V) curves uit de metingen,
% voor 3 waarden van de DC spanning
load U_Vw_binned_P30.dat
data=U_Vw_binned_P30;
V1=data(:,1);
P1=data(:,2);
V2=data(:,4);
P2=data(:,5);
V3=data(:,7);
P3=data(:,8);

% directory voor plots:
plotdir='D:/1_Pemswecs/Model_Opbrengst';
filenaam='opbrengstPEMSWECS3.m'
% plots van tussenresultaten:
intermediate_plots=0;

% 3 Udc bins en alle bins tesamen
% worden met elkaar vergeleken:

for Uchoise=1:4

if Uchoise==1
  Vw=V1;
  Ptur=P1;
  Ulabel='Ulow';
end
if Uchoise==2
  Vw=V2;
  Ptur=P2;
  Ulabel='Umedium';
end
if Uchoise==3
  Vw=V3;
  Ptur=P3;
  Ulabel='Uhigh';
end
if Uchoise==4
   load D:/1_Pemswecs/Meetdata/Binned_data/PVbinnedTav30.dat
  V4=PVbinnedTav30(:,1);
  P4=PVbinnedTav30(:,2);
  Vw=V4;
  Ptur=P4;
  Ulabel='AllU';
end

Paero=0.5*rho*Vw.*Vw.*Vw*pi*D*D/(4*1000);
Cp=Ptur./Paero;
clf
subplot(2,2,1),plot(Vw,Paero,'*')
xlabel('windspeed (m/s)')
ylabel('Pearo (kW)')
title(sprintf('D = %6.2f m, %s',D,filenaam))
subplot(2,2,2),plot(Vw,Ptur,'*')
xlabel('windspeed (m/s)')
ylabel('Ptur (kW)')
subplot(2,2,3),plot(Vw,Cp,'*')
xlabel('windspeed (m/s)')
ylabel('Cp (-)')
```

```
if intermediate_plots==1
   pause
end


% 2. Opbrengstberekening
%
% bereken de opbrengst voor de waarden in de P(V) tabel
% dan is geen interpolatie nodig
%
% invoer voor Weibull berekening: "Continue windvector"
VwindCont = [0.1:0.1:20]';
% deze vector is anders dan de vector VwHis
% waarvoor de urenverdeling
% wordt uitgerekend;

% maximum van VwHis:
VwHis_max=max(Vw);
% eventueel begrenzen: moet lager zijn dan max Vw
% anders kan niet geinterpoleerd worden in de P(V) curve
% en is de opbrengst NaN
VwHis_interval=0.5;

% 3. Weibull berekening
% bereken het aantal uren in een bepaalde windklasse:
% VwHis,NhourHis
weibull2

% P(V) curve uitbreiden met nullen aan onderzijde
% dit moet om iets te laten uitrekenen in lage Vw gebied
extra_nullen=0;
if extra_nullen==1
Vstart=min(Vw);
if Vstart>0
   dV=Vw(2)-Vw(1);
   Va=Vw(1)-dV;
   Vw=[0 Va Vw']';
   Ptur=[0 0 Ptur']';
end
end

% het volgende dient om de P(V) curves voor 3 Udc
% met dezelfde Vw te laten beginnen
% voor hoge Udc nl geen Vw waarden in lage bins
remove_low_Vw=0
if remove_low_Vw==1
   % alles onder 5 m/s nul:
   sizeVw=size(Vw,1)
   for n=1:sizeVw
      if Vw(n)<5
         Ptur(n)=0;
      end
   end
end
% OPMERKING:
% dit geeft randeffecten rond V=5
% die de vergelijking van de verschillende opbrengsten vertekenen
% daarom is het beter om het volledige Vw bereik uit te rekenen
% en later alleen voor dezelfde Vw range en waarden
% de Etur op te tellen!

extend_to_cutout=0;
if extend_to_cutout==1
% en Prated aan bovenzijde
 Vw=[Vw' v_cutout]';
 Ptur=[Ptur' max(Ptur)]';
end


% 4. Interpolatie van de P(V) curve voor de VwHis
%          windsnelheidswaarden uit Weibull
PturHis=interp1(Vw,Ptur,VwHis,'linear');
PaeroHis=0.5*rho*VwHis.*VwHis.*VwHis*pi*D*D/(4*1000);
CpHis=PturHis./PaeroHis;
plot(Vw,Ptur,VwHis,PturHis,'*')
xlabel('windspeed (m/s)')
ylabel('Ptur (kW)')
title('Power curve interpolation')
if intermediate_plots==1
   pause
end

ujaar=8328;
% verschil met 8760: onderhoud en beschikbaarheid
avail=8328/8760;
uren=avail*NhourHis;
Etur=uren.*PturHis;
Eaero=uren.*PaeroHis;
Eratio=Etur./Eaero;
```

```
% dit is weer de Cp
Eturtot=sum(Etur)
Eaerotot=sum(Eaero)
controletabel=[VwHis NhourHis uren PturHis Etur Eaero Eratio]
% gemiddeld continu geleverde vermogen in kW:
% totaal aantal kWh/jaar*jaar/uur=kW
Pmean=Eturtot/8760
CF=Pmean/Prated;
Extr=Eturtot/Eaerotot;
clf
subplot(321),bar(VwHis,NhourHis)
ylabel('h/y')
title(sprintf('V_a_v = %1.2f, S_w_e_i_b_u_l = %1.2f ',v_mean,s_weib))
subplot(325),bar(VwHis,Eaero)
ylabel('E_a_e_r_o (kWh)')
xlabel('Windspeed (m/s)')
subplot(326),bar(VwHis,Etur)
xlabel('Windspeed (m/s)')
ylabel('E_t_u_r (kWh)')
subplot(323),bar(VwHis,PaeroHis)
ylabel('P_a_e_r_o (kW)')
subplot(324),bar(VwHis,PturHis)
ylabel('P_t_u_r (kW)')
axis([0 20 0 5])
top=2.7*Prated;
del=0.25*Prated;
text(0,top,(sprintf(filenaam)))
text(0,top-del,(sprintf(Ulabel)))
text(0,top-2*del,(sprintf('E_a_e_r_o = %5.0f kWh/y',Eaerotot)))
text(0,top-3*del,(sprintf('E_t_u_r   = %5.0f kWh/y  -> EF=%4.2f',Eturtot,Extr)))
text(0,top-4*del,(sprintf('P_t_u_r^a^v  = %6.2f kW  -> CF=%4.2f',Pmean,CF)))

pause

if Uchoise==1
   shis=size(VwHis,1);
   Vvec=zeros(shis,0);
   Pvec=zeros(shis,0);
   Evec=zeros(shis,0);
end

Vvec=[Vvec VwHis];
Pvec=[Pvec PturHis];
Evec=[Evec Etur];

eval(['print -deps ' plotdir '/Opbrengst_' Ulabel '.eps']);

end % of Uchoise

clf
plot(Vvec(:,1),Evec(:,1),'o',Vvec(:,2),Evec(:,2),'*',Vvec(:,3),...
Evec(:,3),'+',Vvec(:,4),Evec(:,4),'d')
xlabel('Windspeed (m/s)')
ylabel('E_t_u_r (kWh)')
title(sprintf('%s          %s',filenaam,date))
ymax=500
if v_mean==6
   ymax=700
end
if v_mean==7
   ymax=800
end
axis([4 12 0 ymax])
hold on
% legenda:
x1=5;
x2=x1+0.5;
y1=150;
dy=30;
plot(x1,y1-dy  ,'o')
text(x2,y1-dy  ,'Udc < 125 V ')
plot(x1,y1-2*dy,'*')
text(x2,y1-2*dy,'125 < Udc < 135 V')
plot(x1,y1-3*dy,'+')
text(x2,y1-3*dy,'Udc > 135 V')
plot(x1,y1-4*dy,'d')
text(x2,y1-4*dy,'All Udc')
x1=10;
y1=450;
if v_mean==6
   y1=650;
end
if v_mean==7
   y1=650;
   x1=5;
end
dy=30;
text(x1,y1,sprintf('V_a_v = %1.2f ',v_mean))
text(x1,y1-dy,sprintf('S_w_e_i_b_u_l = %1.2f ',s_weib))
```

```
VavLabel=int2str(v_mean);
eval(['print -deps ' plotdir '/Opbrengst_CompareVav' VavLabel '.eps']);

% opbrengst in het gebied waar alle P(V) waarden hebben:
% zie volgende tabel voor de keuze:
Nummers=[1:shis]'
Totvec=[Nummers Vvec(:,1) Evec]


% Vw tusse 5 en 11 m/s:
n1=11;
n2=22;
Elow=sum(Evec(n1:n2,1))
Emed=sum(Evec(n1:n2,2))
Ehig=sum(Evec(n1:n2,3))
Eall=sum(Evec(n1:n2,4))

fid = fopen('OpbrengstCompTabel.tex','w');
fprintf(fid,'Vav = %1.2f, Sweibul = %1.2f ///n',v_mean, s_weib)
fprintf(fid,'  U low      &    %8.0f      /////n',Elow)
fprintf(fid,'  U medium   &    %8.0f      /////n',Emed)
fprintf(fid,'  U high     &    %8.0f      /////n',Ehig)
fprintf(fid,'  all U      &    %8.0f      /////n',Eall)
fclose(fid);
```

C.7 Weibull routine

```
%  weibull.m
%
%  input:
%       VwindCont = "continue" wind vector, kleine stapgrootte
%       s_weib en v_mean
%       VwHis_max
%       VwHis_interval = windsnelheidinterval grote stap
%
%       uit v_cutout en interval wordt VwHis bepaald
%       voor de VwHis windvector wordt aantal uren bereken
%       VwHis hoeft niet gelijk te zijn aan windvector in PV curve
%
%       buiten deze routine wordt Pel geinterpoleerd voor VwHis
%       en de jaaropbrengst berekend
%
%  bereken uit Weibull kansdichtheid:
%       1. aantal uren in windsnelheidsintervallen van VwindCont
%       2. sommatie van aantal uren in grotere intervallen
%          van VwHis voor opbrengst via powercurve
%
%  output:
%       VwHis, NhourHis
%
%  wijzigingen:
%       23mrt01
%       interval VwindCont wordt nu uitgerekend (was 0.1)


factor=(0.287/s_weib+0.688/(s_weib^0.1))^(1/s_weib);
c_weib=v_mean/factor;

%%%%%%%%%%%%%%%%%%%%%%%%%%%%%%%%%%%%%%%%%%%%%%%%%%%%%%%%%%%%%%%%%%%%%%%%%%%%%%%
% VwindCont is de windvector met kleine stapgrootte:
% bepaal eerst de continue windsnelheidsverdeling:
%%%%%%%%%%%%%%%%%%%%%%%%%%%%%%%%%%%%%%%%%%%%%%%%%%%%%%%%%%%%%%%%%%%%%%%%%%%%%%%

iup=min(find(VwindCont>=VwHis_max));
nclfix=iup-1;
nhour=zeros(nclfix,1);
vband=zeros(nclfix,1);
vcentr=zeros(nclfix,1);

% EERSTE DE KLEINE INTERVALLEN:

for i=1:nclfix,
 nhour(i,1) = (  exp(-(VwindCont(i) / c_weib)^s_weib) - ...
                 exp(-(VwindCont(i+1)/c_weib)^s_weib) ) * 8760;
 vband(i,1) = VwindCont(i+1)-VwindCont(i);
 vcentr(i,1) = 0.5*(VwindCont(i+1)+VwindCont(i));
end

% CONTROLE OP WAT ER GEBEURT:
Vcen=vcentr(:,1);
Nhour=nhour(:,1);
clg
plot(Vcen,Nhour)
```

```
xlabel('wind speed [m/s]');
ylabel('number of hours in production wind class [-]');
title('Weibull Continu (klein interval)')
if intermediate_plots==1
   pause
end

% AANTAL DATAPUNTEN DAT WORDT SAMENGENOMEN PER INTERVAL:
% 0.1 IS NL. DE OORSPRONKELIJKE STAPGROOTTE:

VwindCont_interval=VwindCont(2)-VwindCont(1);
nsum=VwHis_interval/VwindCont_interval;
istop=VwHis_max/VwHis_interval;

% NU DE GROTE INTERVALLEN DOOR OPTELLEN:

for i=1:istop-1,
  VwHis(i,1) = 1/nsum*sum(vcentr((i-1)*nsum+1:i*nsum) );
  NhourHis(i,1) =  sum(nhour((i-1)*nsum+1:i*nsum));
end;

clg
plot(VwHis,NhourHis,'*');
xlabel('wind speed [m/s]');
ylabel('number of hours in production wind class [-]');
title('Weibull gesommeerd (groot interval)')
ymax=max(NhourHis);
xm=mean(VwHis);
dy=ymax/10
text(xm,ymax,'Weibull windspeed distribution:');
text(xm,ymax-dy,sprintf('mean windspeed = %4.1fm/s',v_mean));
text(xm,ymax-2*dy,sprintf('shape factor = %3.1f',s_weib));
text(xm,ymax-3*dy,sprintf('scale factor = %3.1f',c_weib))
if intermediate_plots==1
   pause
end

tabel=[VwHis NhourHis]
save vwfreqWB.dat tabel  -ascii
%stop

% DELEN DOOR AANTAL UREN MAAL INTERVAL BREEDTE GEEFT WEER
  DE KANSDICHTHEID:

NhBc=NhourHis/(8760*VwHis_interval);

% BIJ NORMEREN NIET ALLEEN AANTAL UREN PER JAAR MAAR OOK
  DE INTERVALBREEDTE
% GEEFT ZELFDE WAARDEN ALS DE CONTINUE VERDELING (weibull3.m)

plot(VwHis,NhBc,'*');
title('Weibull kansdichtheid')
xlabel('wind speed [m/s]');
ylabel('number of hours in production wind class [-]');
if intermediate_plots==1
   pause
end
```

	Date: August 2001	**Report No.:** ECN-C–01-032
Title	PEMSWECS, Performance Evaluation Methods for Autonomous, Applications Orientated Wind Turbine Systems: Systems with batteries	
Author	J.T.G. Pierik	
Principal(s)	European Community	
ECN project number **Principal's order number**	7.4063 JOR3-CT98-0262	
Programmes	Joule 3	

Abstract
This report describes measurements and simulations to determine a method for the power performance evaluation of autonomous wind turbine systems. The method applies to small systems, equipped with a permanent magnet generator in the turbine, a diode rectifier and batteries. The analysis concentrates on the effect of the load on the power-wind speed curve of the turbine. It is shown that, although the effect of the load on the DC voltage is substantial, a 30% variation is not unusual, the effect on the power curve is relatively small. The effect on the annual averaged energy production, although dependent on the wind regime, is also expected to be small: in the range of 5%. This justifies a simple method for the measurement of the power curve.

Keywords
power performance, stand-alone wind turbines, wind energy, electric power, electrical models

Authorization	**Name**	**Signature**	**Date**
Checked			
Approved			
Authorised			